SEISMIC RESPONSE
OF
LATERITE MASONRY STRUCTURES

Thesis

submitted in partial fulfillment of the requirements for the degree of

DOCTOR OF PHILOSOPHY

by

SUJATHA UNNIKRISHNAN
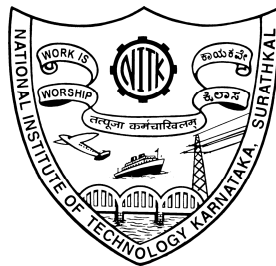
DEPARTMENT OF CIVIL ENGINEERING

NATIONAL INSTITUTE OF TECHNOLOGY KARNATAKA

SURATHKAL, MANGALORE-575025, INDIA

JUNE 2013

D E C L A R A T I O N

I hereby declare that the Research Thesis titled, **SEISMIC RESPONSE OF LATERITE MASONRY STRUCTURES**, which is being submitted to the **National Institute of Technology Karnataka, Surathkal** in partial fulfillment of the requirements for the award of the Degree of **Doctor of Philosophy** in **CIVIL ENGINEERING** *is a bonafide report of the research work carried out by me*. The material contained in this Research Thesis has not been submitted to any University or Institution for the award of any degree.

<div align="center">

SUJATHA UNNIKRISHNAN
Reg. No. CV04P2

Department of Civil Engineering

</div>

Place: NITK-Surathkal

Date:

C E R T I F I C A T E

This is to certify that the Research Thesis entitled, **SEISMIC RESPONSE OF LATERITE MASONRY STRUCTURES**, submitted by **Sujatha Unnikrishnan** (Register Number: **CV04P2**) as the record of the research work carried out by her, *is accepted as the Research Thesis submission* in partial fulfillment of the requirements for the award of degree of **Doctor of Philosophy**.

Dr. Mattur C. Narasimhan
Research Guide
Professor in Civil Engineering

Dr. Katta Venkataramana
Research Guide
Professor in Civil Engineering

Professor and Head
and Chairman – DRPC
Department of Civil Engineering

Place: NITK-Surathkal

Date:

Vakra-Tunndda Maha-Kaaya
Surya-Kotti Samaprabha
Nirvighnam Kuru Me Deva
Sarva-Kaaryessu Sarvadaa

ACKNOWLEDGEMENTS

ABSTRACT

Laterite is the most favored masonry material in south-west coastal areas of India due to its availability in abundance. However, not much research has been carried out so far on the structural performance of laterite masonry. The studies addressing the seismic performance of laterite masonry buildings are almost nil and hence there is a need for research in this area.

The strength and elastic properties of laterite masonry are influenced by the individual properties of laterite blocks and mortar used and the nature of bond between them. Experimental investigations were carried out on the strength characteristics of laterite blocks, cement mortar specimens and stack-bonded laterite masonry prisms under uniaxial compression. From these studies laterite masonry may be classified as weak-soft unit and strong-stiff mortar masonry. Stack bonded laterite masonry prism was modeled using commercially available finite element software and analyzed to understand the stress distribution pattern. Parametric studies were also conducted.

In south-west coastal areas of India masonry structures are normally box-type structures with either a light roof or a rigid roof. Efficiency of different types of seismic strengthening measures like lintel band, roof band etc. were studied on both these types of structures. A method of reinforcing laterite masonry with vertical reinforcement called 'containment reinforcement' has also been tried. Different configurations of box-type laterite masonry structures with these strengthening measures were modeled. Free vibration studies were conducted to find the natural frequencies and mode shapes of box-type laterite masonry structures without and with roof. Response of single storeyed box-type laterite masonry structures, to El-Centro acceleration input was obtained using time-history analysis. The effect of strengthening factors like lintel band, roof band and containment reinforcement on the natural frequencies, mode shapes and time-history responses were analyzed. Responses of some of these structures to Kobe and Koyna accelerations were also studied.

Keywords: Laterite, box-type structure, natural frequency, mode shape, seismic response.

CONTENTS

LIST OF FIGURES

x

LIST OF TABLES

CHAPTER 1

INTRODUCTION

1.1 GENERAL

Laterite is a prime masonry material for housing construction in western coastal areas of India. Laterite stone blocks are being used in these areas, for ages. Laterite is used for the construction of both load-bearing and 'partition walls'. It is also used as in-fills in framed structures. Exposed laterite walls have, in recent times, become fashionable, giving the building an antique look. There are many historical monuments built of laterites in this region. Some examples are Tippu's fort in Tellicherry, Basilica of Bom Jesus in Goa, and Fort St Agnelo in Kannur. The Bekal Fort in Kerala is the most recognized example.

Laterite is used in its natural form without any manufacturing process and hence proves a sustainable material. The term laterite was first proposed by Buchanan in 1807 to describe the reddish ferruginous, vesicular, unstratified and porous material with yellow ochres, occurring extensively in Malabar, India. This material is locally used as building blocks and is hence called "laterite" derived from the Latin word "lateritis" meaning brick [Gidigasu 1974]. The freshly dug material is soft enough to be cut easily into brick-like blocks with iron instruments but rapidly hardens on exposure to air and is fairly resistant to the weathering effects.

A National Geological Monument (Fig. 1.1) was erected at Angadipuram town in Malappuram district in the southern Indian state of Kerala. It is one of the 26 monuments declared as National Geological Monuments, on the occasion of the "International Conference on Laterization" held in 1979. The special significance of Angadipuram to laterites is that it was here that Dr. Francis Buchanan-Hamilton, a professional surgeon, gave the first account of this rock type, in his report of 1807, as "indurated clay", ideally suited for building construction.

1

He wrote: "What I have called indurated clay is one of the most valuable materials for building. It is diffused in immense masses, without any appearance of stratification and is placed over the granite that forms the basis of Malayala. It is full of cavities and pores, and contains a very large quantity of iron in the form of yellow and red ochres. In the mass, while excluded from the air, it is so soft, that any iron instrument readily cuts it, and is dug up in square masses with a pick-axe, and immediately cut into the shape wanted with a trowel, or large knife. It very soon after becomes as hard as brick, and resists the air and water much better than any brick that I have seen in India. … **The most proper English name would be laterite, from lateritis, the appellation that may be given to it in science**" [Buchanan 1807].

Fig. 1.1 National geological monument at Angadipuram (Wikipedia)

Laterite is a surface formation in hot and wet tropical areas, and is rich in iron and aluminium. It develops by intensive and long-lasting weathering of the underlying parent rock. Laterites are widely distributed throughout the world, especially in humid tropical climates within 30°N and 30°S of the equator. The distribution of laterite in regions of Africa, Australia, India, South-East Asia and South America is shown in Fig. 1.2 and the distribution in south-west India is shown in Fig. 1.3 [Kasturba 2005a]. In India, Laterite occurs in the states of Kerala, Karnataka, Goa, Maharashtra, Tamil Nadu, Andhra Pradesh, Bihar, Assam, Meghalaya and Orissa [IS 3620- 1979].
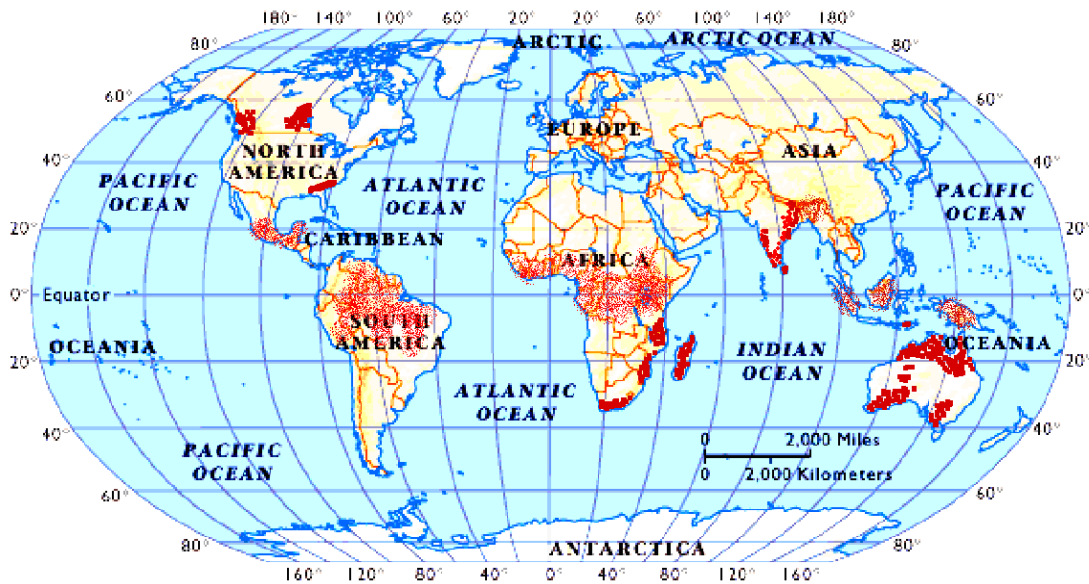
Fig. 1.2 World wide distribution of laterite (Kasturba 2005a)

Laterite cannot be placed in the triplet family of rocks, namely igneous, sedimentary or metamorphic. It may be considered to be a metasomatic rock [Kasthurba 2005b]. Metasomatism is a metamorphic process by which the chemical composition of a rock or rock portion is altered in a pervasive manner and which involves the introduction and/or removal of chemical components as a result of the interaction of the rock with aqueous fluids (solutions). During metasomatism, the rock remains in a solid state [Zharikov et al. 2007].

Laterites are mainly used as building blocks for construction of masonry in buildings and also as aggregate in road construction. In spite of the fact that geologists, soil scientists, mineralogists, geographers, geomorphologists, mining and construction engineers have participated in laterite research, publications on laterite as a masonry material is scarce. Great regional variations have hindered in-depth research to characterize laterite as a masonry material [Das 2008].
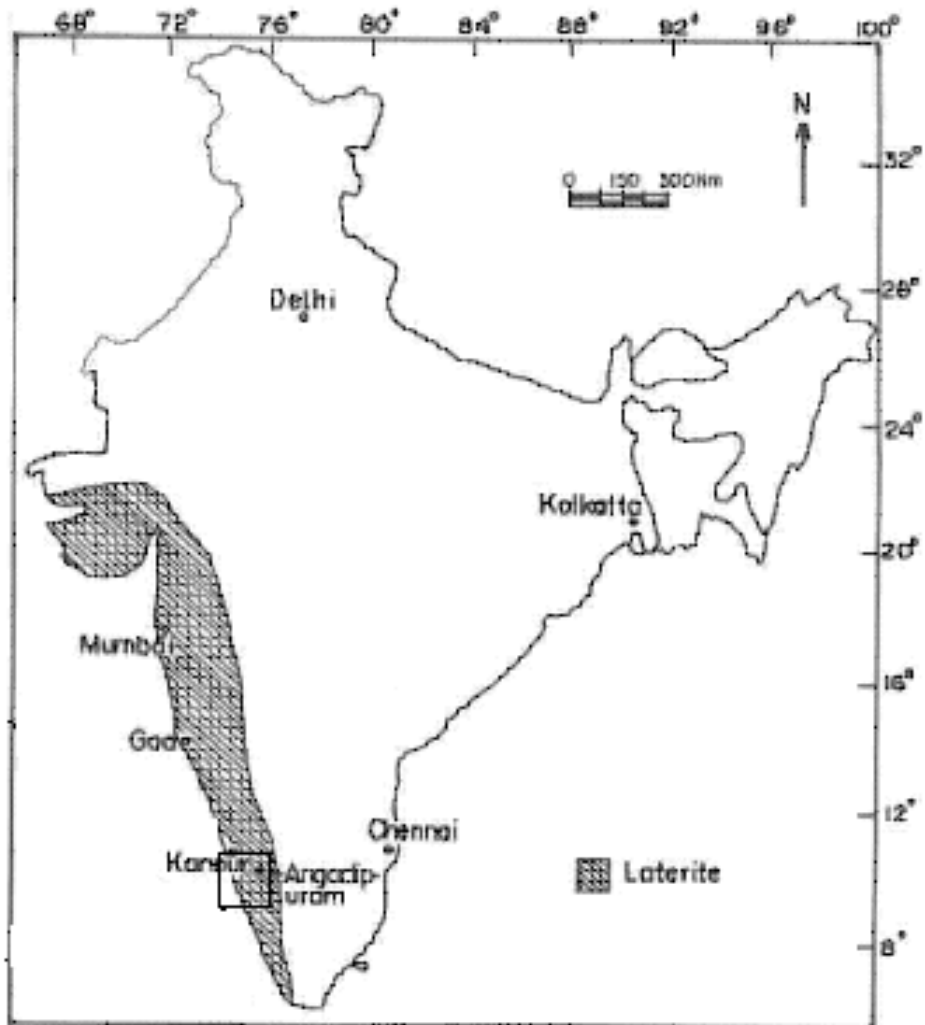
Fig. 1.3 Distribution of laterite in west-coast of India (Kasturba 2005a)

When subjected to an earthquake ground motion, inertia forces, which are proportional to the masses of building components and induced accelerations, cause the vibration of the structural system. As a result of such vibration, additional bending and shear stresses develop, which often exceed the strength of the materials and cause damage to structural elements. Since masonry, though can be stressed relatively higher in compression, is not a suitable material for carrying the bending and shear stresses, the resulting damage is severe and often causes the collapse of a building [Tomazevic 1999].

Ductility is one of the most desirable properties in a structural system for earthquake resistance. To achieve a ductile effect in the overall behavior of the component, appropriate ductile materials must be proportioned and placed so that they come in tension and are subjected to yielding. Thus a necessary requirement for good earthquake resistant design is to have sufficient ductile materials at points of tensile stresses. From the point of view of seismic strengthening of masonry walls, reinforcement is essential to prevent catastrophic collapse of walls by enhancing its ductility, especially in flexure.

Horizontal bands are provided to prevent the growth of vertical and diagonal cracks in masonry elements apart from acting as beams across the openings. They also perform the job of holding the corners of the walls together. These bands seem to provide ductility at discrete levels in a masonry wall, whereas the rest of the wall remains un-reinforced and hence brittle. Also, these bands may not prevent the growth of horizontal cracks. The growth of horizontal cracks can be prevented by the provision of vertical reinforcement along the height of the wall.

The opening in a wall is a weak zone. When a wall with an opening deforms during earthquake shaking, the shape of the opening distorts and becomes more like a rhombus – two opposite corners move away and the other two come closer (Fig. 1.4). Under this type of deformation, the corners that come closer develop cracks. The cracks are bigger when the opening sizes are larger. Steel bars provided in the wall masonry all around the

openings restrict these cracks at the corners (Fig. 1.5). Lintel and sill bands above and below the openings, and vertical reinforcement adjacent to vertical edges, provide protection against this type of damage [Murty 2005].
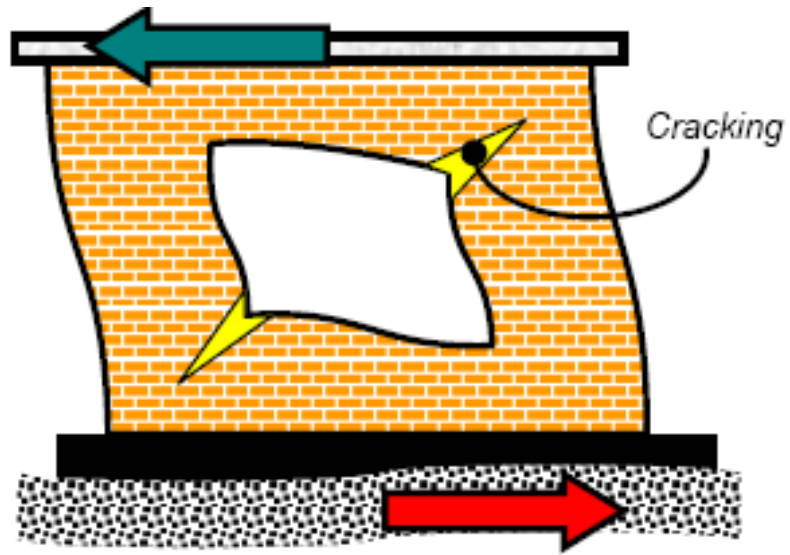
Fig. 1.4 Cracking in building with no corner reinforcement (Murty 2005)
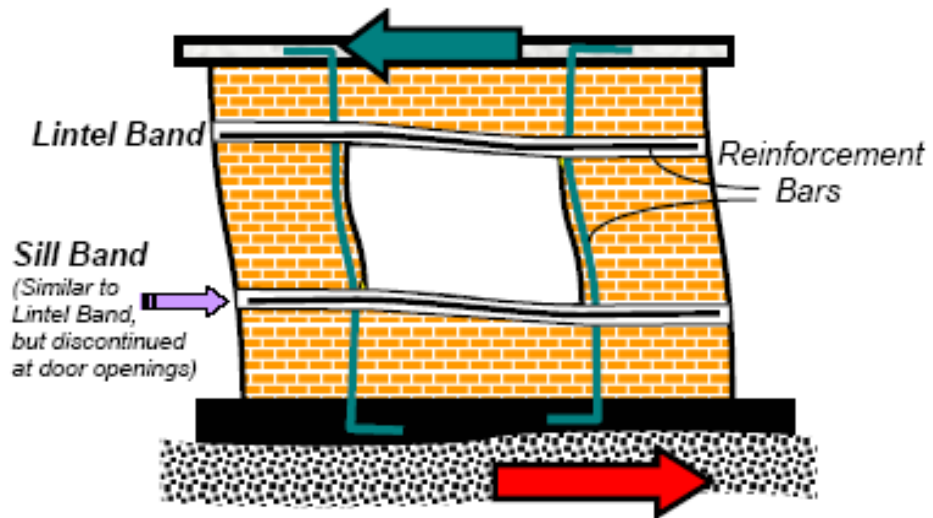
Fig. 1.5 Building with vertical reinforcement (Murty 2005)

1.2 CONTAINMENT REINFORCEMENT

In 'containment reinforcement', vertical reinforcement is wrapped around the masonry unit at the base and tied at the top. Such vertical reinforcement is to be provided at an appropriate spacing along the length of the wall. The reinforcements on the two faces are tied together through links/ties provided at a definite vertical spacing. As the masonry wall bends, one face of masonry would be subjected to tension and the reinforcement on that side would bend to its profile while the reinforcement on the compression side would tend to become slack and the reverse happens as the wall bends the other way. Here the reinforcement is intended to prevent the growth of flexural tensile cracks that lead to failure. The 'containment reinforcement' will prevent brittle failure due to tension cracks and permit larger deflections and hence a much higher absorption of energy without a substantial increase in strength [Raghunath 2003].

1.3 BACKGROUND TO THE STUDY

In general, masonry structures are very good in resisting gravity loads, but do not perform so well when subjected to an earthquake. The National Seismic Zone Map of India presents a large scale view of the seismic zones in the country. The south-west coastal areas of India lie in zone III according to IS 1893-2002 (Fig. 1.6). In spite of the fact that laterite is the most favored masonry material in these regions of India, the structural performance of laterite masonry has not been systematically investigated, the studies addressing the seismic performance of laterite masonry buildings are almost nil. Now that these areas are becoming more and more important from point of view of trade and commerce, there is a need for research on the seismic response of laterite masonry structures located in these areas.
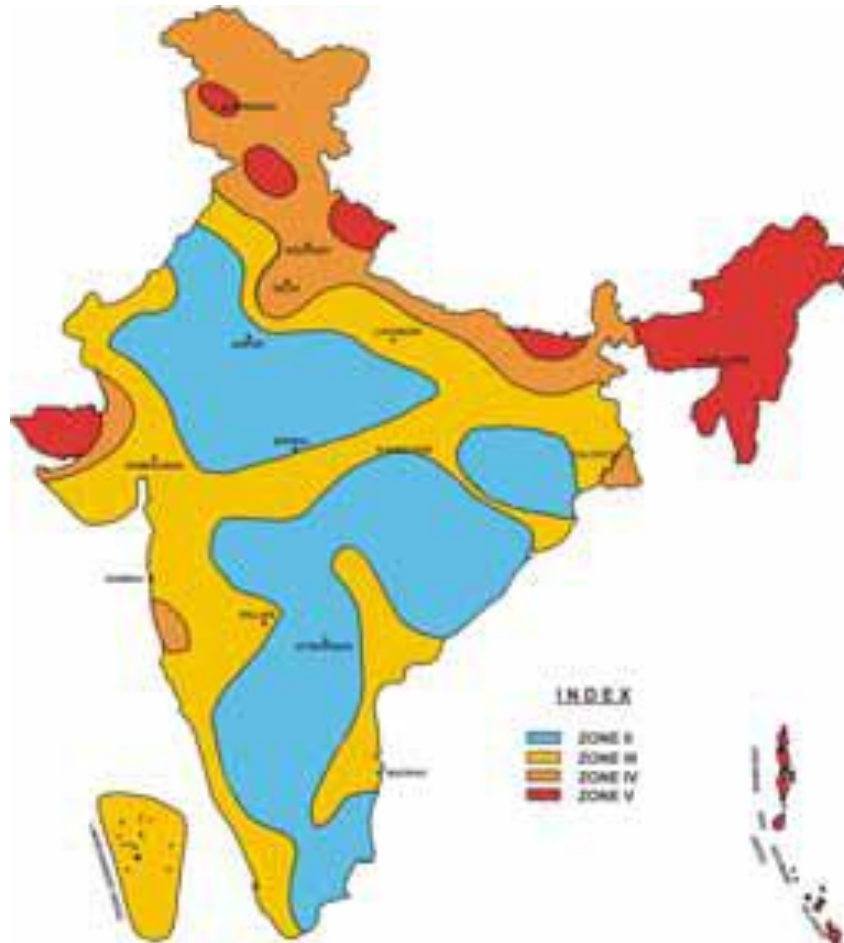
Fig. 1.6   Indian seismic zone map as per IS:1893 (Part 1) – 2002

1.4 SCOPE OF THE PRESENT STUDY

The aim of the present study is to analyze the potential seismic performance of single-storeyed box-type laterite masonry structures. Preliminary experimental work to determine strength and elasticity characteristics of laterite blocks, cement mortar and laterite masonry in cement mortar was conducted. Initial dynamic analysis consisting of determination of natural frequencies and mode shapes of different configurations of single-storeyed box-type laterite masonry structures was attempted using finite element method. Seismic response of such structures was studied in detail using acceleration

8

records of El-Centro earthquake. The effect of providing containment reinforcement on such seismic response of these structures has been evaluated.

1.5 ORGANISATION OF THESIS

The thesis is presented in six chapters. Chapter-1 gives a brief introduction about the material of laterite, seismic zoning in India and seismic behavior of masonry structures in general. The need for undertaking the present study is brought out.

Detailed literature review on laterite as a masonry material is presented in Chapter-2. Literature review on evaluation of properties of laterites, testing of masonry prisms, finite element modeling and seismic response of brick masonry structures is also presented. All the details of the experimental work that was carried out on laterite blocks, mortar specimens and laterite masonry prisms and triplets are presented in Chapter-3. Results obtained in analytical studies based on micro-mechanics based FE modeling of laterite masonry prisms are discussed in detail.

Natural frequencies and mode shapes of single-storeyed box-type laterite masonry structures are presented in Chapter-4. Masonry structures, both without roof and with roof are considered. Effects of provision of RC bands in these structures vis-à-vis vertical containment reinforcement on the free-vibration response characteristics of these structures are evaluated. Responses of box-type laterite masonry structures to accelerations of El-Centro earthquake are presented in detail in Chapter-5. Responses of some of these structures to Kobe and Koyna earthquakes are also presented to bring out clearly the effect of vertical containment reinforcements, qualitatively and quantitatively, on the seismic performance of such structures.

The Chapter-6 summarizes the conclusions drawn based on the results obtained during the present investigation. Topics with potential for further research are identified and are presented.

CHAPTER 2

LITERATURE REVIEW

2.1 INTRODUCTION

Literature on laterite soil and geological study on laterite is available, but study on laterite as a masonry material is scarce. For an understanding on properties of laterite, some papers on laterite are included. For information on prism studies as well as for response of masonry structures to lateral loads or earthquake accelerations, papers on block/brick masonry are included.

Gidigasu (1974) has attempted to assemble available information useful for the identification and evaluation of all grades of lateritic materials for engineering purposes. From a study of literature it is concluded that the genesis and degree of decomposition, laterisation or dehydration of laterite materials give them diverse genetic, morphological, chemical and mineralogical characteristics. Each of these exerts considerable influence upon their geotechnical characteristics and engineering behaviour. The properties of laterite as a masonry material have not been included in this study.

West (1936) has reported on the Quetta (Baluchistan) earthquake of 1935 with photographs of earthquake-proof masonry buildings which withstood the earthquake without much damage. These masonry buildings were constructed with horizontal and vertical railings with brick infill panels. It has been cited that adjacent buildings without such railings have been completely ruined showing the efficiency of such bands.

Krishna and Chandra (1965) have suggested different methods of strengthening brick houses against earthquake forces based on their experimental studies conducted at research school, Roorkee. They have concluded that:

1. the ultimate load carrying capacity against extensive cracking is not increased by the provision of a lintel band alone. The overall stiffness against cantilever action is, however, increased and would certainly delay the actual collapse of the structure.

2. vertical steel at corners is very effective and increases the strength of the structure considerably. It will delay the initial cracking and take much more load before the final collapse.

3. vertical steel at jambs only does not prevent the initial failure of the structure but does increase the overall resistance of the structure since corners near jambs are vulnerable to failure due to diagonal tension.

4. combination of horizontal steel at lintel level and vertical steel at corners is still stronger a combination and of course, if vertical steel at jambs is also present, the effect is very much pronounced.

McNary and Abrams (1985) investigated strength and deformation of clay-unit masonry under uniaxial concentric compressive force. Biaxial tension-compression tests of bricks and triaxial compression tests of mortar were also done for various brick types and mortar strength. This study considered the soft cement-lime mortar and stiff fired-clay bricks. Shear stresses at the brick mortar interface result in an internal state of stress which consists of triaxial compression in the mortar and bilateral tension coupled with axial compression in the brick. Such a stress state initiates vertical splitting cracks that lead to failure. Again measured properties of brick and mortar were used as input to a numerical model. The prism strengths and deformations calculated using the numerical model were then compared with experimental results to verify the theory. Although failure of prism occurred as a result of lateral tensile splitting of masonry unit, it was the mortar that induced the tensile stresses. These stresses increased disproportionately with compressive forces because of the nonlinear deformational properties of the mortar. Prism strength was also dependent on the strength of the masonry units which were under bi-axial tensile and uniaxial compressive stresses.

Karantoni and Fardis (1992) have studied the behaviour of and damage inflicted on stone-masonry buildings during the Kalamata, Greece, earthquake of 1986. The results from a finite element analysis show that out-of-plane bending and the transfer of out-of-plane lateral loads to the transverse walls cause most of the damage. They have concluded that finite element analysis can be used to improve our understanding of the seismic behaviour of masonry buildings and to develop and assess techniques of seismic strengthening.

Bruneau (1994) has made a number of observations on the seismic performance of unreinforced masonry buildings (URM). He has discussed different types of failures which also include:

- Lack of anchorage between floor and walls
- Anchor failure when joists are anchored to walls
- In-plane failure
- Out-of-plane failure
- Combined in-plane and out-of-plane effects

The fact that URM buildings are most vulnerable to flexural out-of-plane failure has been emphasized. In-plane failure may not right away lead to collapse since the load carrying capacity of a wall is not completely lost by diagonal cracking, whereas, out-of-plane failure leads to unstable and explosive collapse. Sometimes an initial in-plane failure may weaken the wall and subsequent out-of-plane motion can lead to collapse. Bruneau has also pointed out that when masonry construction of poor quality often show total failure, monumental/institutional masonry buildings of high quality often perform quite well.

Jain et al. (1994) have reported on 1993 Killari earthquake in Central India. It is mentioned that a number of dwellings in the affected villages had timber columns connected together with transverse and longitudinal beams. The roof planks in these houses were supported by the timber beams and columns rather than the rubble masonry

walls. When securely anchored to the floor and to the roof beams, the posts tended to hold up the roof and prevent the inward collapse of the walls, thereby saving the inhabitants.

Some of the poorest people in the villages lived in the thatch-type houses consisting of wooden vertical posts and rafters connected with coir type ties. Roofs were of thatch, and thatch panels or a series of small stocks or slit bamboo woven together formed the walls. Mud plaster provided a wall finish in some of these cases. These houses performed extremely well with only minor cracks in the mud-plaster walls. A few brick masonry houses in the area were found to have concrete lintel bands. Such houses also performed very well with no damage.

Rao et al. (1995) studied strength characteristics of soil-cement block masonry. They have concluded that bed joint thickness has significant influence on masonry strength and its effect will depend on the ratio of mortar strength to block strength. Based on experimental results they have recommended 10 to 12mm thickness of bed joints for soil-cement block masonry.

Andreaus (1996) investigated the failure criteria of masonry panels under in-plane loading, which has been attributed to three simple modes: slipping of mortar joints, cracking of clay bricks and splitting of mortar joint, and middle plane spalling. In this paper, a suitable strength criterion is connected to each collapse mode. A frictional law is associated with the slipping, which accounts for the shear strength depending nonlinearly on normal stress. Splitting can be explained by the maximum tensile strain criterion (Saint Venant), orthotropic non-symmetric elasticity being assumed for the material. Eventually panels exhibit spalling when the maximum compressive stress (Navier criterion) was attained under biaxial loading. Strength parameters were identified on the basis of experimental results and were compared with reliable criteria found in the literature. The proposed failure criteria were in good agreement with experimental

results, within the limits of small-size panels, single wythes, solid units, regular mortar joints, and in-plane loads. The potential application of the proposed criteria to actual cases is also illustrated. A specific example is worked out to show as to how to apply these criteria to predict the failure load and failure mode of a particular masonry panel. The discussion is confined to the in-plane behaviour of solid-brick, single-wythe masonry and does not consider the effects of out-of-plane bending produced by eccentrically applied loads or lateral instability.

Rai and Goel (1996) studied the seismic strengthening of un-reinforced masonry piers with steel elements. They considered the in-plane behaviour of masonry piers. The strengthening system showed significant improvement in stiffness and ductility.

Jain et. al. (1997) have presented their observations on engineering aspects of Jabalpur earthquake of May 1997. During that earthquake some houses in rural as well as urban areas built with burnt brick masonry in mud mortar had sustained significant cracking. Unlike the traditional construction practice, the mud mortar was not reinforced with straw in this type of construction. There were examples of load-bearing masonry houses built of brick with cement mortar and having a reinforced concrete roof slab, with good quality of construction. Those structures had performed well during the earthquake, in spite of not having any special earthquake resistant features such as a "lintel band".

Felix (1999) studied the compressive strength and modulus of elasticity of masonry prisms by computer simulation and laboratory testing of masonry units, mortars and prisms. Low and high strength masonry units (30 -100 MPa) in combination with low and high strength mortar mixes (2 -15 MPa), in different combinations were tested. But in all the cases, units were much stronger than mortar, which is generally the case in western countries. During the numerical simulations, when Poisson's ratio of the masonry unit was reduced, without changing the other parameters, the tensile stress of the elements in the masonry unit in the horizontal directions, increased. The higher the difference of

Poisson's ratios between the masonry unit and the mortar, the faster the prisms fail. Similar is the case with modulus of elasticity: the higher the relative difference, the higher the tensile stress in the masonry unit and lower the prism strength. The computer simulations identified the interface of the mortar and the unit as the most critical area. Again it is found that modulus of elasticity of prisms is mainly controlled by the properties of the masonry unit.

Tomazevic (1999) and his colleagues carried out a large number of studies on earthquake resistant masonry structures. Following are some of the concepts mentioned by them for designing earthquake resistant masonry:

1. Traditional stone masonry walls with horizontal RC bond beams connecting the walls around the building at vertical spacing of 1m or 2m depending on the expected seismic intensity.
2. Masonry confined in its own plane by RC bond beams and columns. The columns have to be connected to the walls through shear keys. The spacing of columns should not be more than 4m.
3. Vertical reinforcement is provided in grouted holes of hollow block masonry and small pockets inside brick masonry. Horizontal reinforcements in the shape of truss like arrangements are also provided in bed joints. There are Eurocode specifications for such reinforcements.
4. Horizontal tie rods are provided as a retrofitting measure in grooves cut in the mortar, below the floor level, on both sides of a wall. They are anchored to steel plates at both ends of the wall.
5. Steel mesh is anchored to the walls on both faces and covered with plaster.

Thakkar and Agarwal (2000) have conducted a seismic evaluation of earthquake resistant and retrofitting measures of stone masonry houses. Model tests of stone masonry structures indicated that the damage started from the corners of model and the corners of door and window openings. Hence, it was suggested that strengthening of corners will

not only improve the lateral resistance capacity significantly but will also improve energy dissipation without much strengthening of wall piers. On the basis of shock table tests the following recommendations are made to reduce the damage in stone masonry structures,

(i) an integrated roof system with shear connection with walls

(ii) bands at sill and lintel level

(iii) extra strengthening at corners in the form of vertical bars and dowels

(iv) strengthening around the door and window openings.

They have concluded that the Indian codal provisions of earthquake resistance measures such as lintel band, roof band, corner and jamb reinforcement, as given in IS 4326-1993, are effective in improving the behaviour of stone masonry models: the cracks are reduced, corner separation does not occur, roof does not collapse. But the cracking in the piers of walls, below the lintel band, still occur.

Raghunath et al. (2000) have carried out studies on the ductility of brick masonry walls with containment reinforcement. Containment reinforcement consists of thin ductile wires provided on both faces of masonry wall, held together with the help of lateral ties provided through the bed joints. Characterization of static and dynamic behavior of unreinforced masonry and masonry provided with containment reinforcement is done. Initially unreinforced masonry walls were tested to obtain their strength and elastic properties. Later, brick masonry units provided with containment reinforcement, were tested to obtain moment-curvature relationships. Containment reinforcement has not only increased ductility but has also resulted in increasing the ultimate moment capacity.

Jagadish et al. (2002) studied brick masonry buildings with containment reinforcement using shock table testing. Containment reinforcement is intended to control post-cracking deflections and impart flexural ductility to masonry walls. From test results on $1/6^{th}$ scaled models, it is observed that reserve energy capacity of the masonry building is vastly enhanced due to the presence of ductile 'containment reinforcement'.

Jagadish et al. (2003) studied the behaviour of brick masonry structures during the Bhuj earthquake of January 2001. They have reported that (i) higher bond strength improves the earthquake resistance of masonry (ii) use of lintel band, seems to introduce a rigid box-like behaviour in the upper portion of the buildings while the portions below the lintel bands cracked badly suggesting the need for more horizontal bands at different levels (iii) provision of corner reinforcement in corners and junctions, as suggested by IS 4326-1993, has to be properly bonded with the surrounding masonry possibly with dowels or keys to prevent separation.

According to them the horizontal bands might not be adequate in strengthening against out-of-plane flexure, especially for flexural cracks that run horizontally. They suggest 'containment reinforcement' to contain the flexural tensile cracks from growing. They have studied the effect of containment reinforcement for earthquake resistant masonry buildings. Observed damage patterns of masonry buildings reveals that out-of-plane flexural failure of walls is primarily responsible for collapse of masonry buildings during earthquakes. In order to prevent this kind of failure and to improve the ductility of masonry walls, reinforcement in the form of 'containment reinforcement' was provided. Laboratory studies on masonry building models with such reinforcement in addition to horizontal bands have shown significant improvement in flexural ductility and energy absorption capacity of masonry.

Bakhteri et al. (2004) numerically verified the results of experimental investigations on the effect of mortar joint thickness on compressive strength characteristics of axially loaded brick-mortar prisms. Micro-modeling with two different material assumptions was attempted. In one, both phases of the materials are replaced with an equivalent homogeneous material with derived elastic properties and the other treats the masonry as a composite material consisting of the brick and the mortar. Composite material model gave more accurate prediction of the stress distribution in the prisms and hence this

model is more appropriate than the homogeneous material model. FEM model with mechanical properties taken from the experimental study led to large discrepancies between experimental and FEM results, confirming that the properties of mortar inside the joints are different from the properties of mortar cubes. Even after correcting such material properties, there were differences between the experimental and numerical results. Therefore, to get the actual compressive design strength of brick masonry, the finite element analysis results had to be enhanced by a factor of 1.5.

Rao et al. (2004) have studied the behaviour of brick masonry buildings during earthquakes. They have reported the results of the dynamic analysis of typical Indian brick masonry buildings subjected to three different earthquake ground motions. Based on post earthquake field study and finite element analysis, they have concluded that out-of-plane flexural failure of walls is primarily responsible for collapse of masonry buildings during earthquake. In order to prevent out-of-plane flexural failure and to improve ductility of masonry walls they suggest 'containment reinforcement', the efficiency of which has been confirmed through laboratory studies conducted on scaled models.

Kasthurba et al. (2005b) carried out a detailed study of laterite building stones from four major quarries in widely scattered locations of Malabar region, Kerala. The compressive strength of laterite blocks were evaluated according to Indian standard specifications. According to this study, the strength values of laterites depend on the specimen size and its geometry. Also, the decrease in the size of cube specimens is accompanied by an increase in the compressive strength, as in concrete cubes. In the reported results, compressive strength of most of the specimens tested were below 3.5 MPa, which is the prescribed minimum for use in laterite stone masonry, as per IS 3620-1979. Since the local practitioners vouch for the good quality of these laterites from the local quarries, this study has suggested a relook into the codal provisions. It has also been suggested that

the strength evaluation of laterite be carried out on standard size blocks, used for masonry, like in the case of bricks and hollow blocks, instead of cubes.

Sarangapani et al. (2005) have investigated the influence of bond strength on masonry compressive strength, through an experimental program using local bricks and mortars. The elastic modulus of brick used was 15 times less than that of mortar. For a given mortar, an increase in bond strength resulted in an increase in compressive strength of masonry. It is suggested that the masonry prism compressive strength is more sensitive to brick-mortar bond strength than the compressive strength of the mortar.

Kasthurba et al. (2006) studied the weathering forms and properties of laterite building stones used in historic monuments of Western India. This study found that the deterioration of laterite masonry may be caused due to a variety of causes. They have identified dampness as a major factor which induces deterioration and hence protection from dampness would prolong the life of laterite monuments.

Murty et al. (2006) have studied the performance of structures in the Andaman and Nicobar Islands (India) during the December 2004 Great Sumatra Earthquake and Indian Ocean Tsunami. Several old masonry structures on the islands performed well during the earthquakes, thus revealing the high quality of masonry construction practice prevalent in India upto the first half of the twentieth century, whereas many comparatively newly constructed masonry buildings have collapsed due to out-of-plane instability of the slender walls and poor connection or no connection to the surrounding structural elements. The traditional wood houses constructed of locally available timber also had performed extremely well in response to ground shaking.

Saikia et al. (2006) have studied the effect of provision of RC bands on the dynamic behaviour of masonry buildings. Stress analysis of typical masonry buildings, with and without RC bands, under lateral static and dynamic loads have been discussed. The

natural frequencies and mode shapes of buildings with and without bands have been presented. They have concluded that although reinforced concrete bands enhance the structural integrity by contributing to the connectivity of walls, they are not adequate in preventing out-of-plane collapse of some segments of wall. Need to develop simple methods of providing vertical reinforcement in these regions has been stressed.

Gumaste et al. (2007) studied the properties of brick masonry using table-moulded and wire-cut bricks of India with various types of mortars. The strength and elastic modulus of brick masonry under compression were evaluated for stiff-brick/soft-mortar and soft–brick/stiff-mortar combinations. Both prisms and wallettes were studied. In western countries, brick masonry generally consists of bricks which are strong and stiff compared to the mortar adopted. Such bricks are found to have compressive strengths in the range of 15-150 MPa and elastic moduli anywhere between 3500 and 34000 MPa. On the contrary, bricks of India show relatively lower strengths (3-20 MPa) and elastic moduli (300-15000 MPa). The state of stress developed in brick and mortar components of masonry depends on their relative elastic properties. When bricks are relatively softer than mortar, if the brick-mortar interface bond remains intact until the failure of masonry, the brick will be under triaxial compression and mortar will be under uniaxial compression and bilateral tension. In such a scenario, the failure of masonry is initiated by the tensile splitting of the mortar in the joint. The mortar failure will then extend to the brick causing masonry failure. Other possible mechanisms mentioned are:

1. if the brick-mortar interface fails in shear due to loss of bond, the lateral compression in the brick will vanish and the brick will fail by tensile splitting.
2. if one of the brick is relatively very weak (due to large coefficient of variation), it can also fail by crushing ahead of the splitting failure of other bricks.
3. in the case of masonry walls, mortar in the vertical joint can cause splitting failure in the brick below, since the stress in the mortar is much higher because of its greater stiffness.

Kasthurba et al. (2007) investigated laterite stones used for building purposes by testing laterites from widely located quarries within Malabar region, Kerala. There is a wide variation in the experimental results of compressive strength (1.3 MPa - 4.3 MPa) of commercially available, machine-cut laterites from Malabar region. According to their study, laterite stones show a wide variation in their engineering properties depending on the geographic location of the quarry and within a quarry, with depth. It was noted that specific gravity and compressive strength decrease with depth whereas water absorption increases with depth, which results in a decline in quality of laterite blocks of the deeper layers. Again, from a comparison of wet and dry strengths, it is observed that there is a significant reduction in strength (47-75%) due to saturation. Hence, it is suggested that laterite masonry is to be protected from dampness. Also it was observed that, laterite stones with dark reddish brown to red colour, taken from top portion of the profile, generally possess better strength, higher specific gravity and lower water absorption and hence are good for building purposes.

Kaushik et al. (2007a) observed from experimental results that the modulus of elasticity of brick masonry varied between 250 and 1100 times the prism strength of masonry. The compressive strength of masonry was found to increase with the compressive strength of bricks and mortar. This trend was more prominent in case of masonry constructed with weaker mortar.

Kaushik et al. (2007b) studied stress-strain characteristics of clay brick masonry under uniaxial compression. Using linear regression analysis, a simple analytical model has been proposed for obtaining the stress-strain curves for the masonry. During compression of masonry prisms constructed with stronger and stiffer bricks, mortar of the bed joints are in triaxial compression and the bricks are in bilateral tension coupled with axial compression. Modulus of elasticity of brick, mortar and masonry are given in terms of their compressive strength.

Das (2008) has undertaken decay diagnosis of Goan laterite monuments with the Basilica of Bon Jesus, India, as a case study, along with a combination of field and laboratory tests on freshly quarried stones. Most of the defects in the monument have been found to be because of water ingress. Goan laterite was found to be weak in compression and flexure even compared to standard brick. Hence the durability of masonry was attributed to water tightness rather than strength.

Reddy et al. (2009) studied the influence of bed-joint thickness and elastic properties of the soil-cement blocks and the mortar on the strength and deformation behavior of soil-cement block masonry prisms. Masonry compressive strength was found to be sensitive to the ratio of modulus of block to that of the mortar (E_b/E_m) and masonry compressive strength decreases as the mortar joint thickness is increased for the case where the ratio of block to mortar modulus is more than 1. Again the lateral tensile stresses developed in the masonry unit are sensitive to the E_b/E_m ratio and the Poisson's ratios of mortar and the masonry units.

Vyas and Reddy (2010) have developed a three dimensional non-linear finite element model based on micro-modeling approach to predict masonry prism compressive strength and crack pattern of solid block masonry. The FE model uses multi-linear stress-strain relationships to model the non-linear behaviour of solid masonry unit and the mortar. Masonry prism compressive strengths predicted by the proposed finite element model are about 19% less than the experimental values.

Sahin A. (2010) has developed a simple assistant program named ANSeismic, for implementing earthquake analyses of structures with ANSYS and SAP2000, finite element codes. Structural system is constructed in ANSYS by using GUI or APDL. The seismic records are loaded from PEER Strong Motion Database and earthquake analysis files are produced in ANSYS or SAP2000. The structural models constructed in ANSYS may be analyzed by just loading the analysis file developed with ANSeismic. SAP2000

time history source data file may also be produced with ANSeismic. ANSeismic program is free software and can be used as a tool in time history analysis of structures by researchers. It can be downloaded from MATLAB central. The flowchart developed to implement seismic analysis with ANSYS is presented in Fig. 2.1.

Existent literature reveals that most of the study on laterite is on the geological aspects. Though study on engineering properties of laterite is less, it is available. But study on laterite masonry is not available in literature. Studies on seismic response of brick masonry structures are available in literature but review of the existent literature shows that no research has been carried out on the seismic response of laterite masonry structures.

2.2 RESEARCH OBJECTIVES

The primary objectives of the present investigation are as follows:

1. To analyze laterite masonry prisms using finite element method.

2. To conduct a detailed free vibration analysis of box type laterite masonry structures for determining their natural frequencies and the mode shapes and to study the effect of various parameters on such free vibration response.

3. To find the response characteristics of box type laterite masonry structures subjected to typical ground accelerations and to study the effect of 'containment reinforcement' on such seismic response characteristics.
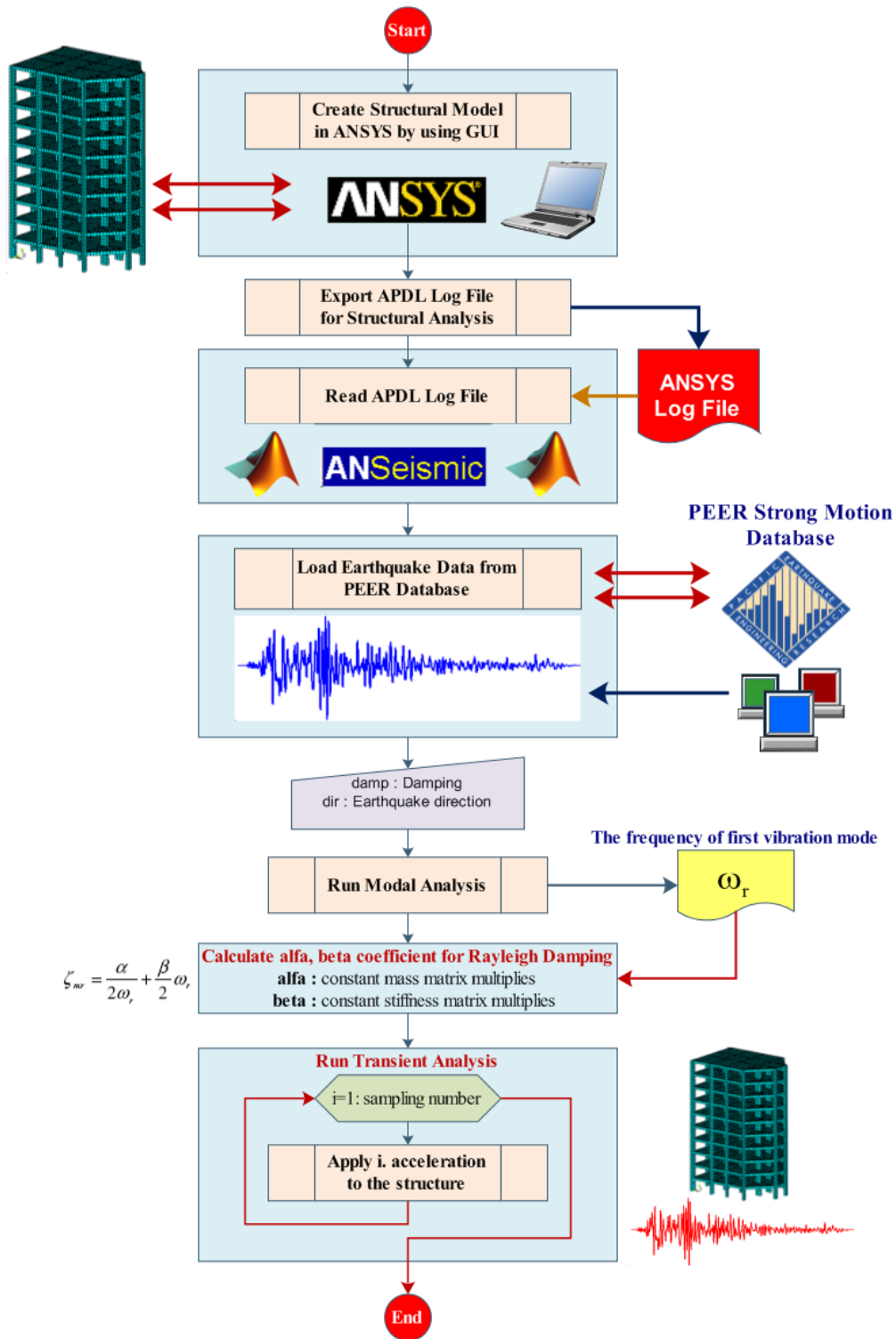
Fig. 2.1 Flowchart for time-history analysis using ANSeismic (Sahin 2010)

CHAPTER 3

CHARACTERIZATION OF LATERITE MASONRY

3.1 INTRODUCTION

Laterite is well known in Asian countries as a conventional building material. Laterite stone blocks are being used as masonry material for housing construction in western coastal areas of India, for ages. In India, Laterites are found in the states of Goa, Kerala, Karnataka, Maharashtra, Tamil Nadu, Andhra Pradesh, Bihar, Assam, Meghalaya and Orissa [IS 3620-1979]. In spite of widespread use of laterite in buildings, no systematic research study has been undertaken on this material, on its engineering properties, particularly on the strength and durability aspects [Kasturba 2005a].

The strength and elastic properties of laterite masonry are influenced by the individual properties of laterite blocks and mortar used and the nature of bond between them. Hence characterization of laterite block, mortar and laterite masonry prisms was attempted using detailed laboratory experiments.

3.2 EXPERIMENTAL INVESTIGATIONS

Experiments were conducted in accordance with IS codes in order to find the following:

- compressive strength, modulus of elasticity, water absorption and specific gravity of laterite stones
- compressive strength and modulus of elasticity of cement mortar specimens
- compressive strength and modulus of elasticity of laterite masonry prisms
- shear strength of laterite masonry triplets

3.2.1 Compressive Strength of Laterite Stone Blocks

The compressive strength of a masonry unit may be defined as the maximum stress to which the unit can be subjected by a gradually increasing compressive load applied perpendicular either to the bedding plane or normal position [Agarwal and Shrikhande 2007]. Compressive strength of laterite blocks, as per guidelines of Indian standard codes IS 3620-1979 and IS 1121(Part 1)-1974, is to be determined by testing 50mm cubes. But it is difficult to cut laterite blocks into 50 mm cubes. Moreover, generally larger laterite blocks are used in masonry construction and hence, laterite blocks of such sizes as used in masonry were tested in this study. Laterite blocks, from three different quarries of Mangalore region of Karnataka state, were tested. As prescribed in the code, the two faces of the laterite blocks were capped using rich cement mortar. Before testing, the blocks were immersed in water for 72 hours and tested in saturated condition. The blocks were subjected to gradually increasing axial compressive loading in a compression testing machine. Fig. 3.1 and Fig. 3.2 show a laterite block capped with cement mortar and the failure pattern, observed after testing the block in compression, respectively. The test results are shown in Table 3.1.

Fig. 3.1 Laterite block capped with cement mortar for compression test

Fig. 3.2 Failure pattern in laterite under compression

As observed by Kasturba et al. (2007), there can be large variations in the compressive strengths of laterites from one quarry to those of another. In the present investigation, the average compressive strength of laterite blocks varied from 2.06 MPa to 4.58 MPa. The

minimum compressive strength specified for laterites for use in masonry, by IS: 3620-1979 is 3.5 MPa. It is to be noted that the compressive strength reported in this study is for blocks of size as used in construction, whereas minimum strength prescribed by IS: 3620-1979 is for 50mm laterite blocks. In case of masonry materials, a decrease in specimen size is normally accompanied with an increase in the compressive strength [Kasturba 2005a].

Table 3.1 Compressive strength of laterite blocks

No.	Size (LxBxH) (All in mm)	Failure load (kN)	Compressive strength (MPa)
Quarry 1			
1	360x230x170	400	4.83
2	370x220x160	330	4.05
3	360x220x170	350	4.42
4	360x220x160	400	5.05
Average			**4.58**
Quarry 2			
1	360x230x160	200	2.4
2	370x230x160	240	2.8
3	375x215x170	210	2.6
4	370x220x160	220	2.7
Average			**2.63**
Quarry 3			
1	360x220x180	180	2.27
2	355x215x200	150	1.97
3	360x230x190	150	1.81
4	365x225x210	180	2.19
Average			**2.06**

The compressive strengths of commercially available machine cut laterites from Malabar region are in the range 1.3-4.5 MPa [Kasturba et al. 2006]. Manu et al. (2009) have reported that laterite blocks used in masonry construction in most parts of Ghana, generally have, compressive strengths in the range of 3.1 MPa to 17.2 MPa. Thus it can be said that, the values of compressive strength of laterite blocks tested herein are comparable to values reported by other investigators.

3.2.2 Modulus of Elasticity of Laterite Stone Blocks

The modulus of elasticity of the individual unit is not generally determined and is therefore not specified in most of the codes. But an estimate of the value of modulus of elasticity is required in finite element modeling. The modulus of elasticity of the units may be obtained as secant modulus under compression, which is the slope of a line on the stress-strain curve, joining the origin to the point corresponding to 33% of the unit compressive strength [Agarwal and Shrikhande 2007].

An attempt was made in this study, to find the modulus of elasticity of laterite blocks. For testing of modulus of elasticity, blocks of size as used in construction practice, were selected from the 1st quarry, as they had a higher compressive strength. Six laterite blocks, each immersed in water for 72 hours, were tested in a compression testing machine in saturated condition. Strains were measured using a demec gauge of gauge length 100 mm and of accuracy 0.002 m/m [Fig. 3.3].

Fig. 3.3 Demec buttons glued on laterite blocks

Results were plotted using the stress strain data noted. The stress-strain variations for blocks with minimum and maximum moduli are as shown in Fig. 3.4. Secant modulus calculated at 30% of ultimate stress, was considered as the modulus of elasticity of the block which varied from 749 MPa to 1240 MPa.
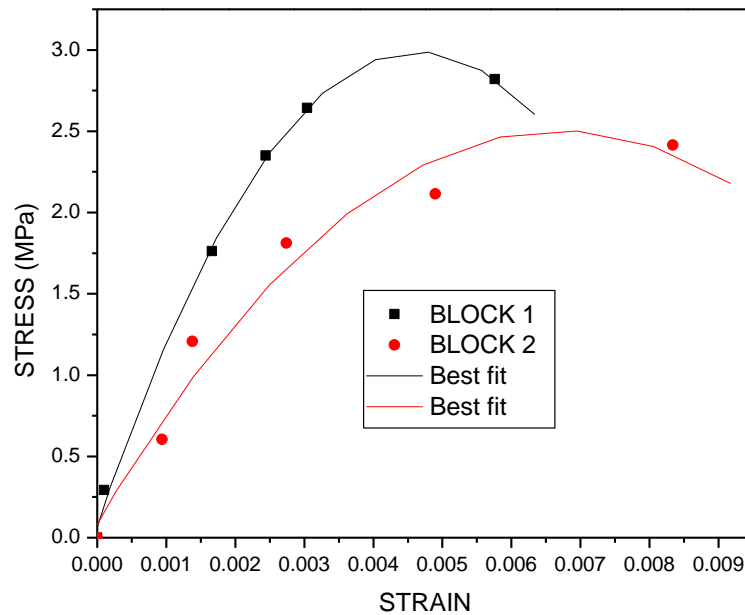
Fig. 3.4 Stress-strain relations for laterite blocks

3.2.3 Water Absorption & Specific Gravity of Laterite

Water absorption and specific gravity were determined as per IS 1124-1974 as suggested by IS Code for laterite stone masonry IS 3620-1979. Laterite stone was crushed and the material passing 20mm IS sieve and retained on 10mm IS sieve was used for the test. Fig. 3.5 shows sample of test specimen. The test sample weighing about 1 kg was washed to remove particles of dust and immersed in water at room temperature for 24 hours. The vessel was then emptied and the test sample allowed to drain. The surface dried sample was weighed (B). The sample was then carefully introduced in a 1000 ml capacity measuring cylinder and water was poured, until the level of water in the cylinder reaches 1000ml mark. The quantity of water thus added was recorded (C).

The water in the cylinder was drained and the sample was taken out and dried in an oven at 100 to 110^0C for 24 hours. It was then cooled in a desiccator to room temperature and weighed (A). Test results are shown in Table 3.2.

Apparent specific gravity = A/ (1000 − C)

where

A = weight of oven-dry test sample in gm.

C = quantity of water added in 1000 ml jar containing the sample in gm.

Water absorption = [(B − A) /A] x 100

where

A = weight of oven-dry sample in gm.

B = weight of saturated surface-dry sample in gm.

Fig. 3.5 Laterite sample for water absorption & specific gravity

Table 3.2 Water absorption and specific gravity of laterite

No.	Weight of oven-dry sample (A)	Weight of saturated surface-dry sample (B)	Quantity of water added in 1000 ml jar containing the sample (C)	Water absorption [(B – A) /A] x 100	Specific gravity A/(1000 – C)
1	953 gm	1062 gm	500 ml	11.44	1.91
2	965 gm	1071 gm	500 ml	10.98	1.93
3	973 gm	1086 gm	495 ml	11.61	1.93
	Average			**11.34**	**1.92**

As per the limits specified by IS Code for laterite stone masonry IS 3620-1979, specific gravity of laterite should not be less than 2.5 and water absorption should be less than 12% by mass. Specific gravity was obtained as 1.92, which is less than 2.5 specified by code. Water absorption was obtained as 11.34% which is within the limit of 12% specified in code.

3.2.3 Compressive Strength of Cement Mortar Cubes

Generally, 1:6 cement mortar is used for laterite masonry construction, in south-west coastal areas of India. Hence this type of cement mortar was selected for this study. Ordinary Portland cement (43 grade) and river sand were used for the preparation of the mortar mixes.

Compressive strength of mortar depends on the water cement ratio and the cement content. Code specifies quantity of water as that required for working consistency. Working consistency of a mortar is usually judged by the mason during its application. Water should be enough to maintain the fluidity of the mortar during application, but at the same time it shall not be excessive [IS: 2250-1981]. In this study water-cement ratio of mortar specimen was maintained at 0.8.

Compressive strength of the mortar was determined by testing 70mm cubes, according to IS: 2250-1981. The results obtained during compression tests of mortar cubes are shown in Table 3.3. In the present investigation, the average 28-day compressive strength of 1:6 cement mortar cubes with water-cement ratio 0.8 was obtained as 7.33 MPa and the average density as 2179 kg/m^3.

Table 3.3 Compressive strength of cement mortar cube

No.	Weight (gm)	Density (kg/m^3)	Load at failure (kN)	Compressive strength (MPa)	Average compressive strength (MPa)
1	756	2204	40	8.0	
2	752	2192	40	8.0	
3	710	2070	40	8.0	7.33
4	756	2204	40	8.0	
5	761	2218	30	6.0	
6	751	2190	30	6.0	

Sarangapani et al. (2005) have reported compressive strength of similar cubes with water-cement ratio 0.8 as 7.32 MPa. Kaushik et al. (2007b) have reported 28-day compressive strength of 1:6 cement mortars with water-cement ratio 0.7 to 0.8 as 3.1 MPa. Gumaste et al. (2007) have reported 28-day compressive strength of 1:6 cement mortar cubes (70 mm) with water-cement ratio of 1.1 as 6.6 MPa and 28-day compressive strength of 150 mm x 150 mm x 300 mm prisms as 5.14 MPa. Pradhan et al. (2009) have reported ultimate strength of 1:6 cement mortar with 0.7 water-cement ratio as 4.06 MPa. Thus it is seen that large variations exist between the compressive strength of mortars depending on mix proportions, water-cement ratio, age, size and shape of the specimens.

3.2.4 Modulus of Elasticity of Cement Mortar

Mortar cylinders of size 150 mm diameter and 300 mm length were cast using ordinary Portland cement-43 grade and river sand in the ratio 1:6 and with water-cement ratio 0.8. After keeping them immersed in water for 28 days, they were taken out and tested in saturated surface-dry condition in a compression testing machine. Modulus of elasticity

was determined by applying a gradually increasing axial compressive load to the mortar cylinder and measuring the compression at different load levels. A compressometer with gauge length of 200 mm was fixed on to the mortar cylinder to measure the axial compression and hence the strain. With the help of these readings, stress-strain graphs were plotted as shown in Fig. 3.6. Modulus of elasticity was calculated from the stress strain curves by measuring the slope of secant at 25% of ultimate stress as 2879 MPa. For finite element modeling of laterite masonry further in this study, a reference value of 3000 MPa was taken for modulus of elasticity of mortar.
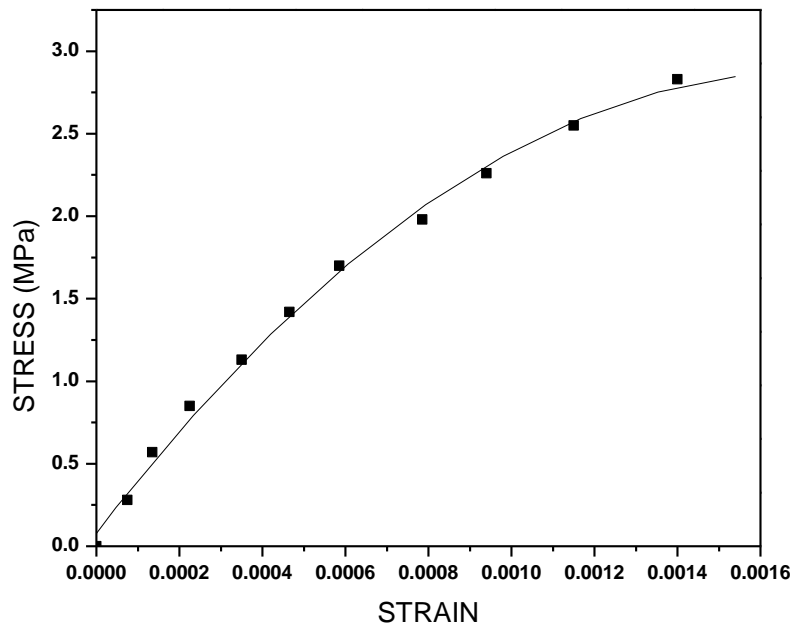
Fig. 3.6 Stress-strain curve of cement mortar

Sarangapani et al. (2005) have reported secant modulus at 25% of ultimate stress of 1:6 cement mortar with water-cement ratio of 0.8 as 5766 MPa, while Gumaste et al. (2007) have reported such modulus with water-cement ratio 1.1 as 8568 MPa, both using 150 mm x 150 mm x 300 mm prisms. Kaushik et al. (2007b) have reported average secant modulus considering the chord joining ordinates at 5% and 33% of ultimate stress, of 1:6

cement mortar with water-cement ratio of 0.7 to 0.8 as 545 MPa. Pradhan et al. (2009) have reported modulus of elasticity of similar mortar with water-cement ratio of 0.7 as 2616 MPa. Thus literature reveals a wide variation in modulus of elasticity for cement mortar specimen [545 MPa to 8568 MPa], depending on size and shape of the specimens, water-cement ratio and the way in which the modulus of elasticity is calculated.

3.2.5 Testing of Laterite Masonry Prisms

IS:1905-1987 recommends two methods for finding the compressive strength of masonry:

      (1) using a table of masonry strength based on strength of block and mortar

      (2) testing stack bonded prisms.

There is no universal, rational procedure for prism testing to determine compressive strength that is representative of masonry structures [Hamid and Chukwunenye 1986]. Compressive strength of laterite masonry was determined by testing stack-bonded prisms as per guidelines of IS: 1905-1987.

Laterite blocks from 3 quarries were tested for compressive strength and the best quality ones, i.e., from the 1st quarry, were selected for prism testing. Five-block high, stack-bonded, laterite masonry prisms were cast using laterite blocks of size 360 mm x 220 mm x 170 mm in 1:6 cement mortar. Six prisms as shown in Fig. 3.7 were cast. Ordinary Portland cement (43 grade) and river sand were used for the preparation of mortar mixes. Joint thicknesses were maintained at 10mm as recommended in SP 20-1991.

The prisms were capped with the same mortar in order to get a level surface. A steel plate of 10 mm thickness was kept on top of the prism to distribute the load. The prisms were cured for periods of 7-days and 28-days by covering them using wet gunny bags. The prisms were tested in wet condition. Three prisms were tested after 7 days and the remaining three after 28 days. Demec buttons were glued to the masonry surface on the front face of the prism in order to measure the strains. An axial compressive load was applied through a hydraulic jack and the same was measured with a proving ring.

Fig. 3.7 Laterite masonry prisms cast for testing

Table 3.4 gives the compressive strength of the prisms tested and Fig. 3.8 shows the typical failure patterns.

Table 3.4 Compressive strength of laterite masonry prisms

No.	Age (days)	h/t	Size (LxBxH) All dimensions in mm	Load at failure (kN)	Compressive strength (MPa)
1		3.955	360 x 220 x 870	92.31	1.17
2	7	3.82	360 x 220 x 840	100.00	1.26
3		3.48	370 x 230 x 800	53.85	0.63*
4		3.82	360 x 220 x 840	92.31	1.17
5	28	3.77	360 x 220 x 830	107.69	1.36
6		3.82	360 x 220 x 840	100.00	1.26

* failure of the prism occurred at an early stage

Fig. 3.8 Failure of stack-bonded laterite masonry prisms

Masonry prisms were tested 7 days and 28 days after casting. Average compressive strength of laterite prisms tested was 1.24 MPa and the ratio of compressive strength of masonry prism to that of laterite block 0.27. It can be seen that significant strength improvement was not observed due to extension of curing from 7 days to 28 days. This could be because laterite is weaker than mortar and the failure of prism occurred by the failure of laterite blocks.

It was observed that for compressive load acting normal to bed joints, the failure primarily occurred by vertical tensile splitting of the blocks. Even though the block compressive strength is lower than the mortar compressive strength, with the compressive strength of prism being much lower than the compressive strength of the laterite blocks, failure was not due to crushing of the blocks. Uniaxial compressive testing of laterite masonry prism has shown bond failure along with splitting of blocks, in all the prisms tested herein.

Gumaste et al. (2007) have studied the bond strength of bricks of modulus of 500 MPa with 1:6 cement mortar and have reported that failure of prism is by bond failure. The failure of masonry is initiated by the tensile splitting of the mortar in the joint, if the brick mortar bond is intact. The mortar failure will then extend to the brick causing masonry failure. On the other hand, if the brick-mortar interface fails in shear due to loss of bond, the lateral compression in the bricks will vanish and the bricks will fail by tensile splitting. Bond between mortar and masonry unit is thus more important, in this case, than compressive strength of mortar.

During the testing of laterite masonry prisms under axial compression, strains were also measured, normal to bed joints, using demec gauge, of gauge length 100mm. Using the stress-strain data obtained, graphs were plotted. Typical stress strain curves for laterite masonry prisms are shown in Fig. 3.9. Secant modulus at 25% of ultimate stress was calculated as the modulus of elasticity of laterite masonry. In this study, the elastic moduli of laterite masonry prisms varied from 447 MPa to 1168 MPa.
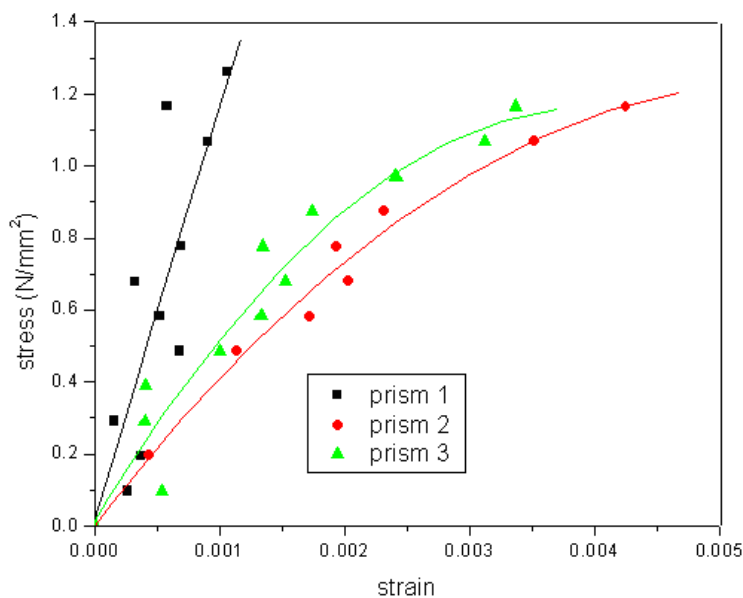
Fig. 3.9 Stress strain curves of laterite masonry prisms

3.2.6 Shear Bond Strength of Laterite Masonry

Shear bond strength of laterite mortar joints was determined for laterite blocks joined with cement mortar. Laterite masonry triplets were cast as per scheme A and scheme B, shown in Fig. 3.10.

(a) Scheme A   **(b) Scheme B**
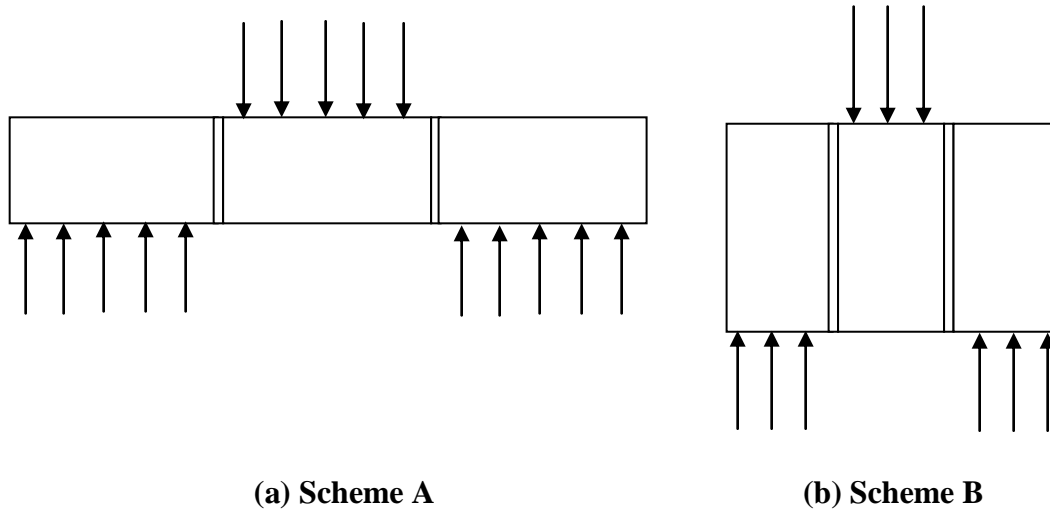
Fig. 3.10 Pattern of laterite masonry triplets cast for testing shear bond strength

Three triplet specimens were cast as shown in Fig. 3.11, using laterite blocks of size 360 mm x 220 mm x 170 mm in 1:6 cement mortar. Ordinary Portland cement (43 grade) and river sand were used for the preparation of mortar mixes. Mortar joint thickness of 10mm was maintained. Triplets were cured for 28 days by covering them with wet gunny bags. Direct shear load was applied on the middle laterite block in the triplet. The other two blocks were restrained. A steel plate of 10 mm thickness was kept on top of the central block and load was applied through a hydraulic jack and was measured with a proving ring. Load was gradually increased on the central laterite block till the bond between laterite block and mortar joint failed. Shear bond strength was calculated based on the failure load. Shear bond strength was calculated from the formula

$$\sigma_v = P_v/2A \tag{3.1}$$

where σ_v is the shear bond strength, P_v is the failure load

A is the sectional area across laterite/mortar joint

The shear bond strength values are given in Table 3.5. Fig. 3.12 shows the typical failure patterns of laterite triplets tested. In all the three cases, failure was observed to be due to joint failure.

Fig. 3.11 Laterite masonry triplets cast for testing (scheme A)

Table 3.5 Shear bond strength of laterite masonry triplets (scheme A)

No.	Load at failure (N)	Shear bond strength (MPa)
1	7000	0.093
2	6370	0.085
3	5120	0.068
Average shear bond strength		**0.082**

Fig. 3.12 Shear bond failure of laterite masonry triplets (scheme A)

Shear bond strength of laterite masonry was also determined from triplet specimens cast as shown in Fig. 3.13. Ordinary Portland cement (43 grade) and river sand were used for the preparation of mortar mixes (1:6 cement mortar). Mortar joint thickness of 10mm was maintained. Triplets were cured for 7days by covering them with wet gunny bags. The middle block was free to move vertically, whereas the other two blocks were restrained to move in the vertical direction. Vertical shear load was gradually applied on the middle block using the hydraulic jack till the bond between laterite block and mortar joint failed and the bond strength was calculated from the equation 3.1.

The shear bond strength values are given in Table 3.6. Fig. 3.14 shows the typical failure patterns of laterite triplets tested. In all the three cases, failure was observed to be due to joint failure.

Fig. 3.13 Laterite masonry triplets (scheme B)

Table 3.6 Shear bond strength of laterite masonry triplets (scheme B)

No.	Load at failure (N)	Shear bond strength (MPa)
1	7650	0.097
2	6400	0.081
3	8900	0.112
Average shear bond strength		**0.097**

Fig. 3.14 Shear bond failure of laterite masonry triplets (scheme B)

3.3 FINITE ELEMENT ANALYSIS OF LATERITE MASONRY PRISMS

Depending on the level of accuracy and the computational effort required, the numerical analysis of masonry can be performed by following two different approaches: the micro-modeling and the macro-modeling. In micro-modeling approach, the difference in mechanical behavior of block and mortar is taken into account by adopting suitable constitutive laws for each component. On the other hand, when large real structures have to be studied in order to capture their global response, macro-modeling is a more effective option. Within such an approach, masonry is regarded as an equivalent material, where mortar and blocks are melted together and appropriate relations are established between averaged masonry strains and averaged masonry stresses [Berto et al. 2005].

Micro-modeling approach is best suited to analyse the real behaviour of masonry particularly concerning the local response of the masonry unit, joint and unit/mortar interface. Such modeling yields accurate results, but requires intensive computational effort [Vyas and Reddy 2010]. This method is suitable for modeling of masonry prisms and hence was used in the present study.

A five blocks-high stack-bonded laterite masonry prism was modeled using micro modeling approach with ANSYS software. The prism size of 360 mm x 220 mm x

41

890mm, made up of 5 laterite blocks of size 360 mm x 220 mm x 170 mm and 4 mortar joints of 360 mm x 220 mm x 10 mm, was considered. The blocks and joints were meshed using SOLID45 elements, available in ANSYS. SOLID45 element is defined by 8 nodes having three degrees of freedom at each node: translations in the nodal x, y and z directions. The element geometry is shown in Fig.3.15 [ANSYS Version 10].
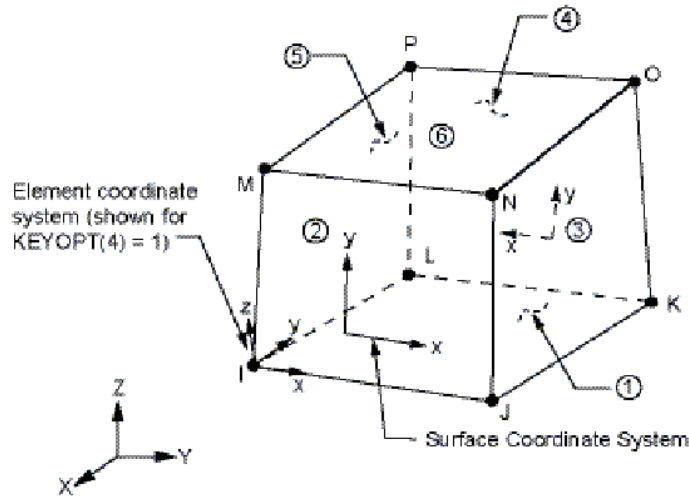
Fig. 3.15 SOLID45 Element

A linear elastic analysis was carried out to understand the nature and distribution of stresses in the laterite block and mortar joint. Modulus of elasticity of laterite and mortar determined experimentally were given as input in the analysis. Poisson's ratios of laterite and mortar were assumed. The blocks and the joints were modeled by micro-modeling approach, assuming a perfect bond between them. With the data sets employed, analyses results shows that under uniaxial compressive load, laterite blocks are in triaxial compression and mortar joints are in uniaxial compression and bilateral tension as shown in Fig. 3.16. There being a difference in stiffness between the two materials, i.e., laterite and mortar, for strain compatibility at the interface, with a good bonding between the two materials, the stiff mortar will try to pull the soft laterite inwards. In the event of bond failure at the brick-mortar interface, the horizontal compression induced by the shear stresses will vanish and the brick will fail by lateral tension [Sarangapani 2005].
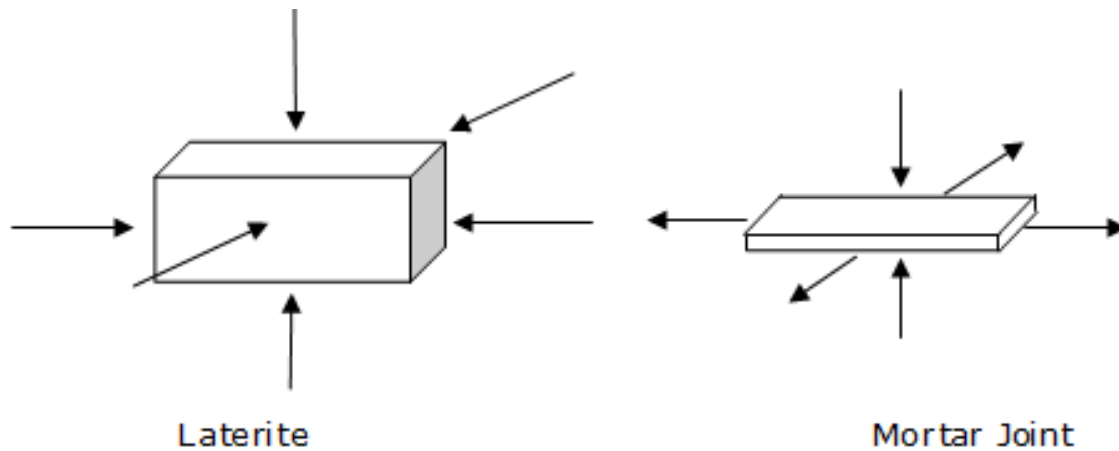
**Fig. 3.16 State of stresses in laterite block and mortar joint in a
laterite masonry prism under uniaxial compression**

Literature review shows a large variation in the values of elastic modulus of 1:6 cement mortars, even in the Indian context [545 MPa to 8568 MPa]. Even in the present investigation, an average value of 2879 MPa was obtained for the mortar. These values of modulus of elasticity were used as an input in the finite element model. Incorporating such large variation in values of modulus of elasticity of mortar will definitely have an effect on the results of finite element analysis. Hence an extensive parametric study is required to understand the effect of this parameter on the state of stresses in the laterite masonry prism and possible prediction of failure. Studies have shown that, more than the individual values of modulus of elasticity of the block and the mortar; it is the ratio of modulus of elasticity of the block to that of the mortar which plays a major role in the distribution of stresses within the masonry prism [Felix 1999].

3.4 PARAMETRIC STUDIES

In order to understand the influence of different factors on the laterite masonry prism strength, it was analyzed by varying certain parameters. For all the analyses, a representative pressure of 2 MPa was applied on the top surface of the laterite masonry prism. The parameters used in this parametric study were Poisson's ratios of laterite and mortar, the moduli of elasticity of laterite and mortar and the thickness of the mortar

joint. When one parameter was varied, all other parameters were kept unchanged. Table 3.7 gives the reference values and range of values of these different parameters considered. It is difficult to do such a study experimentally. Moreover, the stress distribution, patterns in both the mortar and the blocks would also be available from the analyses results.

Table 3.7 Reference values and range of parameters

No.	Parameter	Reference value	Range
1	Poisson's ratio of laterite (υ_{lt})	0.15	0.15, 0.2
2	Poisson's ratio of mortar (υ_{m})	0.15	0.1, 0.15
3	Modulus of elasticity of laterite (E_{lt}), MPa	1300	300, 750, 1300
4	Modulus of elasticity of mortar (E_{m}), MPa	3000	3000, 6000
5	Thickness of mortar (t_{m}), mm	10	10, 20

3.4.1 Poisson's Ratios of Laterite and Mortar

Poisson's ratios of the masonry unit and the mortar are normally neither tested for nor reported in the traditional compression testing of the masonry prisms. But they are important in computer simulation as they influence the lateral expansion of the masonry unit and the mortar under compressive loading [Felix 1999]. The effects of varying the Poisson's ratios of laterite block and mortar on the stress distribution of an axially loaded laterite masonry prism was investigated and the results plotted.

In the first analysis, moduli of elasticity of laterite and mortar were taken as 1300 MPa and 3000 MPa respectively and the Poisson's ratios of both laterite and mortar as 0.15. The thickness of mortar joints was taken as 10mm. Fig. 3.17a shows the maximum principal stress (lateral tensile) in mortar joint, for a vertical applied pressure of 2 MPa on the laterite masonry prism, as 381713 N/m^2 (0.382 MPa). Fig. 3.17b shows the

corresponding value as 0.607 MPa when the Poisson's ratio of laterite was changed to 0.2, without changing the other parameters. Thus when, only the Poisson's ratio of laterite was increased from 0.15 to 0.2, there was an increase in maximum principal stress (lateral tensile) in mortar by 59%. In this case, the maximum lateral compressive stress in laterite blocks was observed to have increased by 45%.

When the prism is subjected to vertical loading, the masonry units and the mortar will expand laterally at different rates due to their different moduli of elasticity even if their Poisson's ratio is the same [Felix 1999]. If Poisson's ratio of laterite is increased, the difference in the rate of lateral expansion is further increased, causing an increase in tensile stress in mortar. This might reduce the compressive strength of prism.

Fig. 3.17a shows the maximum principal stress (lateral tensile) in mortar as 0.382 MPa, when the Poisson's ratio of mortar was kept at 0.15. Fig. 3.17c shows the corresponding stress in mortar as 0.465 MPa when the Poisson's ratio of mortar was decreased to 0.1, without changing the other parameters. Thus it can be observed that when only the Poisson's ratio of mortar was decreased from 0.15 to 0.1, there was an increase in maximum principal stress (lateral tensile) in mortar by 22%. However, in this case, there is no significant change in the maximum lateral compressive stresses in the laterite blocks.

If the Poisson's ratio of laterite was increased or that of mortar was decreased, it resulted in an increase in lateral tensile stresses in mortar, which in turn would result in reduction of prism compressive strength. Such an increase in lateral stresses was observed to be more when the Poisson's ratio of laterite was increased. The larger the difference between the Poisson's ratios of the block and the mortar, lower the compressive strength of the prism.
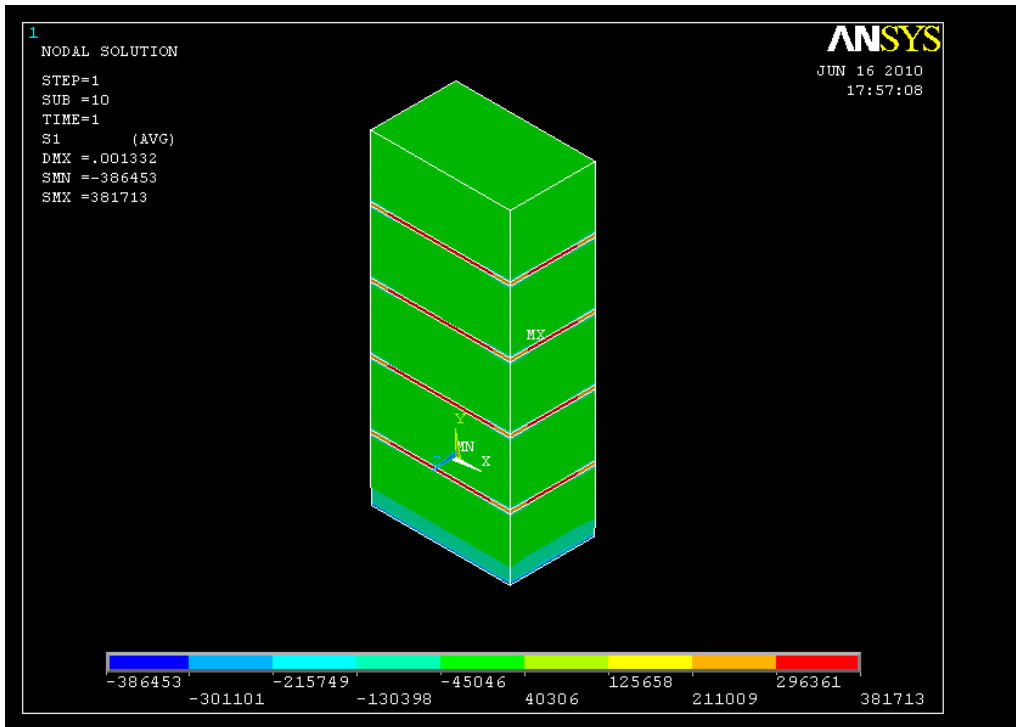
Fig. 3.17a Stress distribution of principal stress σ_1 (N/m^2) (reference case)
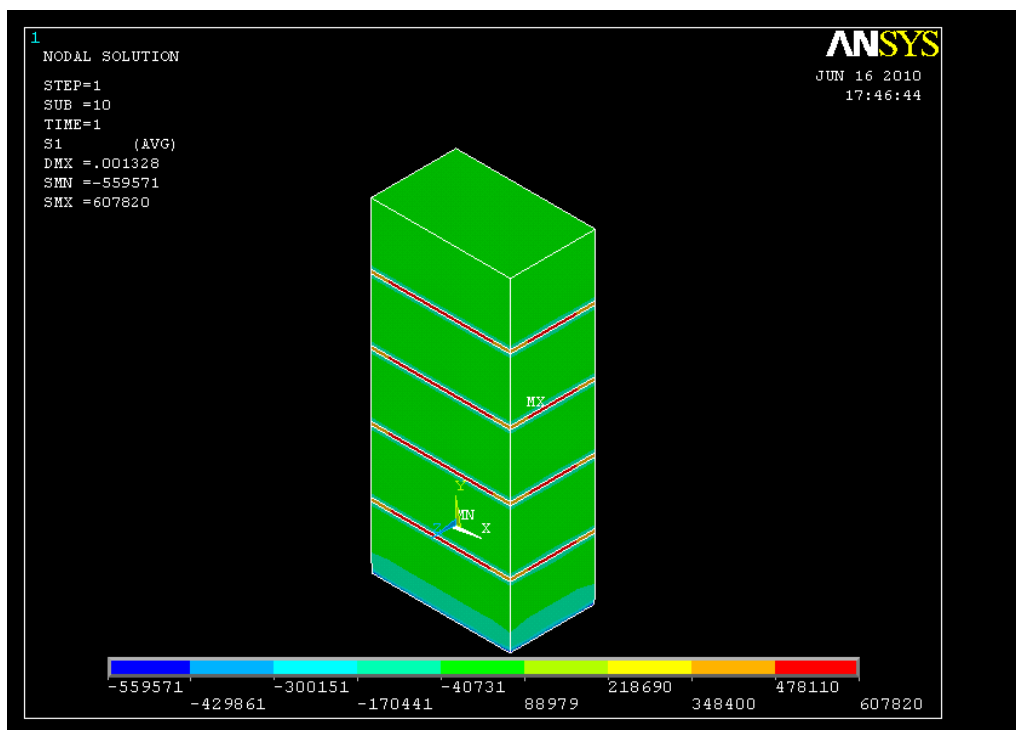
Fig. 3.17b Effect of change in Poisson's ratio of laterite on distribution of principal stress σ_1 (N/m^2) (ν_{lt}=0.2)
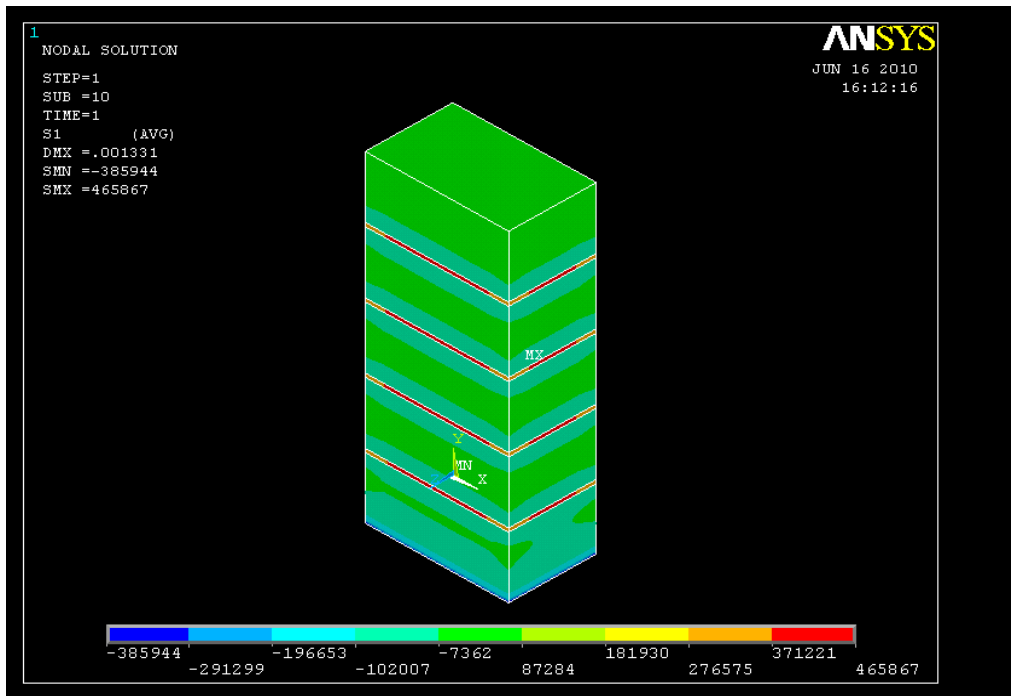
Fig. 3.17c Effect of change in Poisson's ratio of mortar on distribution of principal stress σ_1 (N/m^2) (ν_m=0.1)

3.4.2 Modulus of Elasticity of Laterite and Mortar

Laterite masonry prism was analyzed, keeping the modulus of elasticity of mortar at a reference value of 3000 MPa and varying the modulus of elasticity of laterite. Representative values of 300 MPa, 750 MPa and 1300 MPa were considered for the same. In all the cases, Poisson's ratios of both laterite and mortar were taken as 0.15 and thickness of the mortar joints was kept constant as 10 mm. Fig.3.17a shows the distribution of nodal principal stress σ_1 for the reference case with modulus of elasticity of laterite assumed as 1300 MPa. Fig.3.18a and Fig.3.18b show the corresponding results when the modulus of elasticity of laterite was changed to 750 MPa and 300 MPa respectively.

When modulus of elasticity of laterite was reduced from 1300 MPa to 750 MPa, maximum lateral tensile stress in mortar was observed to have increased from 0.382 MPa to 0.78 MPa. The increase was more than 100 percent. When modulus of elasticity of

laterite was further reduced to 300 MPa, maximum lateral tensile stress in mortar was observed to have further increased to 1.71 MPa, an increase by as much as 4.5 times as compared to the case of E_{lt} = 1300 MPa.
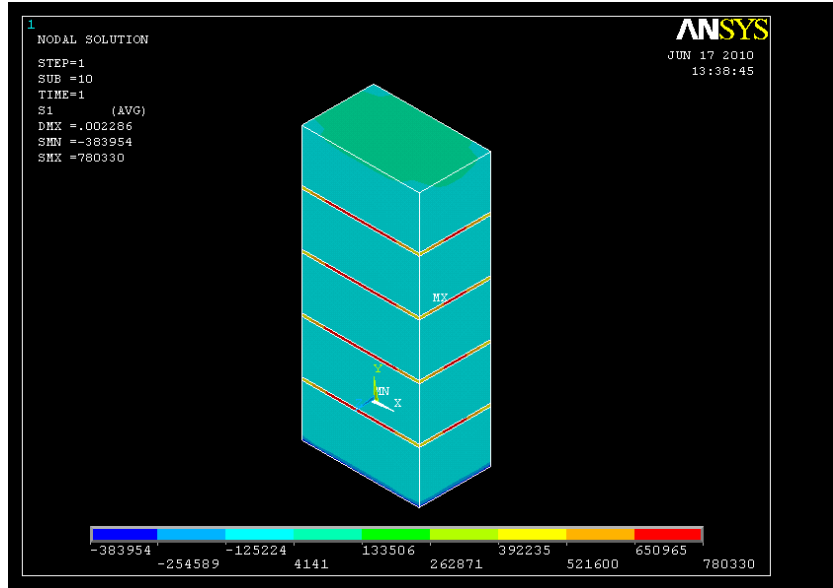
Fig. 3.18a Effect of change in modulus of elasticity of laterite on distribution of principal stress σ_1 (N/m^2) (E_{lt}=750MPa)
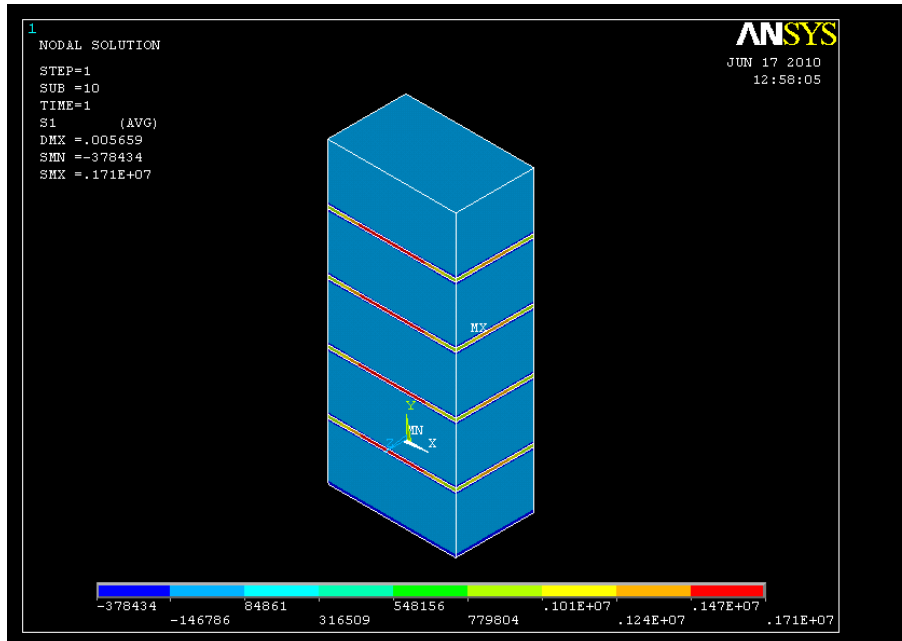
Fig. 3.18b Effect of change in modulus of elasticity of laterite on distribution of principal stress σ_1 (N/m^2) (E_{lt}=300MPa)

Laterite masonry prism was also analyzed keeping the modulus of elasticity of laterite at a reference value of 1300 MPa, and varying the modulus of elasticity of mortar to 3000 MPa and 6000 MPa. The Poisson's ratios of both laterite and mortar were taken as 0.15 and thickness of the mortar joints as 10mm. Fig. 3.17a shows the plot of nodal principal stress σ_1 for modulus of elasticity of mortar, 3000 MPa. Fig. 3.19 shows the corresponding plot when modulus of elasticity of mortar was increased to 6000 MPa. Comparing, it can be observed that when modulus of elasticity of mortar was increased from 3000 MPa to 6000 MPa, without changing any of the other parameters, maximum lateral tensile stress in mortar has increased from 0.382 MPa to 0.905 MPa, the increase being about 2.4 times.
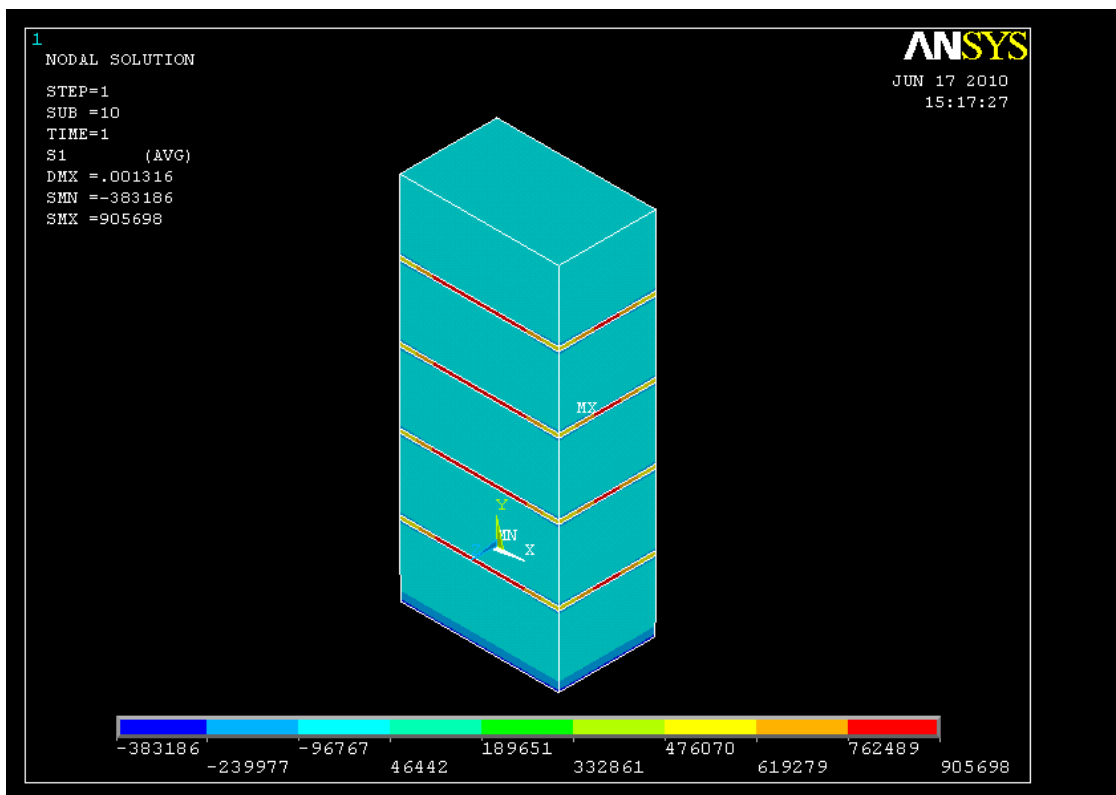
Fig. 3.19 Effect of variation of modulus of elasticity of mortar on distribution of principal stress σ_1 (N/m^2) (E$_m$=6000MPa)

49

The results show that, for a constant modulus of elasticity of mortar, lower the modulus of elasticity of laterite, higher are the tensile stresses in mortar. Similarly, for a constant modulus of elasticity of laterite, higher the moduli of elasticity of mortar, higher are the tensile stresses in mortar. This proves that the ratio of elastic modulus of laterite block to that of mortar is more significant than the individual values of the elastic moduli. As the ratio of modulus of elasticity of laterite block to modulus of elasticity of mortar reduces (only $E_{lt} < E_m$ considered), there is an increase in the lateral tensile stresses in the mortar.

3.4.3 Mortar Joint Thickness

In order to study the effect of thickness of mortar joint, a parametric study was conducted by varying the thickness of mortar joint, keeping the other parameters a constant. In this case, modulus of elasticity of laterite and mortar were taken as 1300 MPa and 3000 MPa respectively, and Poisson's ratios of laterite and mortar as 0.15. Fig. 3.17a shows nodal principal stresses σ_1 for a joint thickness of 10 mm and Fig. 3.20 shows the corresponding case for a joint thickness of 20mm.
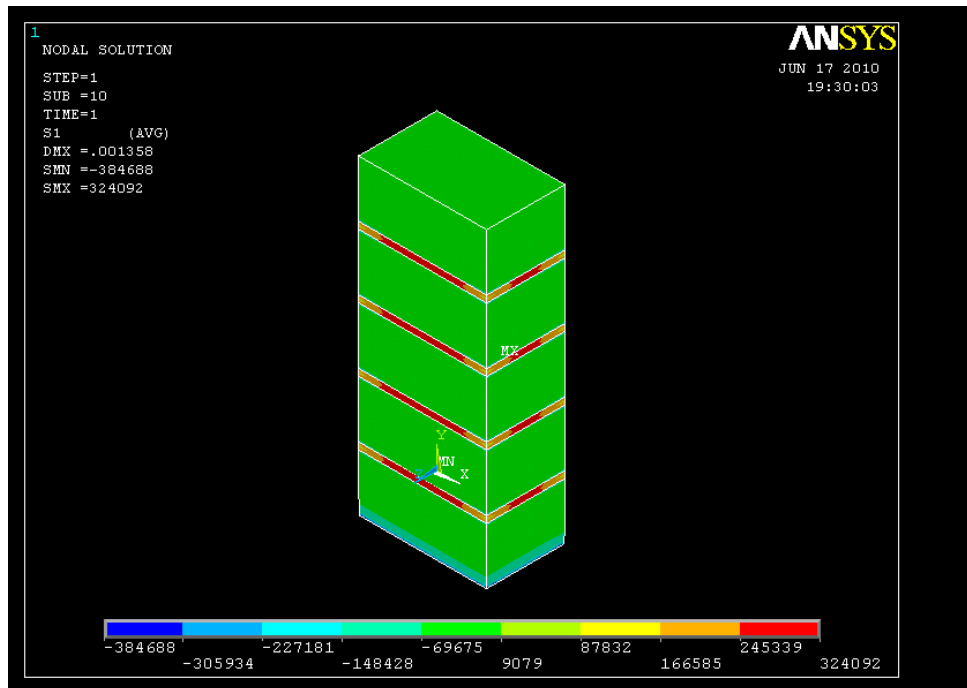
**Fig. 3.20 Effect of variation of thickness of mortar on distribution
of principal stress σ_1 (N/m^2) (t$_m$=20mm)**

In the first case the maximum lateral tensile stress in mortar was observed as 0.382 MPa and in the second case 0.324 MPa. Thus as the thickness of mortar joint was increased from 10 mm to 20 mm the lateral tensile stresses in mortar has reduced by 15%. If the modulus or strength of brick/block is less than that of the mortar, then increase in joint thickness leads to increased masonry prism compressive strength [Rao et al. 1995, Reddy et al. 2009].

3.5 CONCLUSIONS

Experimental investigations were carried out on the strength characteristics of laterite blocks, cement mortar specimens and stack-bonded laterite masonry prisms under uniaxial compression. Parametric studies were also conducted using finite element analyses on laterite masonry prisms. Based on the results of all these studies, the following conclusions are made:

1. When laterite blocks of sizes used in practice were tested, the compressive strengths obtained were much lower than the strengths of the standard-sized mortar cubes tested. Hence laterite masonry tested herein can be classified under weak unit-strong mortar masonry.

2. Average modulus of elasticity of laterite blocks tested was found to be less than that of mortar used in making the laterite masonry; hence, laterite masonry tested herein can be classified as soft unit-stiff mortar masonry.

3. Laterite masonry prisms were observed to have failed by bond failure and subsequent splitting of laterite blocks.

4. Based on analytical results obtained herein, in laterite masonry prisms subjected to uniaxial vertical pressure, the laterite blocks were observed to be in triaxial compression and the mortar joints in uniaxial compression and bilateral tension.

5. A value of Poisson's ratios of the materials used is one of the factors in deciding strength-deformation behavior of laterite masonry prisms. As seen from analytical results, either an increase in Poisson's ratio of laterite blocks or a decrease in Poisson's ratio of the mortar, without changing the other parameters, results in increase in lateral stresses in the mortar joint. This in turn will result in reduction of compressive strength of laterite masonry prism. Lateral stresses in mortar joint are more sensitive to the increase in Poisson's ratio of the laterite blocks than the decrease in Poisson's ratio of the mortar joint.

6. Reduction in the modulus of elasticity of laterite blocks or an increase in the modulus of elasticity of mortar, results in increase in the lateral tensile stresses in mortar joint, in the laterite masonry prism, at a given vertical pressure. As the ratio of modulus of elasticity of laterite block to modulus of elasticity of mortar is reduced (only $E_{lt}/E_m < 1$ considered), there is an increase in the lateral tensile stresses in the mortar.

7. Increase in thickness of mortar joint, results in a decrease in lateral tensile stresses in mortar joint, indicating higher prism strength, if bond remains intact.

8. Prism strength will improve with higher ratio of elastic modulus of laterite and mortar (only $E_{lt}/E_m < 1$ considered) and lower Poisson's ratio of laterite blocks.

CHAPTER 4

NATURAL FREQUENCIES OF BOX TYPE LATERITE MASONRY STRUCTURES

4.1 INTRODUCTION

Laterite masonry is most commonly used in south-west coastal areas of India for the construction of single and two storeyed buildings. Laterite masonry walls are also used in framed structures, as infill panels. Most of the single storeyed laterite structures in southwest coastal areas of India are generally box-type structures.

A load-bearing wall structure without a space frame, in which the horizontal forces are resisted by the walls acting as shear walls, forms a box system. This type of construction may consist of a prefabricated or in-situ masonry, concrete or reinforced concrete wall along both the axes of the building. The walls support vertical loads and also act as shear walls for horizontal loads acting in their own planes. The traditional Indian masonry construction falls under this category [IS 4326-1993].

The forces caused in a structure when an earthquake ground motion passes underneath depend on its own dynamic characteristics, particularly the following:

1. Mass and stiffness distribution: The natural periods, mode shapes and mode participation factors are derived for the structure in the elastic range. The fundamental period T_0 of natural vibrations is crucial in determining the earthquake forces for design.

2. Energy dissipation property: When a structure is vibrated, it dissipates a good amount of the input dynamic energy through its elements, the supports and the foundation and the vibrations get damped. Larger is the damping, less forces are developed.

3. Inelastic energy dissipation: Besides the energy dissipation during the elastic range, well designed ductile structures can dissipate large amount of energy beyond yield deformation. But brittle structures do not have this capacity except through friction which develops after their cracking. Therefore, for earthquake safety against collapse, proper reinforcing of the masonry with steel is considered crucial [BMTPC 2000].

The forces attracted by a structure during an earthquake are dynamic in nature and are functions of ground motion and the properties of the structure itself [SP 22-1982]. The response of the building, within its elastic limit, is mainly dependent on both the frequencies of the ground motion and the natural frequencies and mode shapes of the building. Such a response is magnified when the predominant frequency of the earthquake spectrum is close to the natural frequency of the structure. It is hence essential to obtain the natural frequencies and mode shapes of buildings in order to understand their response to earthquake induced ground motions [Raghunath 2003].

No external forcing functions are involved in a free vibration problem and the natural frequencies and mode shapes are direct functions of the stiffness and mass distribution in the structure. Mode shape is the shape assumed by the body while vibrating with any one of the natural frequencies in order that the inertia forces cancel out elastic stiffness forces. Finite element (FE) analysis is a convenient tool to obtain natural frequencies and mode shapes. There are many advantages in using a FE model, such as ease in modeling the openings in a wall, accommodating different material properties, visualizing the mode shapes etc. [Raghunath 2003].

In south-west coastal areas of India, laterite box type structures are constructed either with light roofing components such as tiled roof or with rigid roofing components such as RCC slab. Light roofing components generally rest loosely on the walls. Such buildings, with light roofs and low rigidity can almost be idealized as a building without roof

[Raghunath 2003]. In the present work, single storeyed box type laterite masonry structures with and without roof were analyzed for their free vibration response. This chapter presents a study of the frequencies and mode shapes of single storeyed box type laterite masonry structures determined using finite element method.

4.2 FE MODELING OF BOX TYPE LATERITE MASONRY STRUCTURES

4.2.1 General

Box type laterite masonry structures were modeled in ANSYS (Version 10). The dimensions of the buildings analyzed were 6m x 3m x 3m (L x B x H). Buildings were provided with openings in accordance with IS 4326:1993 with one door (of size 1.0m x 2.1m) and one window (of size 1.0m x 0.9m) on one longer wall and two windows on the other longer wall. Each of the short walls was provided with one central window opening. Consistent mass matrix formulation was used for the entire model. The walls of the building were assumed to be fixed at their bases all along their lengths. Vertical reinforcement or 'containment reinforcement' was provided on the surface of the walls on both the faces at a spacing of 1m.

Laterite masonry structures were meshed using three-dimensional solid elements (SOLID45) of dimension 0.20 x 0.20 x 0.23 m^3. SOLID45 element is defined by 8 corner nodes having three degrees of freedom at each of these nodes - the translations in the nodal x, y and z directions.

While masonry is quite often modeled with orthotropic material properties, in the present study, it was assumed to be isotropic and values of the modulus of elasticity of laterite masonry obtained from experimental results were made use of. Table 4.1 gives the properties of masonry, RCC and reinforcement bars used in the finite element analysis.

Table 4.1 Material properties used in the FE analysis

Property	Laterite masonry in 1:6 cement mortar	Reinforced concrete	Vertical reinforcement (steel)
Modulus of Elasticity (GPa)	1.2	25	200
Poisson's Ratio (assumed)	0.15	0.15	0.3
Mass Density (kg/m^3)	2500	2500	7850

Eight types of single storeyed box type laterite masonry structures of similar geometry, as given in Table 4.2, were selected for the analyses:

Table 4.2 Types of single storeyed box type laterite masonry structures analyzed

No.	Type	Description of the Structure
1	A	Unreinforced laterite masonry structure without roof
2	AV	Laterite masonry structure without roof and with containment reinforcement
3	ALR	Laterite masonry structure without roof, with lintel band and roof band
4	ALRV	Laterite masonry structure without roof, with lintel band, roof band and containment reinforcement
5	B	Unreinforced laterite masonry structure with roof
6	BV	Laterite masonry structure with roof and containment reinforcement
7	BL	Laterite masonry structure with roof and lintel band
8	BLV	Laterite masonry structure with roof, lintel band and containment reinforcement

Configurations of the eight types of structures analyzed are shown in Figures 4.1 and 4.2.
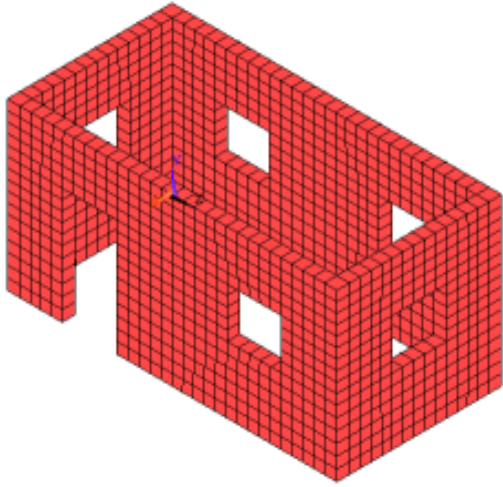
(a) Type A
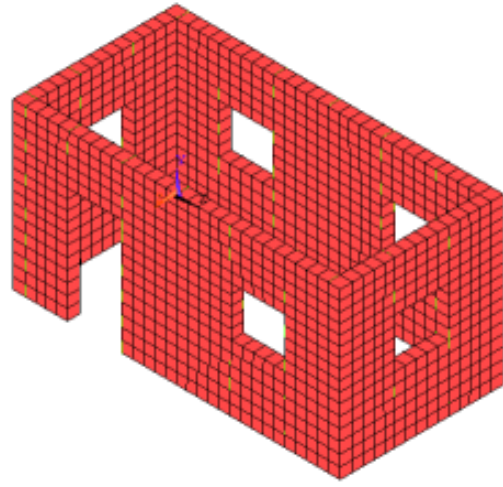
(b) Type AV
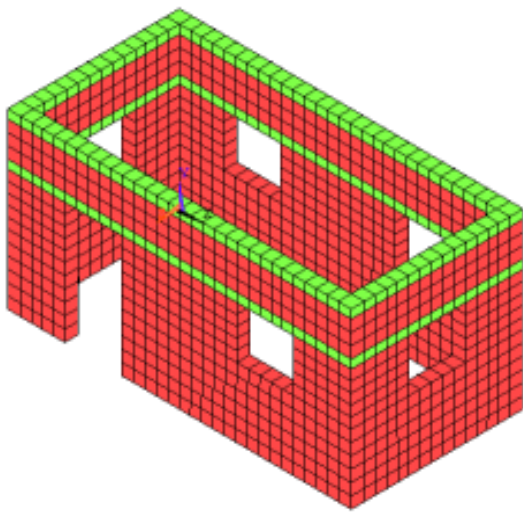
(c) Type ALR
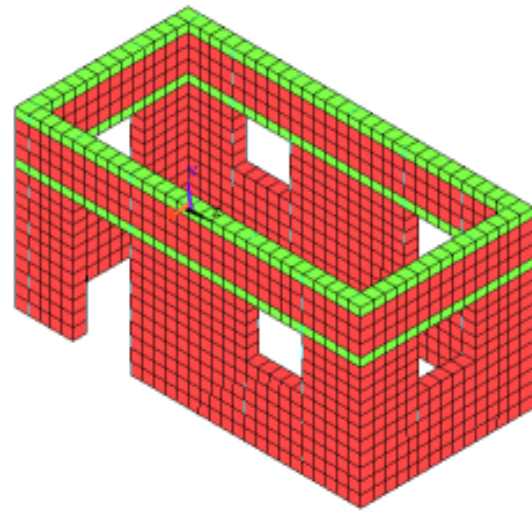
(d) Type ALRV

Fig. 4.1 Configurations of box-type laterite masonry structures without roof
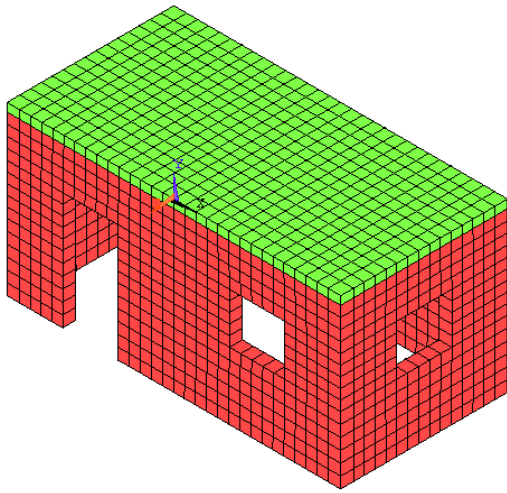
(a) Type B
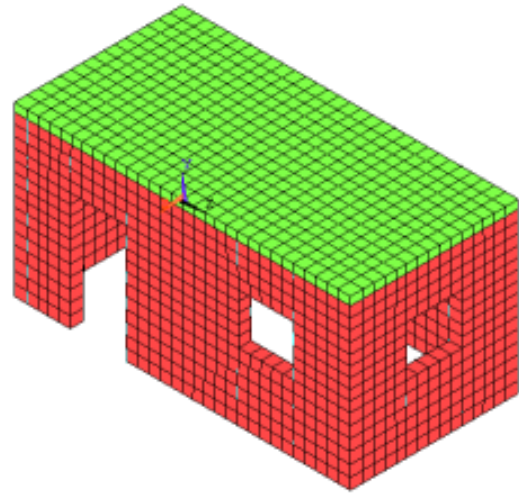
(b) Type BV
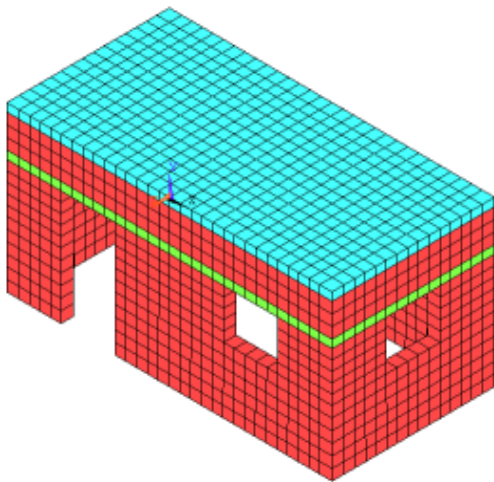
(c) Type BL
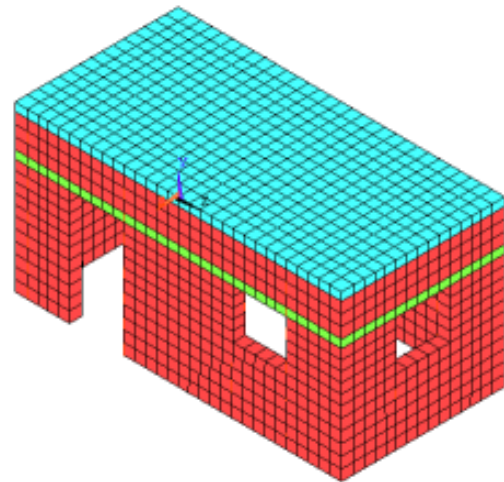
(d) Type BLV

Fig. 4.2 Configurations of box-type laterite masonry structures with roof

4.2.2 Finite Element Modeling of Vertical Reinforcement

A wall subjected to lateral out of plane forces behaves as a plate, bending in two directions. The bending in the vertical direction (normal-to-bed-joints) causes horizontal cracks, while the bending in the other direction (parallel-to-bed-joints) causes vertical cracks. Horizontal bands are provided to prevent the growth of vertical and diagonal cracks in masonry elements apart from acting as a beam at the openings. The growth of horizontal cracks can be prevented by the provision of vertical reinforcement along the height of the wall. Structurally it is more efficient if the vertical reinforcement is provided at the surface of walls where flexural strains are higher [Raghunath 2003].

Embedding vertical reinforcement bars at the edges of the wall piers and anchoring them in the foundation at the bottom and in the roof band at the top, enhances the capability of wall piers, to resist horizontal earthquake forces and delay the X-cracking. Adequate cross-sectional area of these vertical bars prevents the bars from yielding in tension. Further, the vertical bars also help protect the wall from sliding as well as from collapsing in the weak direction. When a wall with an opening deforms during an earthquake shaking, the shape of the opening distorts and becomes more like a rhombus - two opposite corners move away and the other two come closer. Under this type of deformation, the corners that come closer develop cracks. Steel bars are provided in the wall masonry all around the openings to restrict these cracks at the corners [Murty 2005].

Three techniques to model steel reinforcement in finite element models for reinforced concrete have been discussed by Tavarez - the discrete model, the embedded model and the smeared model (Fig. 4.3).

In the discrete model (Fig. 4.3a), the reinforcement is modeled with bar or beam elements that are connected to concrete mesh nodes. Therefore, the concrete and the reinforcement mesh share the same nodes and concrete occupies the same regions occupied by the reinforcement. A drawback to this model is that the concrete mesh is restricted by the

59

location of the reinforcement and the volume of the steel reinforcement is not deducted from the concrete volume.
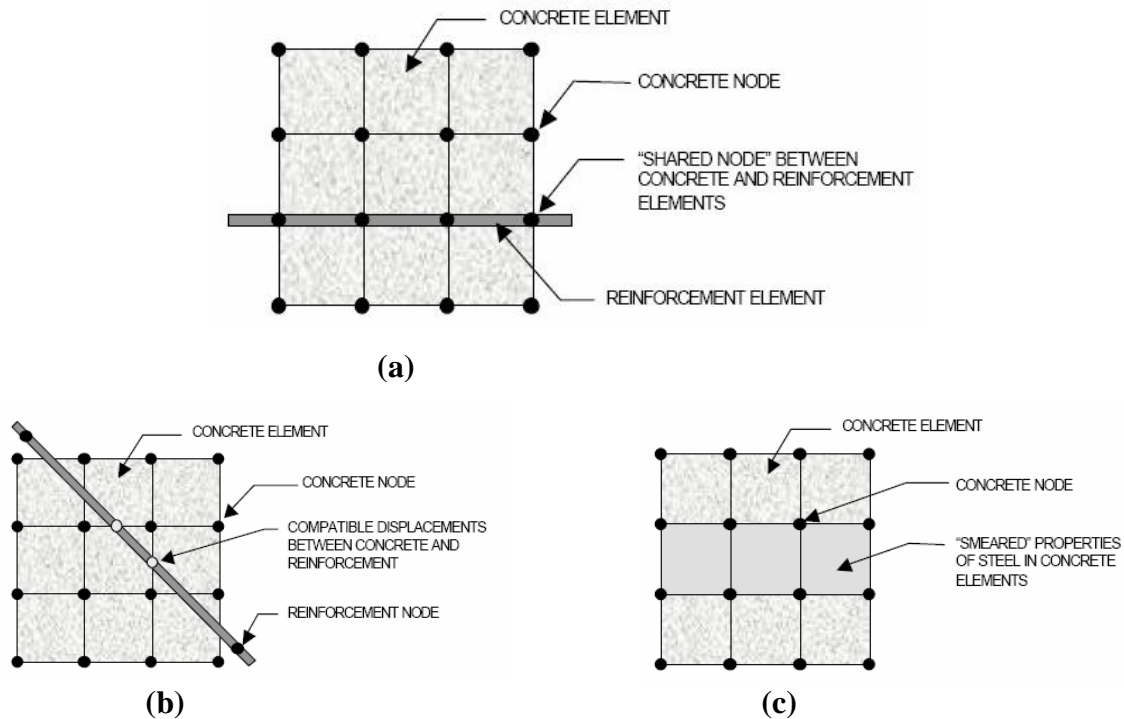
Fig. 4.3 Models for reinforcement in reinforced concrete (Tavarez 2001): (a)discrete (b)embedded (c)smeared

The embedded model (Fig. 4.3b) overcomes the concrete mesh restriction because the stiffness of the reinforcing steel is evaluated separately from that of the concrete elements. The model is built in a way that keeps reinforcing steel displacements compatible with the surrounding concrete elements. This model is usually used in connection with higher order elements. However, the additional nodes required for the reinforcement increase the number of degrees of freedom, and hence the run time.

In the smeared model (Fig. 4.3c), the reinforcement is assumed to be uniformly distributed over the concrete elements. The properties of the material model in the element are constructed from individual properties of concrete and reinforcement using

composite theory. This approach is used for large models where the reinforcement details are not essential to capture the overall response of the structure.

In this study the vertical reinforcing steel attached to the laterite masonry was modeled on similar lines as the discrete model given by Tavarez for RC elements.

The vertical reinforcements were modeled using truss elements (LINK8) of length 0.2 m. LINK8 element of the ANSYS library is a uniaxial tension-compression element with three degrees of freedom at each node: translations in the nodal x, y and z directions. The geometry of this element is shown in Fig. 4.4.
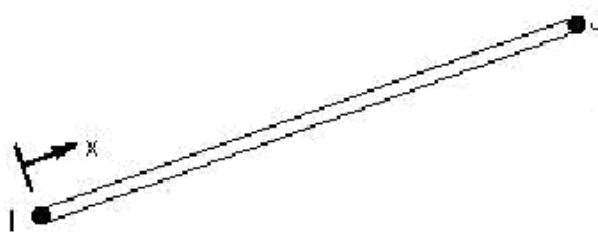
Fig. 4.4 LINK8 Element

Vertical reinforcements called containment reinforcement were provided at a horizontal spacing of 1m on both the faces of the walls, as shown in Fig. 4.5.

LINK8 elements were modeled through the nodes of the SOLID elements and hence meshing of the reinforcement was not required. However, the necessary mesh attributes had to be set before each section of the reinforcement was created [Wolanski 2004]. Separate entities that have the same location (LINK elements and SOLID elements) were merged. Care had to be taken to always merge in the order that the entities appear. All precautions were taken to ensure that all different entities were merged in the proper order. Also, the lowest number was retained during merging. It is assumed that there exists a perfect bond between reinforcement and masonry.
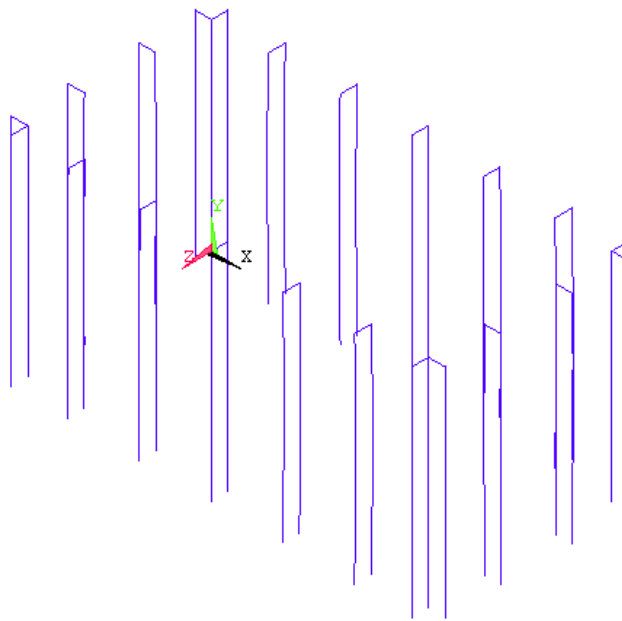
**Fig. 4.5 Configuration of containment reinforcement
in box type laterite masonry structures**

4.3 FREE VIBRATION STUDIES

The natural frequencies and mode shapes are important parameters in the design of a structure under any type of dynamic loads. The equation of motion for an undamped system, expressed in matrix notation, is

$$[M]\{\ddot{u}\} + [K]\{u\} = \{0\}$$
(4.1)

where [M] = mass matrix

[K] = stiffness matrix

{u}= displacement vector

$\{\ddot{u}\}$ = acceleration vector

For a linear system, free vibrations will be harmonic of the form

$$\{u\} = \{\varphi\}_i \cos\omega_i t$$
(4.2)

where $\{\varphi\}_i$ = eigen vector representing the mode shape of the ith natural frequency

ω_i = i[th] natural circular frequency (in radians per unit time)

and t = time

Hence equation (4.1) reduces to the form

$$(-\omega_i^2 [M] + [K]) \{\varphi\}_i = \{0\} \tag{4.3}$$

For a non-trivial solution $| [K] - \omega^2 [M] | = 0.$

This eigen-value problem can now be solved for up to N values of ω_i^2 and the corresponding eigen vectors $\{\varphi\}_i$ which satisfy equation 4.2, where N is the total number of DOFs. Many numerical methods like Block Lanczos, Subspace, Power Dynamics etc. are available in ANSYS. Block Lanczos eigenvalue method is accurate, fast and requires less disk space compared to other methods and hence this method was employed in the present study, for the extraction of the eigen-values and the eigen vectors.

4.3.1 Diameter of Containment Reinforcement

In order to determine the effect of the diameter of containment reinforcement, analyses were conducted on structures with vertical reinforcement of 6mm diameter and 12mm diameter. Three types of single storeyed box type laterite masonry structures of same geometry were selected for the analyses:

     (i)   Type A: unreinforced laterite masonry structure without roof

     (ii)   Type AV1:   laterite masonry structure without roof and with containment reinforcement made up of 6mm diameter bars

     (iii)   Type AV: laterite masonry structure without roof and with containment reinforcement made up of 12mm diameter bars

Free vibration analysis and equivalent static analysis were conducted on all the three types of buildings.

4.3.1.1 Free vibration analysis

Free vibration studies were conducted to find the natural frequencies and mode shapes of all the three types of buildings, the results of which are tabulated in Table 4.3.

Frequencies of Type AV1 (with 6 mm reinforcement) were observed to be slightly more than the frequencies of Type A (unreinforced). The maximum difference in frequencies was observed for a mode where bending is along the height-an increase of 5%. Except the 9th and the 10th mode, all the other mode shapes of Type A and AV1 were similar. In the 9th and 10th modes, a swapping of mode shapes was observed.

Frequencies of Type AV (with 12 mm reinforcement) was observed to be more than that of A and AV1. First 7 modes of building Type AV were similar to that of A. Swapping of mode shapes in the last three listed modes was observed. Maximum increase in frequency of building Type AV compared to A was observed as 18%, again for a mode where bending is along height. This shows that the containment reinforcement will reduce the bending along the height of box type laterite masonry structures without roof.

Table 4.3 Natural frequencies of buildings

Mode No.	Frequency (Hz) A	Frequency (Hz) AV1	Frequency (Hz) AV
1	5.465	5.578	5.872
2	5.853	5.962	6.241
3	11.461	11.543	11.735
4	12.619	12.753	13.033
5	15.792	15.875	16.041
6	17.994	18.179	18.502
7	18.804	19.249	19.976
8	20.035	21.076	22.370
9	20.730	21.476	23.591
10	21.067	21.708	24.125

4.3.1.2 Equivalent-static analysis

Low-rise masonry buildings are generally very stiff and hence undergo inertial type of response during earthquakes. The behaviour of such low-rise buildings can be understood rather easily by carrying out an equivalent-static analysis [Saikia et al. 2006].

Equivalent static analysis is the simplest method to determine a realistic seismic response. In this method, a set of static horizontal forces is applied to the structure. These forces are meant to emulate the maximum effects in a structure that a dynamic analysis would predict. This procedure works well when applied to small, simple structures and also to larger structures if they are regular in their layout [Anderson and Brzev 2009].

A rigorous response analysis of single storeyed box type laterite masonry structures would be the main focus of the present work, as detailed in the next chapter. Anticipating that an equivalent-static analysis of box type laterite masonry structures would prove useful in identifying the vulnerable regions of these structures, the same was attempted, initially.

The design horizontal seismic coefficient for masonry structure, calculated according to IS 1893 (Part 1) – 2002, was obtained as 0.45. Hence, a horizontal acceleration of 0.5g, perpendicular to long walls, was applied on the entire height of the building. Long walls of the laterite masonry buildings underwent a cantilever type of deflection. The maximum deflection was observed on the middle of the top edge in all the three types of buildings. Fig. 4.6 shows a comparison of lateral deflection along the height, at the center of long wall, in the buildings of Type A, AV1 and AV.
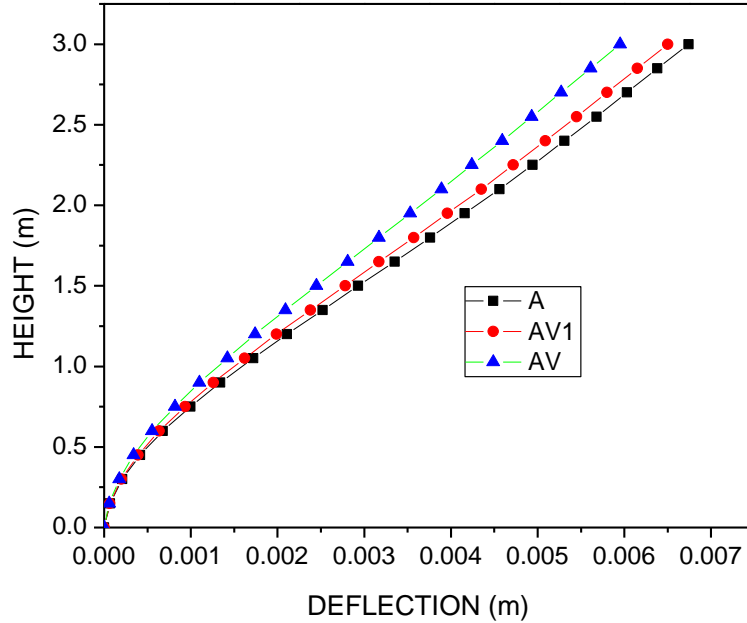
Fig. 4.6 Comparison of deflections u_z along the height, at the center of long wall

In Type A building, the maximum deflection was observed as 6.7 mm. This got reduced to 6.5 mm and 5.9 mm for the buildings of Type AV1 and Type AV respectively, a reduction of 3% and 12% from Type A. This trend of reduction of maximum deflections under same sets of loads suggests sufficient increase in the effective stiffness of the buildings with provision of containment reinforcement and is also in-line with observed increase in natural frequencies.

Again for the same structures under equivalent static analysis, the variation of stresses σ_y along the height at the center of long wall is shown in Fig. 4.7.
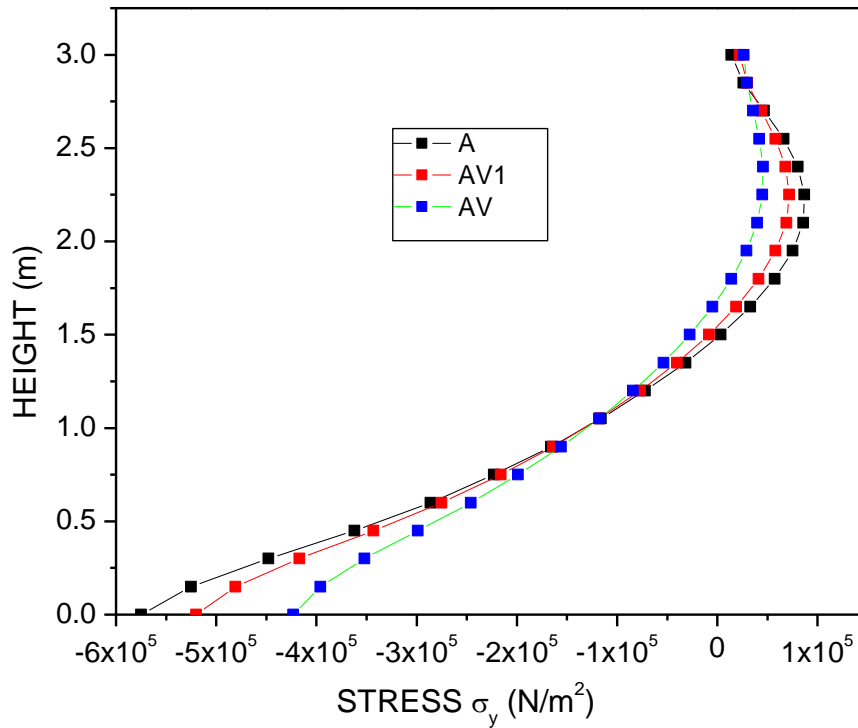
Fig. 4.7 Comparison of stresses σ_y along the height, at the center of long wall

The maximum stress (σ_y) was observed at the center of base of the long wall. The magnitude of such maximum stress σ_y was observed to have reduced from 0.575 MPa in Type A building to 0.52 MPa in Type AV1 building, a reduction of around 10%. In Type AV building the maximum stress σ_y was a low 0.423 MPa, which is 26% less compared to that of Type A building.

Fig. 4.8 shows the variation of stresses σ_x along the length at the top edge of long wall. The maximum value of stress σ_x was observed near the centre of the top edge of long wall. No significant reduction in stress σ_x was observed by reinforcing with 6 mm rods. However the magnitude of maximum stress σ_x was observed to have reduced from 0.353

MPa for Type A building to 0.303 MPa for Type AV building, which is a reduction of 14%.
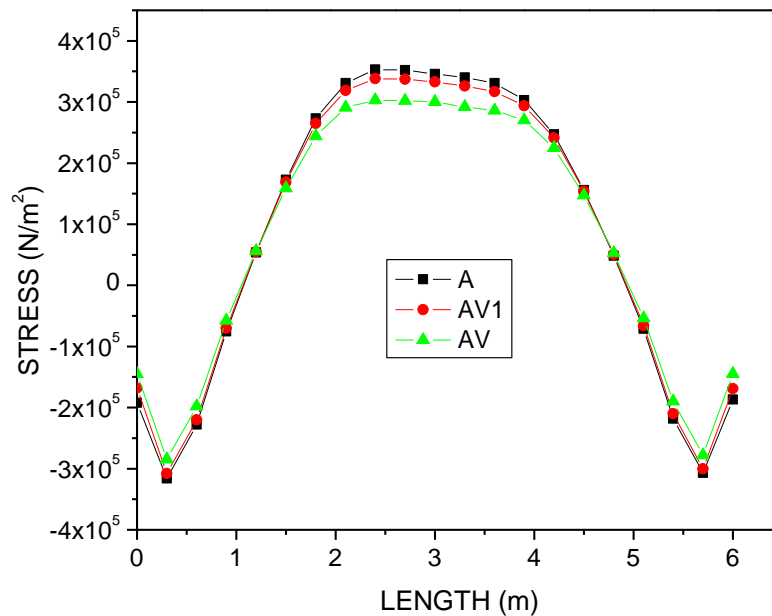
Fig.4.8 Comparison of stresses σ_x along the length at the top edge of long wall

For a lateral acceleration of 0.5g applied perpendicular to long wall, maximum out of plane deflection was observed at the center of top edge of long wall, in all the three type of buildings analyzed. With the introduction of vertical containment reinforcement there is a reduction in such out of plane deflections. The reduction in out of plane deflection depends on the area of cross section of bars. The reduction is quite small (maximum 3%) in case of reinforcing with 6mm bars and maximum 12% in case of reinforcing with 12mm bars. Comparison of stresses σ_x and σ_y for all the three cases shows that, by the introduction of containment reinforcement, the reduction in stresses σ_y is much more than the reduction in stresses σ_x. Containment reinforcement helps to reduce the vertical stresses developed in laterite masonry structures i.e., it helps to reduce bending of walls along the height. The reduction in stresses depends on the area of cross section of vertical reinforcement. The analytical results presented herein shows that 6mm diameter bars are

not very effective in reinforcing the single storeyed box type laterite masonry structures. Hence in the present study, in all further numerical work, 12mm steel bars were used for vertical containment reinforcement.

4.4 FREE VIBRATION OF BOX TYPE LATERITE MASONRY STRUCTURES

Eight types of single storeyed box type laterite masonry structures as given in Table 4.2 were analyzed to find the natural frequencies and mode shapes. The first ten natural frequencies of all the structures analysed are presented in Table 4.4 and Table 4.5.

Table 4.4 Natural frequencies of structures without roof

Mode No.	Freq (Hz) A	Freq (Hz) AV	Freq (Hz) ALR	Freq (Hz) ALRV
1	5.465	5.872	9.407	9.827
2	5.853	6.241	10.145	10.634
3	11.461	11.735	17.909	19.150
4	12.619	13.033	20.802	21.680
5	15.792	16.041	22.744	24.861
6	17.994	18.502	24.026	26.969
7	18.804	19.976	25.658	27.248
8	20.035	22.370	26.221	28.672
9	20.730	23.591	29.088	30.329
10	21.067	24.125	31.129	32.728

Table 4.5 Natural frequencies of structures with roof

Mode No.	Freq (Hz) B	Freq (Hz) BV	Freq (Hz) BL	Freq (Hz) BLV
1	11.953	12.888	12.551	13.508
2	17.945	19.222	18.962	20.223
3	19.420	22.097	20.629	23.245
4	21.859	22.997	23.067	24.162
5	22.328	25.915	23.671	27.213
6	27.883	31.313	31.180	34.438
7	29.172	32.400	31.676	34.754
8	30.051	33.509	33.506	37.124
9	31.180	34.537	34.624	38.083
10	33.207	36.112	37.480	40.950

The addition of containment reinforcement or RC band increases the stiffness of the structure and hence it results in an increase in the natural frequencies of the structure. This was observed both in the case of structures without roof and those with roof. Fig. 4.9 shows a comparison of first ten natural frequencies of all the eight types of structures analyzed.
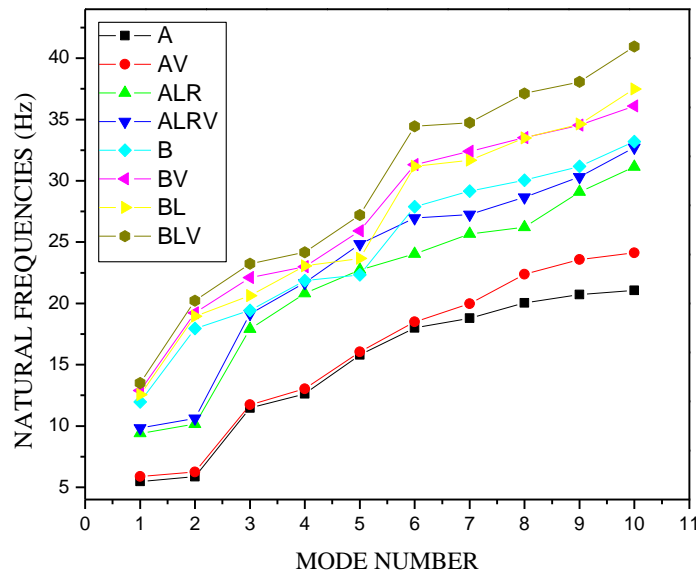
Fig. 4.9 Natural frequencies of box type laterite masonry structures

A comparison of these natural frequencies of unreinforced box-type laterite masonry structure without roof (A) and unreinforced box-type laterite masonry structure with roof (B) is shown in Fig. 4.10. Again a comparison of such natural frequencies of single storeyed box type laterite masonry structures without roof and those with roof are shown in Fig. 4.11 and Fig. 4.12 respectively.
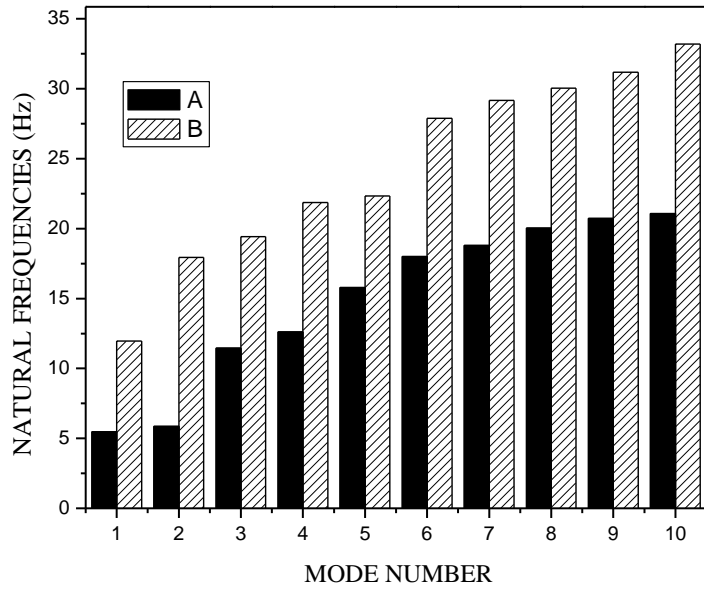
Fig. 4.10 Comparison of natural frequencies of structures A and B
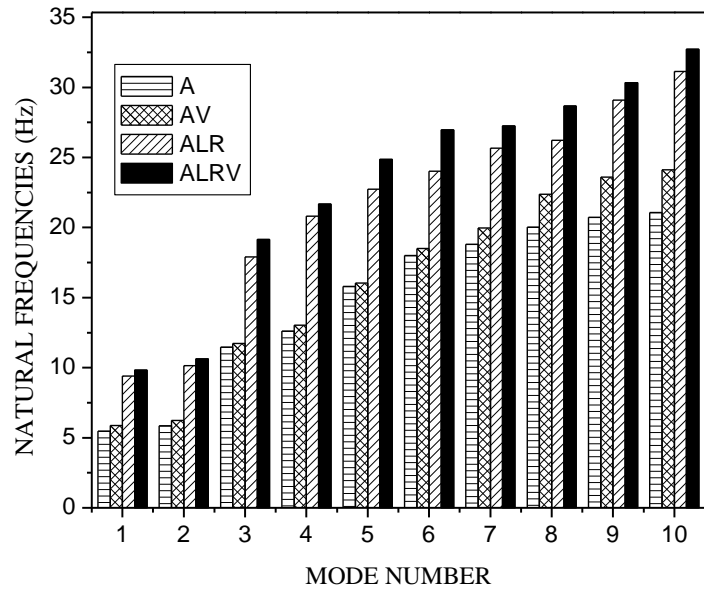
Fig. 4.11 Comparison of natural frequencies of different box-type laterite masonry structures without roof
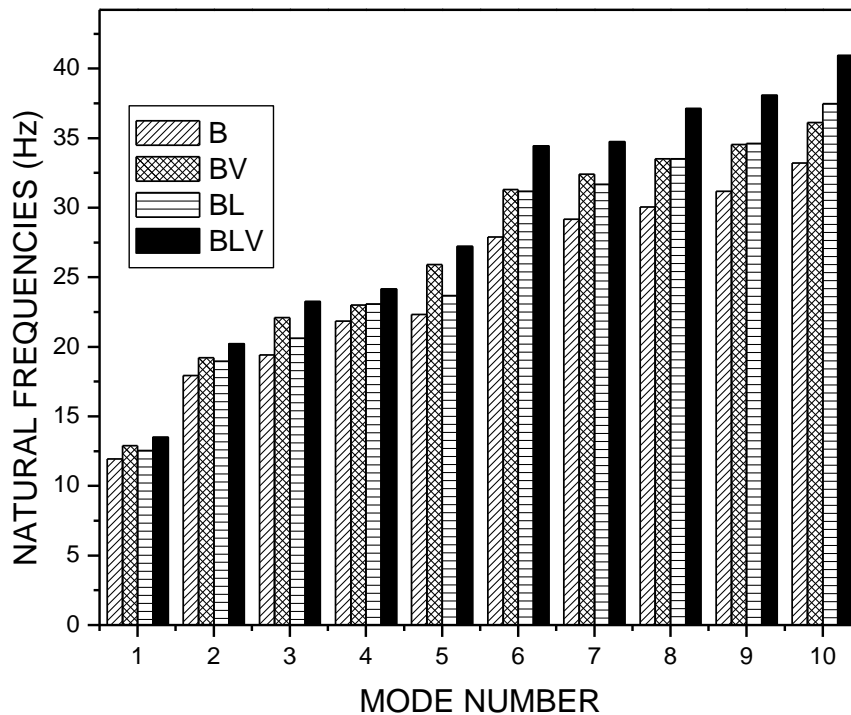
**Fig. 4.12 Comparison of natural frequencies of different
box-type laterite masonry structures with roof**

The fundamental frequency of building Type AV was observed to be 7.45% more than that of building Type A whereas the fundamental frequency of building Type ALR was observed to be 72% more than that of building Type A. In building Type ALRV the increase in fundamental frequency is around 80% compared to building Type A.

The fundamental frequency of building Type BV was observed to be 7.8% more than that of building Type B whereas the fundamental frequency of building Type BL was observed to be 5% more than that of building Type B. In building Type BLV the increase in fundamental frequency is around 13% compared to building Type B. The increase in fundamental frequency of structure from Type A to Type B was noted to be around 119%.

The fundamental mode shape of structures without roof (A, AV, ALR and ALRV) is the 'breathing mode', the opposite walls showing out-of-phase motion with maximum amplitude at the top edge as shown in Fig. 4.13 and Fig. 4.14. The fundamental mode shape of structures with roof (B, BV, BL and BLV) is the 'sway mode', the long walls showing in-phase motion as shown in Fig. 4.15. Provision of RC band or containment reinforcement does not seem to change the fundamental mode shape of box-type laterite masonry structures with or without roof. But the provision of RC roof changes the fundamental mode shape of single storeyed box type laterite masonry structures from a 'breathing mode' to a 'sway mode'.
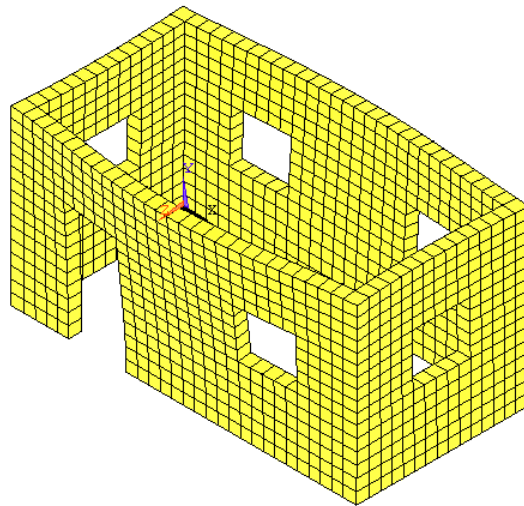
Fig. 4.13 Fundamental mode shape of box type laterite masonry structure without roof - Type A (isometric view)
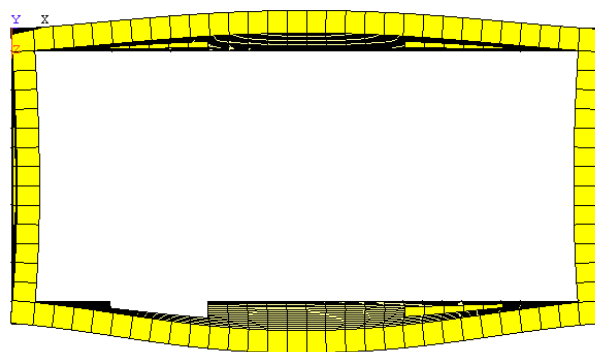
Fig. 4.14 Fundamental mode shape of box type laterite masonry structure without roof - Type A (plan view)
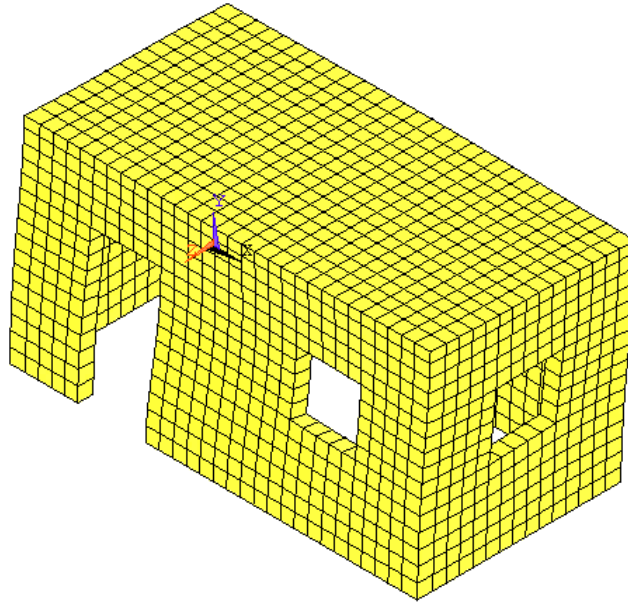
Fig. 4.15 Fundamental mode shape of box type laterite masonry structure with roof - Type B (isometric view)

In structures with roof, torsion mode was observed in the 4th mode in all the four cases (B, BV, BL and BLV). In structures without roof, torsion mode was not observed in the first 10 modes in A and AV but was observed in the 9th mode in ALR and ALRV. Fig. 4.16 and Fig. 4.17 show torsion mode in structure ALR and B respectively.
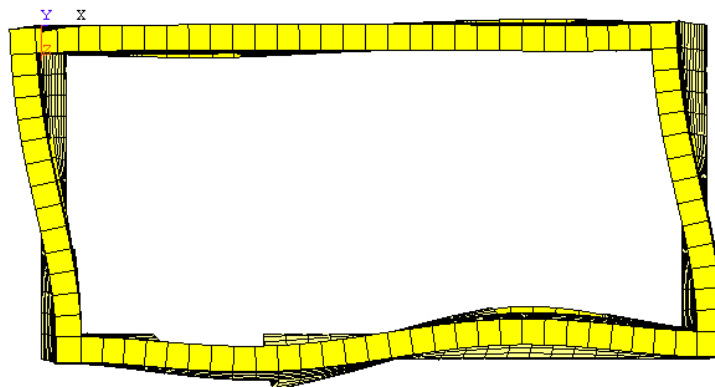
Fig.4.16 Torsion mode of structure ALR (plan view)
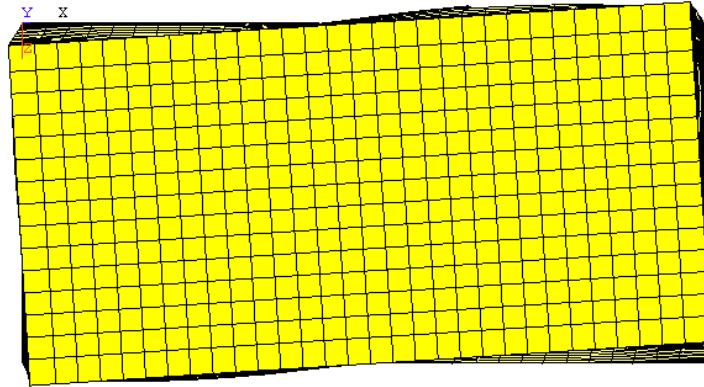
Fig.4.17 Torsion mode of structure B (plan view)

4.5 CONCLUSIONS

Introduction of RC bands or containment reinforcement tends to increase the natural frequencies of box-type laterite masonry structures, both with and without roof. But it does not seem to affect the fundamental mode shapes of these structures. While the fundamental mode shape of box-type laterite masonry structures without roof is a 'breathing mode', it gets shifted to a 'sway mode' for box-type laterite masonry structures with roof. This change in the fundamental mode shape then may bring greater differences in the dynamic response of the structures with provision of a rigid RC roof.

Provision of roof also substantially changes the magnitude of the first few natural frequencies of box type laterite masonry structures. The fundamental frequency of unreinforced laterite masonry structure with roof (B) is more than double that of a structure without roof (A). These changes in the magnitude of the frequencies and the change in the fundamental mode shape then may lead to large differences between the seismic response of the structures with and without roof.

CHAPTER 5

SEISMIC RESPONSE OF BOX TYPE
LATERITE MASONRY STRUCTURES

5.1 INTRODUCTION

Transient dynamic analysis (time-history analysis) is a technique used to determine the dynamic response of a structure under the action of any general set of time-dependent loads. This type of analysis can be used to determine the time-varying displacements, strains, stresses and forces in a structure as it responds to any combination of static, harmonic and transient loads [ANSYS].

In order to understand the seismic response of a single-storeyed box-type laterite masonry structure under earthquake induced vibrations, a linear transient analysis was carried out for all the eight different types of structures described in chapter 4.

The equations of motion, expressed in general matrix, notation is

$$[M]\{\ddot{u}\} + [C]\{\dot{u}\} + [K]\{u\} = -[M]\{\ddot{u}_g(t)\}$$

(5.1)

where
[M] = structural mass matrix $\{\ddot{u}\}$ = nodal acceleration vector

[C] = structural damping matrix $\{\dot{u}\}$ = nodal velocity vector

[K] = structural stiffness matrix $\{u\}$ = nodal displacement vector

and { $\ddot{u}_g(t)$ }= ground acceleration vector

ANSYS software employed herein uses the Newmark time integration method to solve the equations of motion at discrete time instants.

5.2 EQUIVALENT STATIC ANALYSIS

Before attempting detailed time-history analyses, equivalent-static analyses were conducted in order to identify the most vulnerable regions of the laterite masonry structures, undergoing seismic movements. The design horizontal seismic coefficient for masonry structure, calculated according to IS 1893 (Part 1) – 2002, was obtained as 0.45. Hence, a horizontal acceleration of 0.5g, perpendicular to long walls, was applied on the entire height of the building.

The structural response of the buildings were then evaluated in terms of relative magnitudes of out-of-plane displacements of the long walls and the stresses in the masonry walls in horizontal and vertical directions.

5.2.1 Out of Plane Deflection u_z of Long Walls

Fig. 5.1 shows the displacement u_z perpendicular to long wall for building Type A. The out of plane deflection patterns were observed to be similar in all the box type laterite masonry structures without roof - A, AV, ALR and ALRV, the maximum deflection in each case being at the center of top edge of long walls.
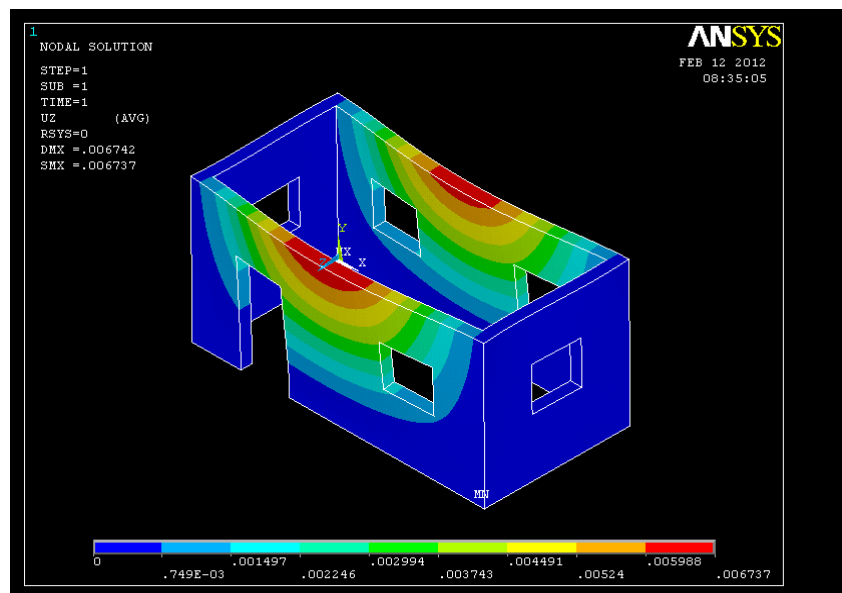
Fig. 5.1 Deflection u_z in building Type A

Fig. 5.2 shows the displacement profile u_z perpendicular to long wall at mid length of the long wall, along the height, for buildings without roof. It can be seen that the long walls of buildings without roof, underwent a cantilever mode of deflection. In building Type A, the maximum deflection u_z was 6.7 mm. This was reduced to 5.95 mm in case of Type AV building, which is a reduction of 11% from that of Type A. The peak deflections in building Types ALR and ALRV were noted as 2.03 mm and 1.91 mm, a large reduction of 70% and 72% respectively from that of building Type A.

The reductions in displacement u_z in case of ALR and ALRV buildings, as compared to Type A building, clearly show the effect of providing a lintel band and a roof band. In box-type laterite masonry structures without roof, provision of a lintel band and a roof band has, thus proved to be more effective in reducing the displacement u_z, than the vertical containment reinforcement, as provided in AV Type building.
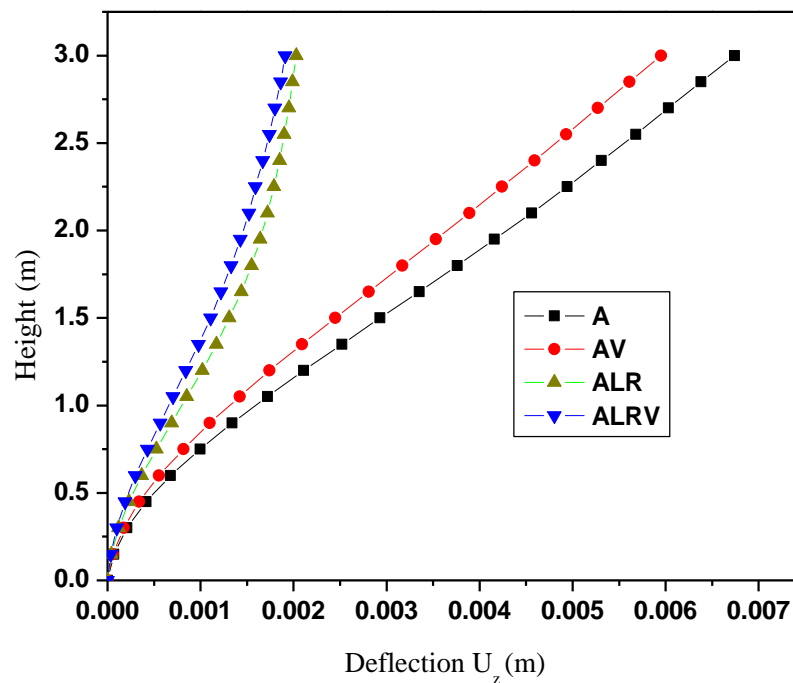
Fig. 5.2 Deflection u_z of long wall at mid-length in structures without roof

Fig. 5.3 shows the displacement u_z perpendicular to long wall for building Type B. The out of plane deflection patterns in box type laterite masonry structures with roof - B, BV, BL and BLV, were observed to be similar. Fig. 5.4 shows the displacement profile perpendicular to long wall u_z at mid-length of long wall, for buildings with roof. The maximum deflection is observed at around 2.25 m height, along the center line of the wall in all the four cases (B, BV, BL and BLV). The deflection seems to increase up to this 2.25 m height and then gradually decreases up to the top edge.
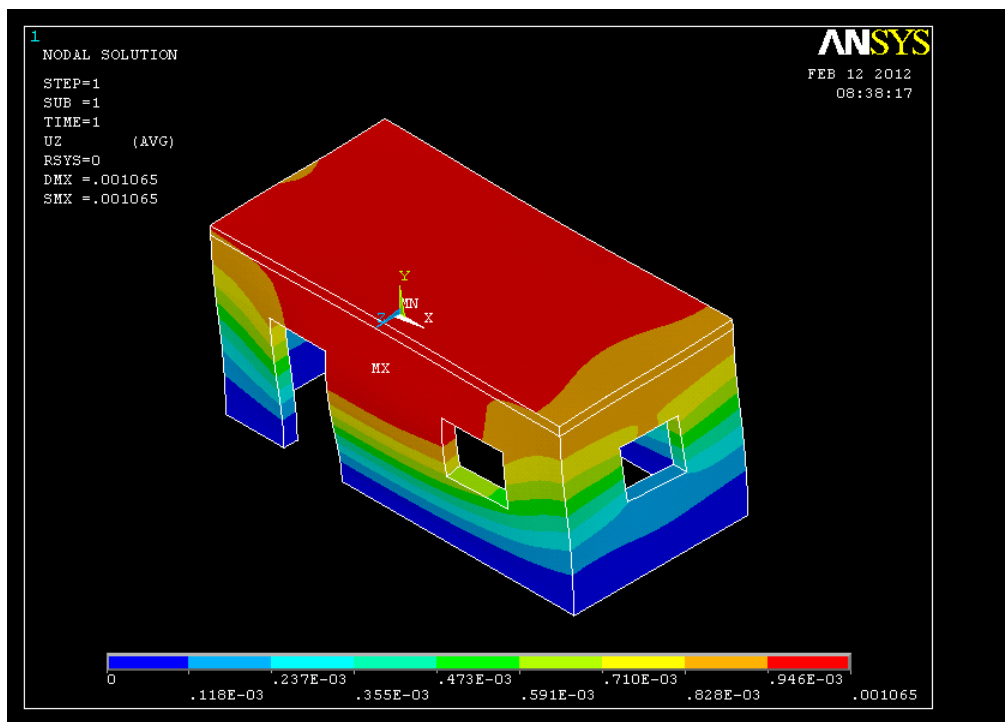
Fig. 5.3 Deflection u_z in building Type B

In building Type B the maximum deflection u_z was 1.06 mm. This was reduced to 0.89mm in case of building type BV, which is a reduction of 16% from that of building Type B. The peak deflections in building Types BL and BLV were noted as 0.95 mm and 0.81 mm, a reduction of 10% and 24% respectively from that of building Type B.

Provision of a heavy rigid RC roof itself helps to reduce the out-of-plane deflection u_z in box type laterite masonry structures. The effect of vertical containment reinforcement in

reducing the out of plane deflection is relatively more in structures with roof, compared to structures without roof.
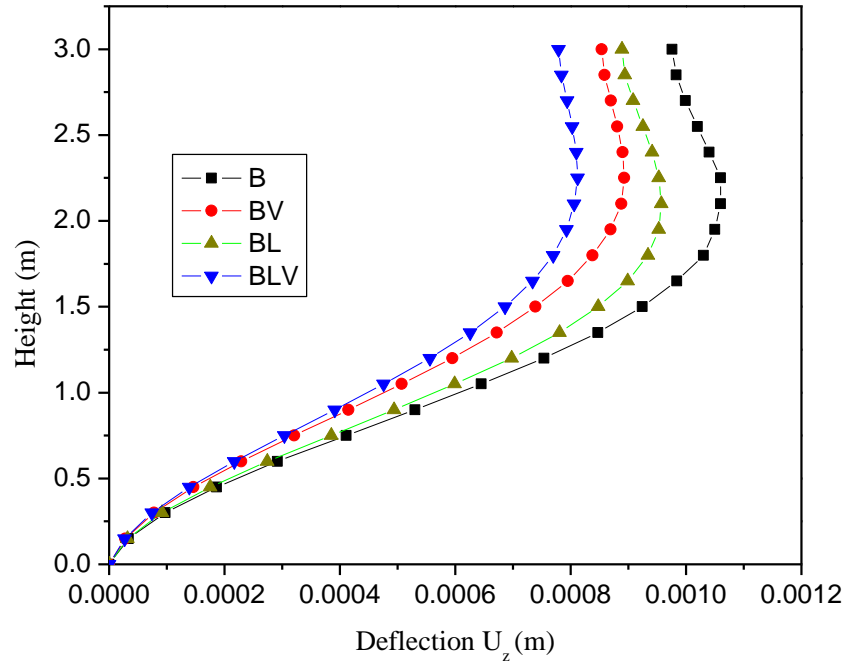
Fig. 5.4 Deflection u_z of long wall at mid-length in structures with roof

5.2.2 Bending Stress σ_y Perpendicular to Bed Joints in Long Walls

Fig. 5.5 shows the variation of stresses σ_y along the height of the long wall at the mid-length, for box-type laterite masonry structures without roof. The maximum value of σ_y was observed near the center of base of the long wall, 0.58 MPa in building Type A. This was reduced to 0.48 MPa in building Type AV, a reduction of 17%. The maximum values of σ_y in building Type ALR and ALRV were noted as 0.34 MPa and 0.275 MPa, a reduction of 41% and 53% respectively, from that of building Type A.

In box type laterite masonry structures without roof, RC bands have helped to reduce the stresses σ_y considerably. Containment reinforcement helped in reducing the stresses σ_y

80

further. Hence, in box type laterite masonry structures without roof, provision of RC bands along with containment reinforcement helps to reduce the stresses σ_y and thus reduce the chances of horizontal cracks in the masonry.
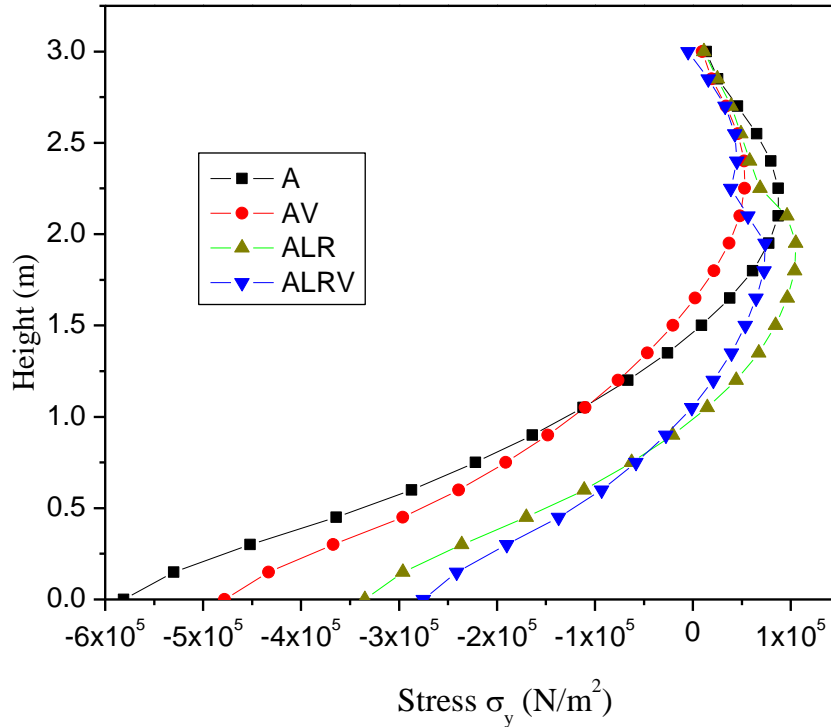
Fig. 5.5 Stresses σ_y near mid length of long wall along height in buildings without roof

The variation of stresses σ_y along the height at a corner of the long wall of box-type laterite masonry structures with roof is shown in Fig. 5.6. The maximum value of σ_y was observed near the corner of base of the long wall, 0.283 MPa in building Type B. This was reduced to 0.251 MPa in building Type BV, a reduction of 11%. The maximum value of σ_y in building Type BL was noted as 0.279 MPa which is nearly the same as the maximum value in building Type B. In case of BLV, the maximum value was 0.245 MPa, a reduction of 13% from that of building Type B.

In box type laterite masonry structures with roof, the maximum value of stress σ_y is observed to be only about 50% of those of structures without roof. Again in these structures with roof, vertical containment reinforcement has played a better role than lintel band in reducing the stresses σ_y.
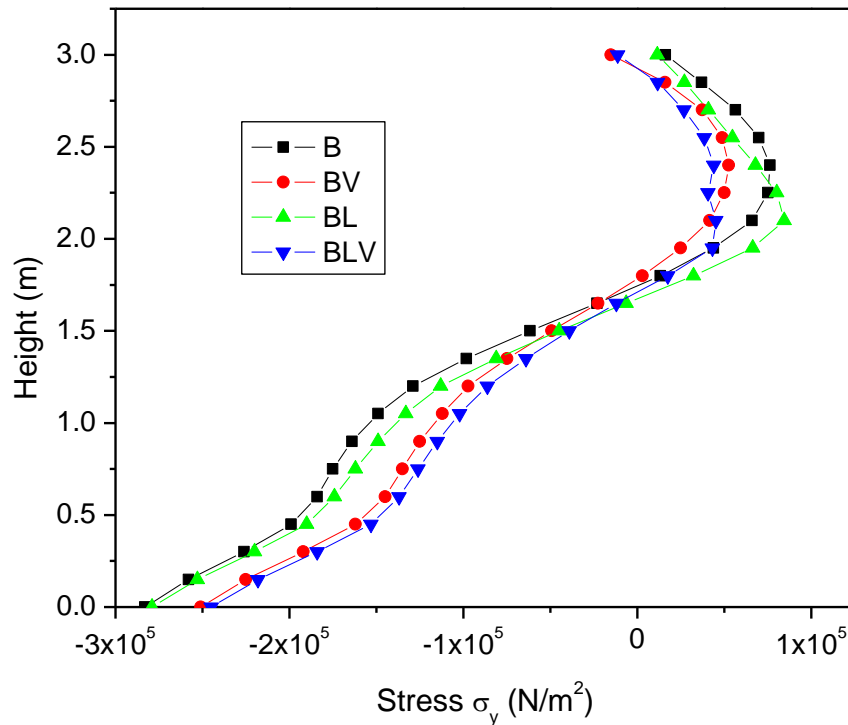
Fig. 5.6 Stresses σ_y at a corner of long wall along height in buildings with roof

5.2.3 Bending Stress σ_x Parallel to Bed Joints in Long Walls

Fig. 5.7 shows the stresses σ_x parallel to bed joints in long walls of box type laterite masonry structures without roof. The maximum value of σ_x was observed around the center near the top edge of the long wall, 0.315 MPa in building Type A. This got reduced to 0.27 MPa in building Type AV, a reduction of 14%. The maximum values of σ_x in building Type ALR and ALRV were noted as 0.09 MPa and 0.084 MPa respectively, which is 71% and 73% less than the maximum in building type A. In box

82

type laterite masonry structures without roof, RC bands have helped to reduce the stresses σ_x considerably and the effect of containment reinforcement is not appreciable.
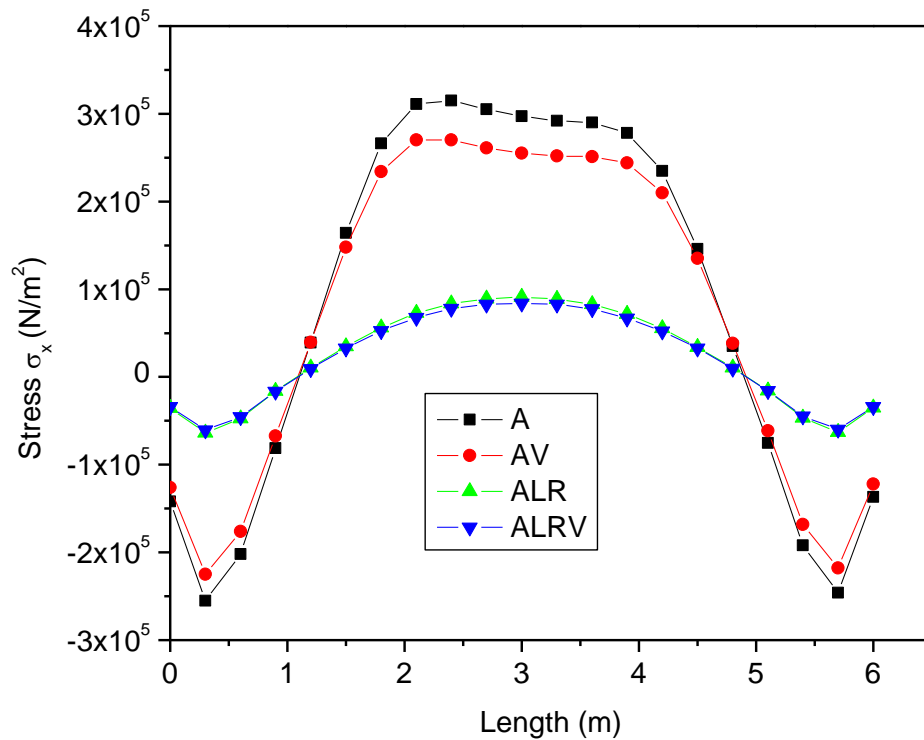
**Fig. 5.7 Stresses parallel to bed joints σ_x near top edge
of long wall in buildings without roof**

Fig. 5.8 shows the variation of stresses σ_x parallel to bed joints at sill level in long walls of structures with roof (B, BV, BL and BLV). The maximum stress in laterite masonry structure B was noted as 0.039 MPa. This was reduced to 0.035 MPa in structure Type BL, a reduction of 10%, 0.026 MPa in structure Type BV, a reduction of 33% and 0.023 MPa in structure Type BLV, a reduction of 41%. The maximum value of stress σ_x in box type laterite masonry structure with roof Type B is almost 88% less than that in structure without roof Type A. In these structures with roof, however, containment reinforcement

has proved to be more effective than just providing a lintel band in reducing the stresses σ_x.
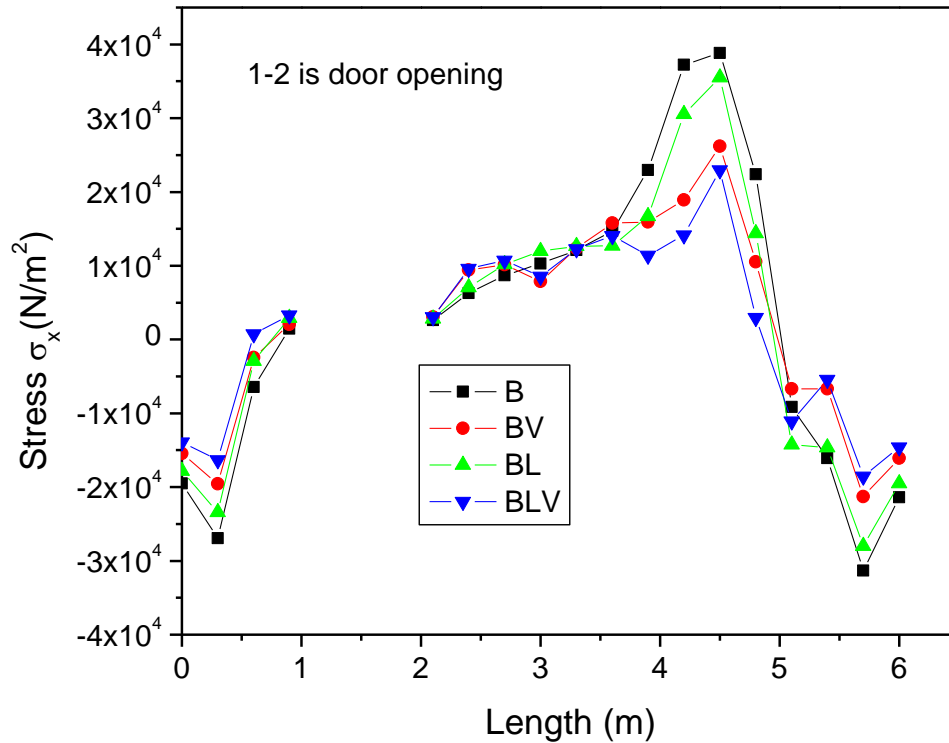
Fig. 5.8 Stresses parallel to bed joints σ_x at sill level in buildings with roof

5.2.4 Shear Stress σ_{yz} in Short Walls

The variation of stresses σ_{yz} along the length of short wall at lintel level of box-type laterite masonry structures without roof is shown in Fig. 5.9. The maximum value of σ_{yz} was observed near the corners of the opening, at lintel level, 0.098 MPa in building Type A. This was reduced to 0.085 MPa in building Type AV, a reduction of 13%. The maximum value of σ_{yz} in building Type ALR was noted as 0.062 MPa, 37% less than that of Type A. In case of ALRV, the maximum value was 0.068 MPa, a reduction of 31% from that of building Type A. In box type laterite masonry structures without roof, RC bands have helped to reduce the shear stresses in short walls significantly.
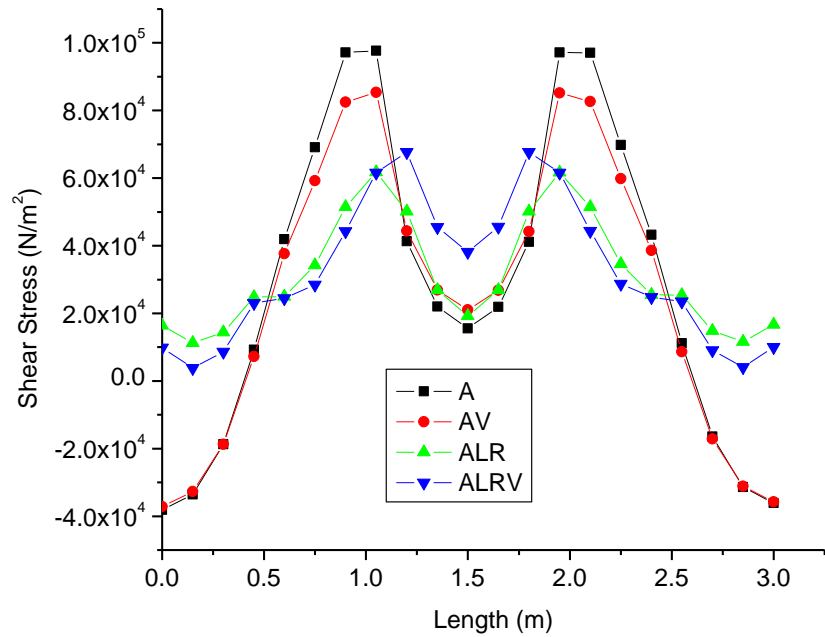
**Fig. 5.9 Shear stress σ_{yz} at lintel level of short wall
along length in buildings without roof**

Fig. 5.10 shows the shear stress distribution in structure with roof, Type B. Fig. 5.11 shows the variation of stresses σ_{yz} along the length of the short wall below sill level, for box-type laterite masonry structures with roof.
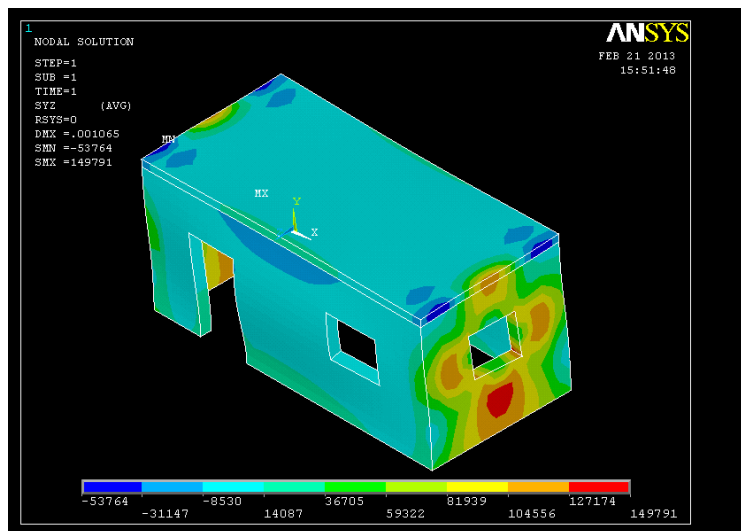
Fig. 5.10 Shear stress σ_{yz} in building Type B
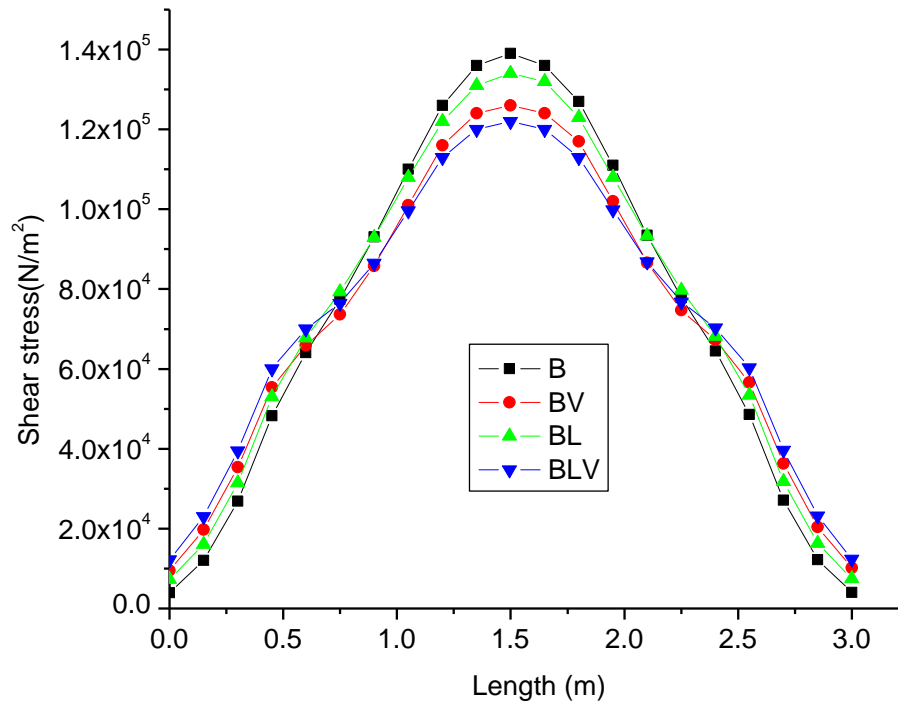
Fig. 5.11 Shear stress σ_{yz} below sill level of short wall along length in buildings with roof

The maximum value of σ_{yz} was observed at the mid-length, 0.139 MPa in building Type B. This was reduced to 0.126 MPa in building Type BV, a reduction of nearly 10%. The maximum values of σ_{yz} in building Type BL and BLV were noted as 0.134 MPa and 0.122 MPa. The reduction in shear stress in case of BLV compared to B was observed to be around 12%.

Compared to box type laterite masonry structures without roof, shear stress was observed to be more in structures with roof. Maximum shear stress in Type B structure was observed to be almost 42% more than that of Type A structure.

5.3 RESPONSE OF BOX TYPE LATERITE MASONRY STRUCTURES TO EL-CENTRO (NS COMPONENT) ACCELERATION

The best way to evaluate seismic performance of structures is by monitoring structural behaviour under real earthquake records. Time history analysis is a part of structural analysis and is the calculation of the response of a structure to any earthquake [Sahin 2010]. Herein a linear transient analysis was carried out with El-Centro (N-S component) earthquake acceleration record as input. A part of the ground motion acceleration record (north-south component) recorded at El-Centro during California earthquake of May 18, 1940 is shown in Fig. 5.12. The maximum peak of the input is 0.319g at time 2.04 s.

Fig. 5.13 shows the Fourier amplitude spectrum of El-Centro NS component. The predominant frequency content of El-Centro acceleration record is around 1.17 Hz, which is significantly lower than the fundamental frequency of the buildings analyzed.
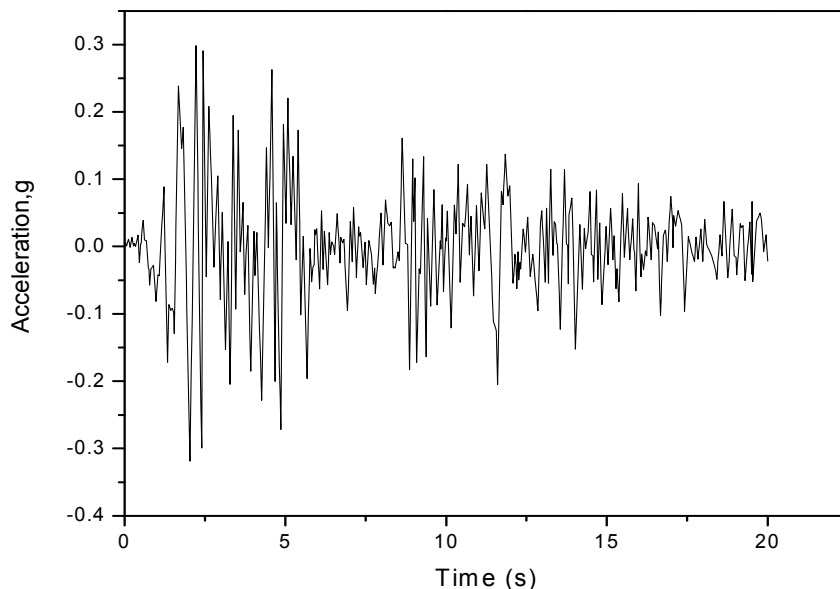
Fig. 5.12   Acceleration time history of El-Centro (NS component)
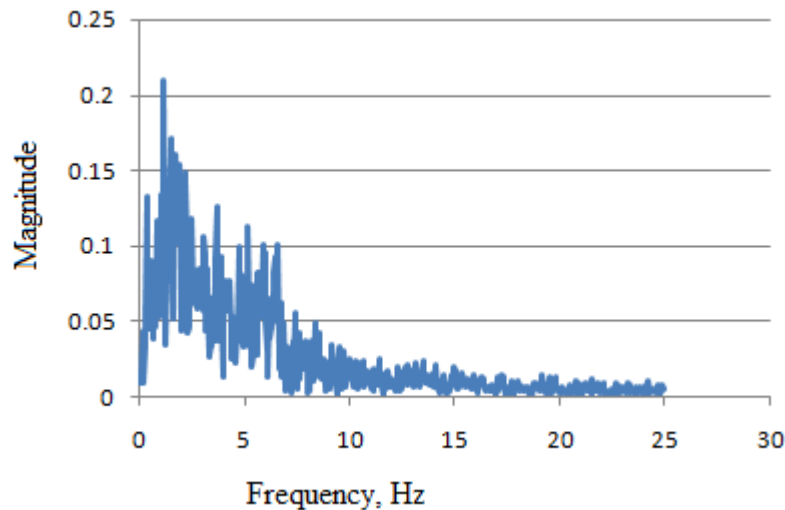
Fig. 5.13 Fourier amplitude spectrum of El-Centro (NS component)

Although ANSYS may be used to implement a step-by-step time history analysis, it is not so easy to achieve the same using its graphical user interface, as a particular tool for seismic analysis is not available. There is no facility to apply a given acceleration time-history directly as base-node excitation, in Version 10 of ANSYS. Sahin (2010) developed an assistant program, named ANSeismic, for earthquake analyses of structures with ANSYS. He proposed application of the acceleration time-histories to the whole model with base fixed using the ACEL command available in ANSYS. The damping coefficients, α and β are calculated depending on damping ratio and fundamental frequency of the system. In their technical report, the researchers from Korea institute of nuclear safety have established the efficacy of this method [Jhung 2009].

The following steps based upon the methods proposed by Sahin were adopted in this study:

The database file of the model prepared in ANSYS is saved in a folder. Program given in Appendix 1 is also saved as a text file in the same folder. A seismic record text file is also created and the downloaded acceleration records multiplied by gravity load is saved in this file. This text file is called by the program in Appendix 1 [Sahin 2010]. The damping

value and earthquake direction are given in the program. First, modal analysis is executed and α and β coefficients for damping are calculated using the first fundamental frequency.

Damping in a structure increases with displacement amplitude since with increasing displacement more elements may crack or become slightly nonlinear. For linear seismic analysis, viscous damping is usually taken as 5% of critical as the structural response to earthquakes is usually close to or greater than the yield displacement. Damping ratio of the model was chosen as 5 %. The time history analysis was executed by applying each acceleration value to the model step by step in time domain.

The time-history analysis of a brick masonry structure was now attempted using the above proposed method. Saikia (2006) has studied the time history analysis of such a structure using finite element software, NISA. An initial model was prepared in ANSYS using shell elements with the dimensions and material properties as given by Saikia. As far as possible, the model was kept similar to Saikia's model. Then time history response results were compared with those of Saikia and good agreement has been found. Based upon such agreement between the results, a study of the seismic responses of box-type laterite masonry structures was undertaken using the above methodology. The same material properties as given in Table 4.1 and the configurations as shown in Fig. 4.1 and 4.2 were considered in this study.

The long cross walls of the box-type laterite masonry structures are the ones that are vulnerable to out-of-plane flexural cracking. And hence the acceleration was applied perpendicular to the long walls of box-type laterite masonry structures.

All the eight types of box-type laterite masonry structures discussed earlier were analyzed to find their responses to El-Centro (NS component) acceleration. The deformed shapes of structures without roof (A, AV, ALR and ALRV) at minimum peak acceleration are

given in Fig. 5.14 to Fig. 5.17 and the deformed shapes at maximum peak acceleration are given in Fig. 5.18 to Fig. 5.21. In box-type laterite masonry structures without roof (A, AV, ALR and ALRV), the maximum deformation was observed at the top edge.
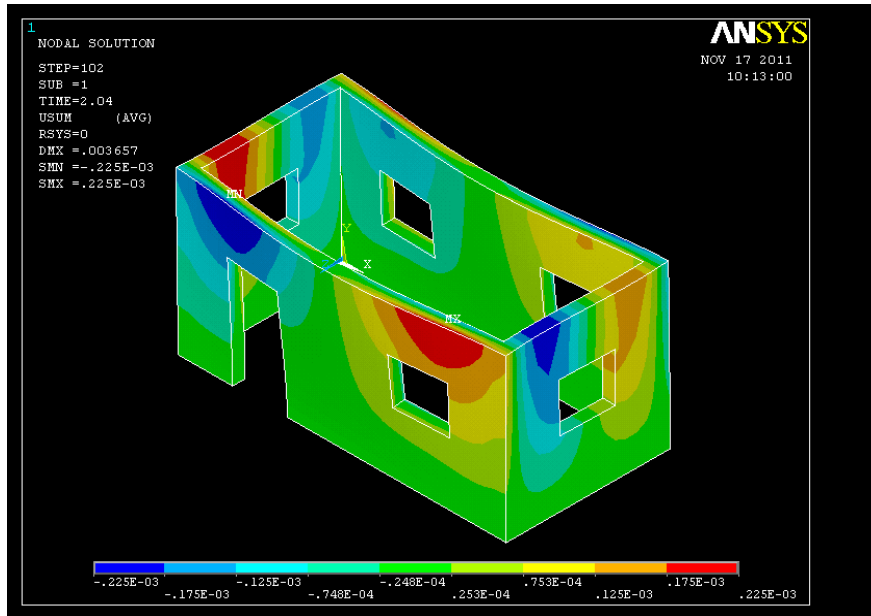
Fig. 5.14 The deformed shape of structure A at min. PGA
time = 2.04s (total displacement in m)
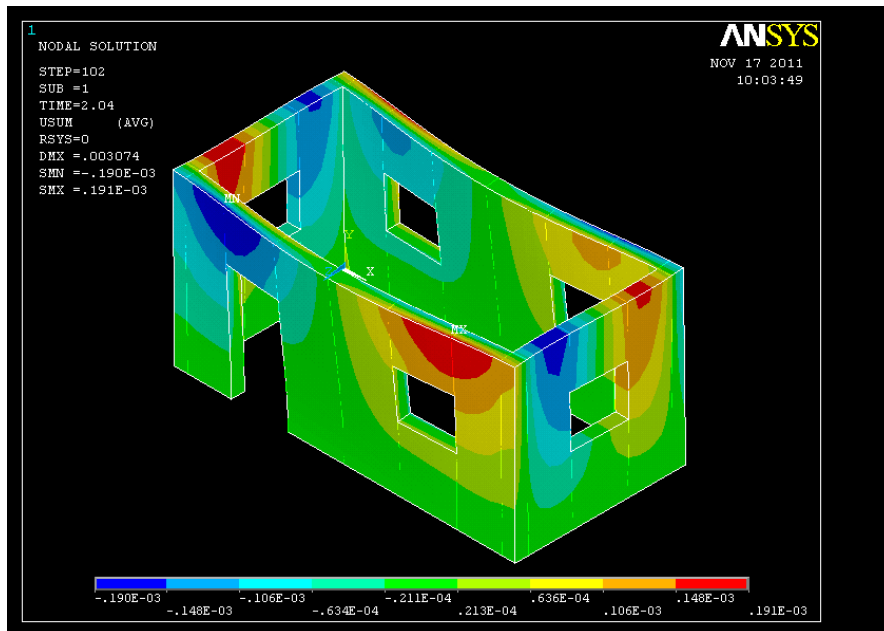
Fig. 5.15 The deformed shape of structure AV at min. PGA
time = 2.04s (total displacement in m)
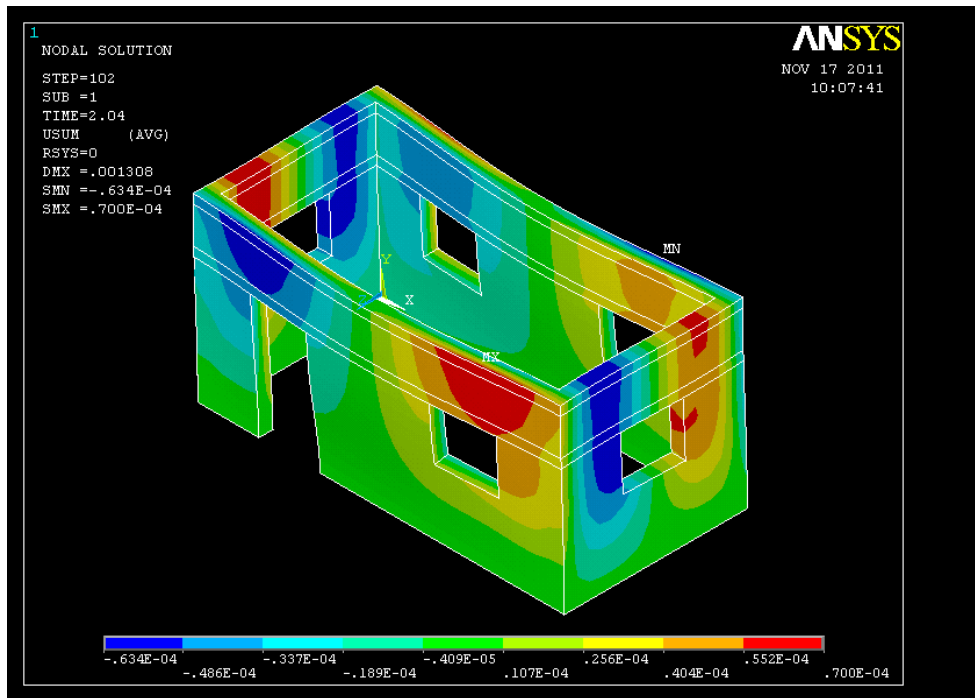
Fig. 5.16 The deformed shape of structure ALR at min. PGA time = 2.04s (total displacement in m)
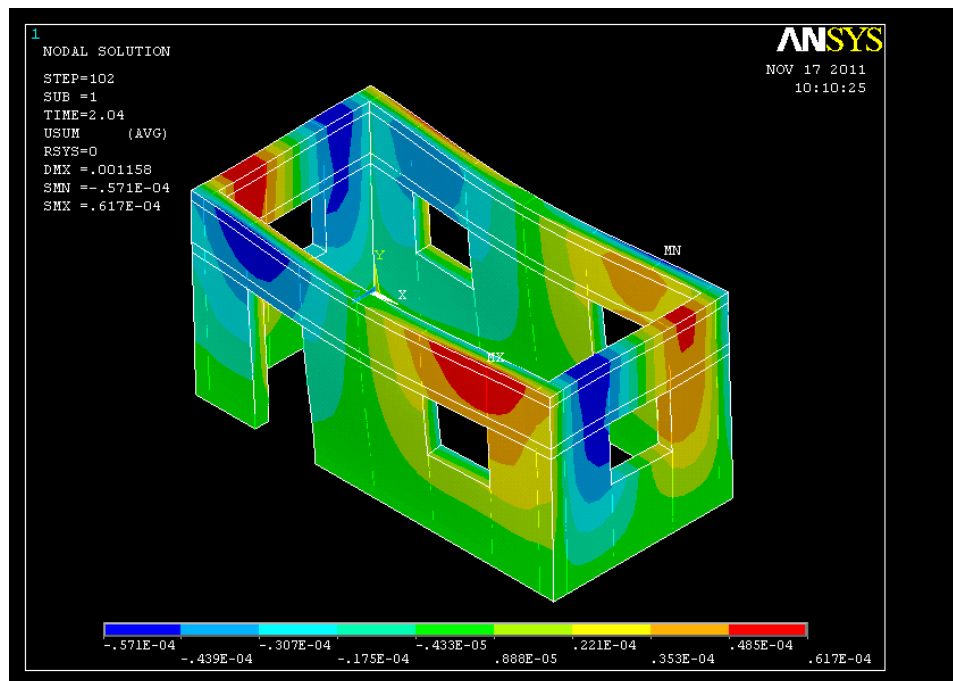
Fig. 5.17 The deformed shape of structure ALRV at min. PGA time = 2.04s (total displacement in m)
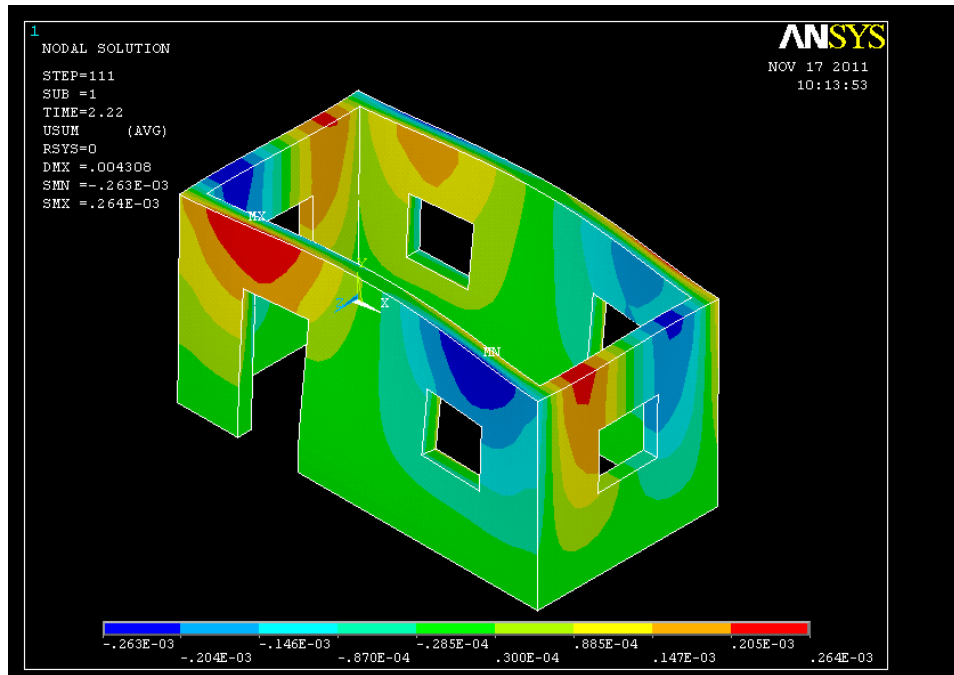
Fig. 5.18 The deformed shape of structure A at max. PGA time = 2.22s (total displacement in m)
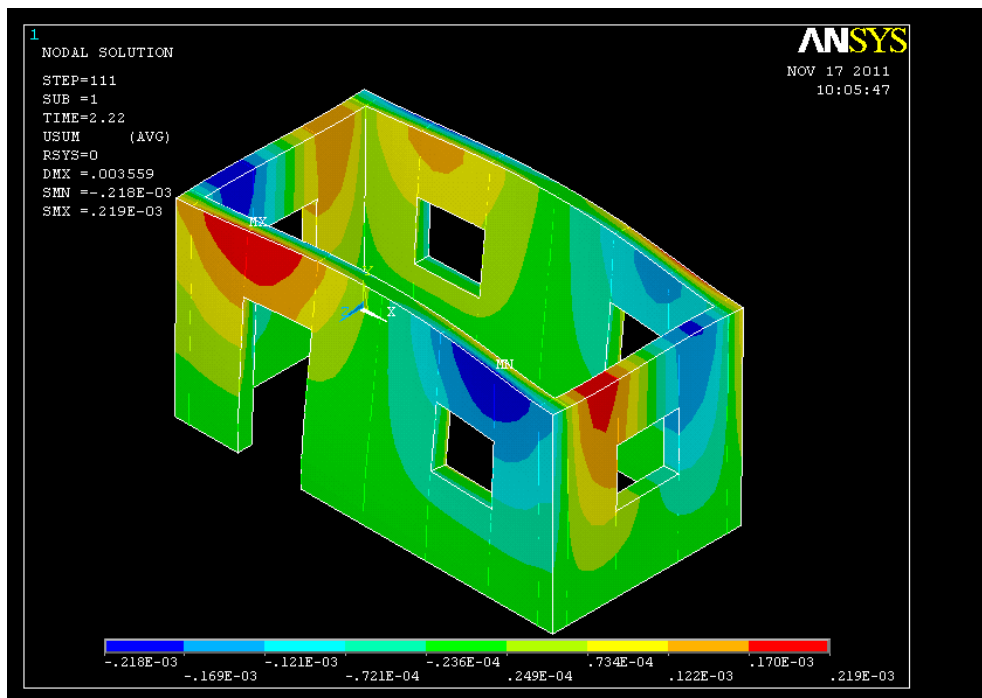
Fig. 5.19 The deformed shape of structure AV at max. PGA time = 2.22s (total displacement in m)
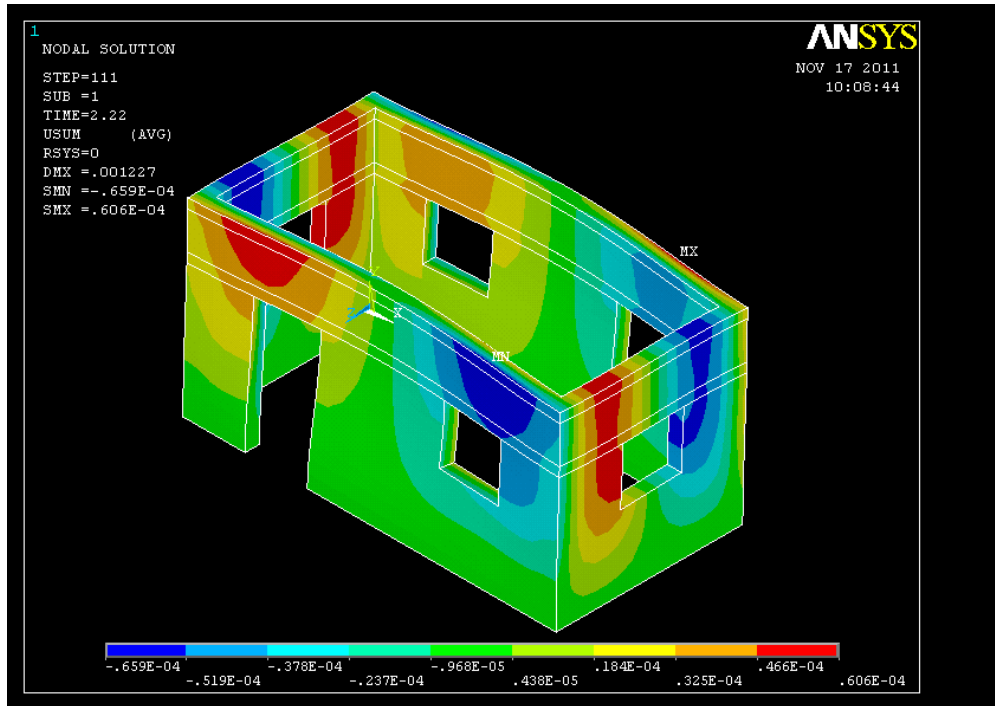
Fig. 5.20 The deformed shape of structure ALR at max. PGA time = 2.22s
(total displacement in m)
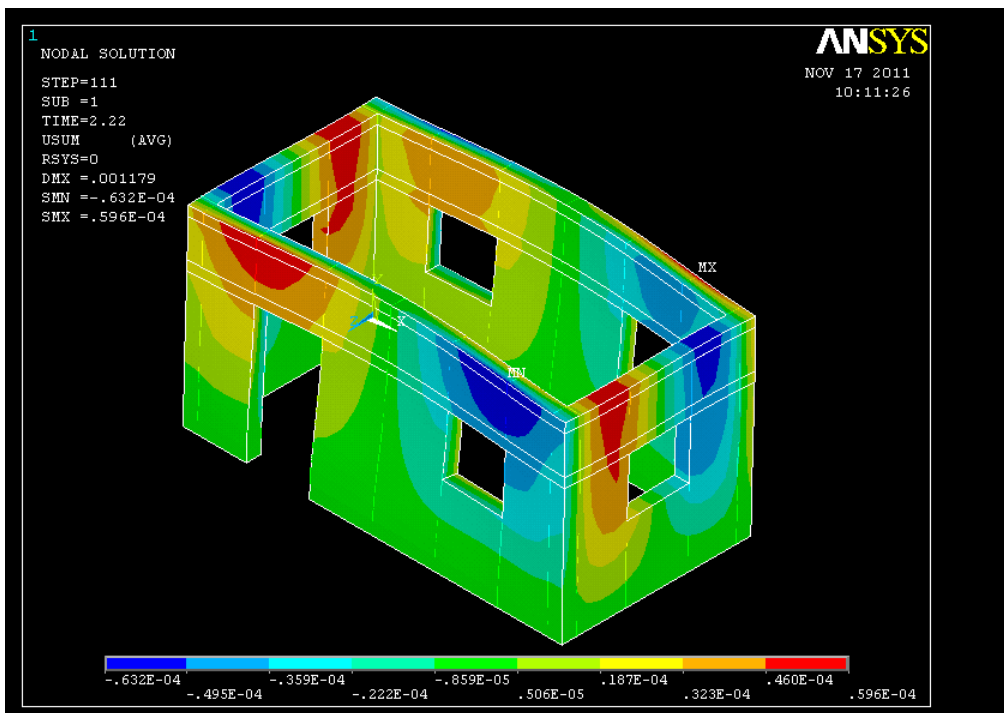
Fig. 5.21 The deformed shape of structure ALRV at max. PGA time = 2.22s
(total displacement in m)

The deformed shapes of structures with roof (B, BV, BL and BLV) at minimum peak acceleration are given in Fig. 5.22 to Fig. 5.25 and the deformed shapes at maximum peak acceleration are given in Fig. 5.26 to Fig. 5.29. In box type laterite masonry structures with roof (B, BV, BL and BLV), the maximum deformation was observed near the openings and at the corners of the rigid roof.
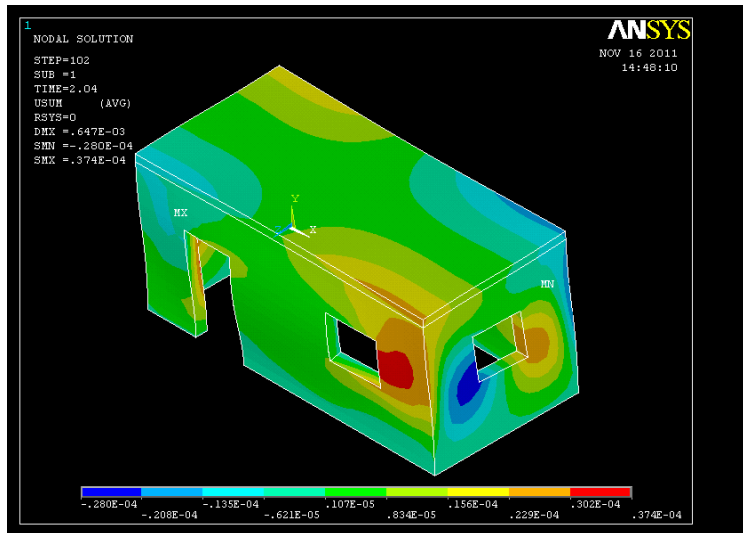
Fig. 5.22 The deformed shape of structure B at min. PGA
time = 2.04s (total displacement in m)
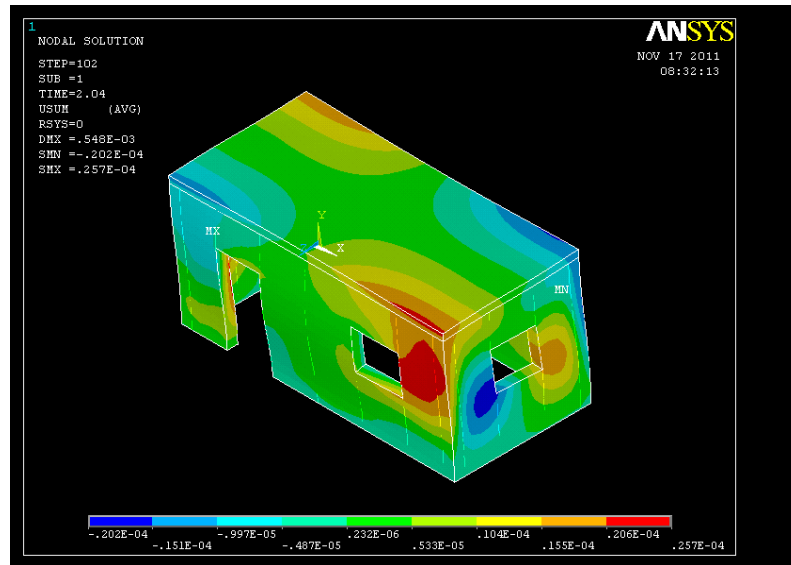
Fig. 5.23 The deformed shape of structure BV at min. PGA
time = 2.04s (total displacement in m)
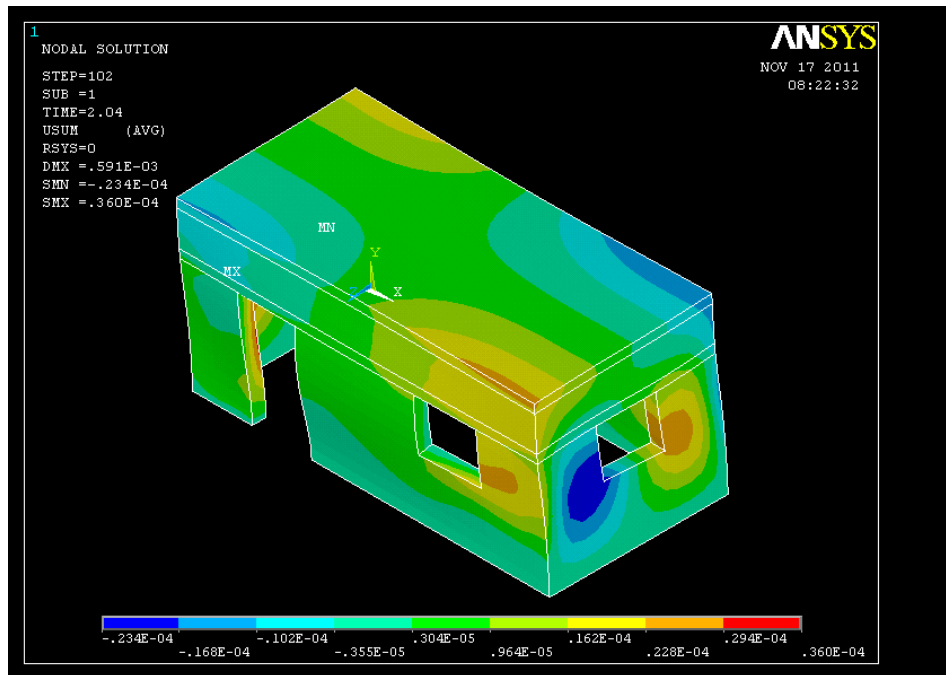
Fig. 5.24 The deformed shape of structure BL at min. PGA time = 2.04s (total displacement in m)
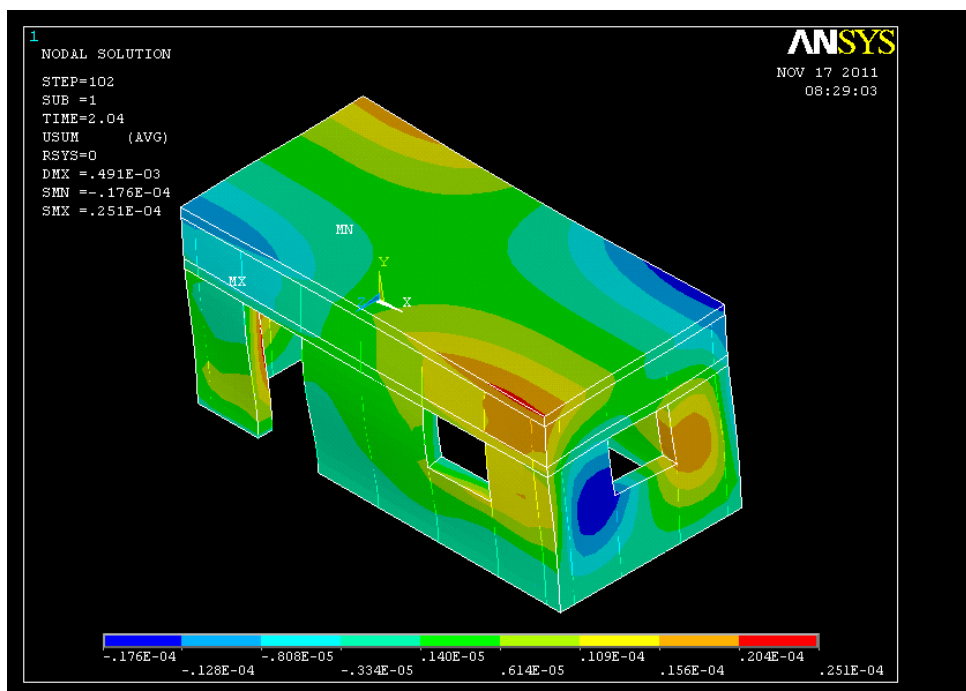
Fig. 5.25 The deformed shape of structure BLV at min. PGA time = 2.04s (total displacement in m)
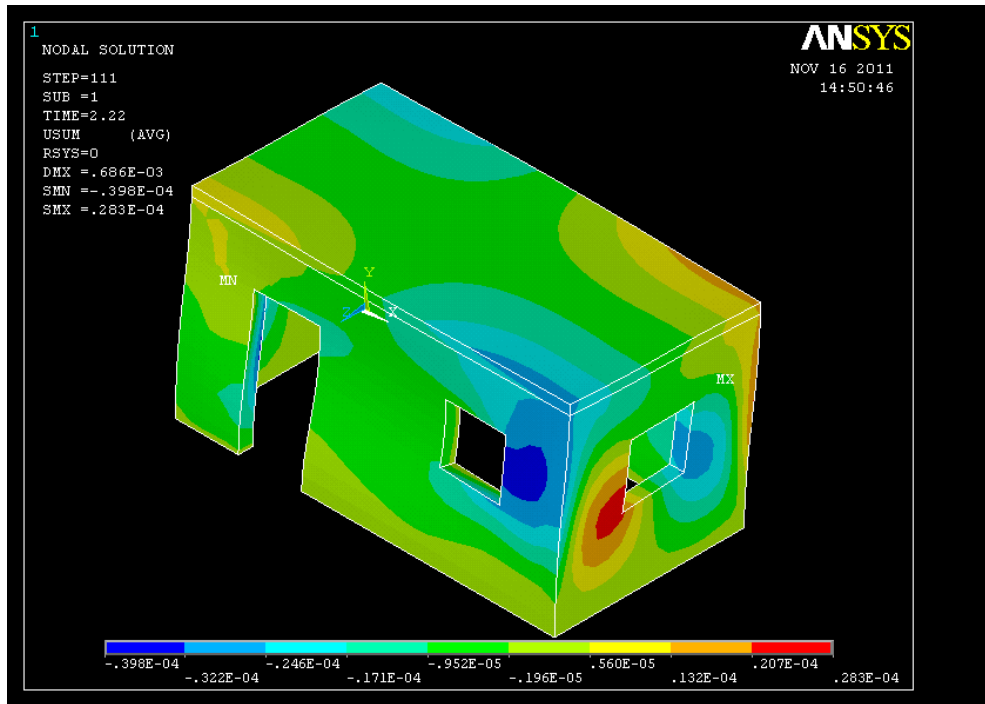
**Fig. 5.26 The deformed shape of structure B at max. PGA time = 2.22s
(total displacement in m)**
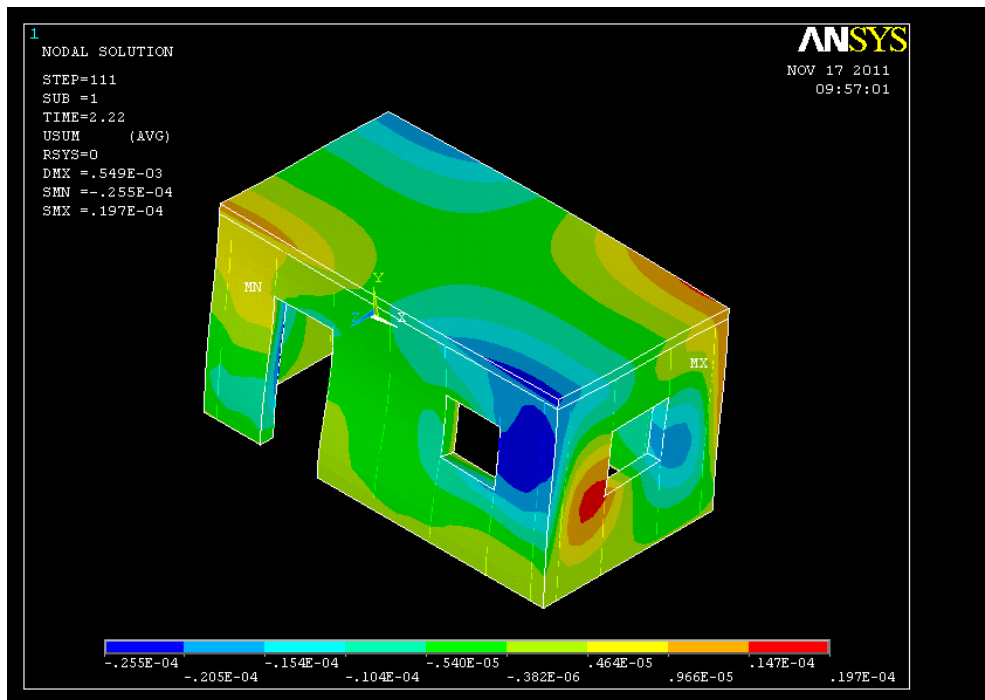
**Fig. 5.27 The deformed shape of structure BV at max. PGA time = 2.22s
(total displacement in m)**
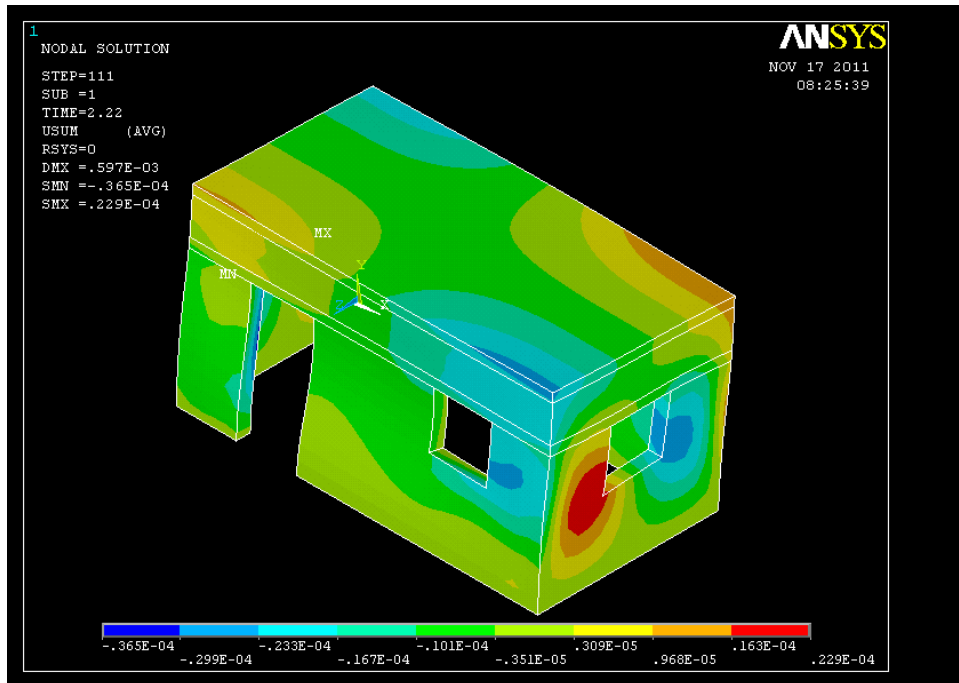
Fig. 5.28 The deformed shape of structure BL at max. PGA time = 2.22s (total displacement in m)
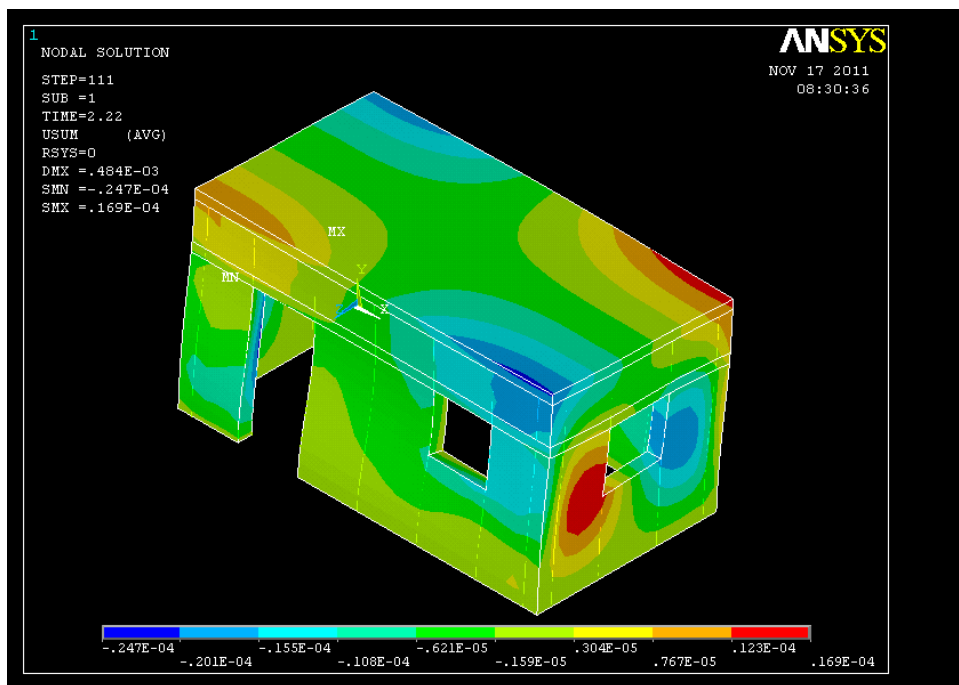
Fig. 5.29 The deformed shape of structure BLV at max. PGA time = 2.22s (total displacement in m)

In structure without roof, A, the maximum total displacement at PGA (time 2.22s) was noted as 0.264 mm. This had reduced to 0.219 mm in case of structure AV, (a reduction of 17%) and to 0.06 mm in structure ALR (a reduction of 77%). In single storeyed box type laterite masonry structures without roof, reinforced concrete bands seem to have helped to control the total deformation significantly.

In structure with roof, B, the maximum total displacement at PGA (time 2.04s) was noted as 0.037 mm, which shows that the rigid roof itself had helped to reduce the total displacement significantly. This had reduced to 0.026 mm in case of structure BV (a reduction of 30%), and to 0.036 mm in structure BL (a reduction of 3%).

Thus in single-storeyed box-type laterite masonry structures with roof, vertical containment reinforcement seems to help in controlling the total deformation significantly. Again the displacements in the various box-type laterite masonry structures with roof are quite small as compared to structures without roof.

5.3.1 Time-History Response of Deflection u_z

Equivalent static analysis conducted earlier had revealed that the node at the center of top edge of the long wall recorded the maximum out-of-plane deflection u_z, for all the cases of structures without roof being considered. Hence the time-history responses of those nodes were plotted.

Fig. 5.30 to Fig. 5.33 show the time-history response u_z of the center of top edge in building Types A, AV, ALR and ALRV respectively.
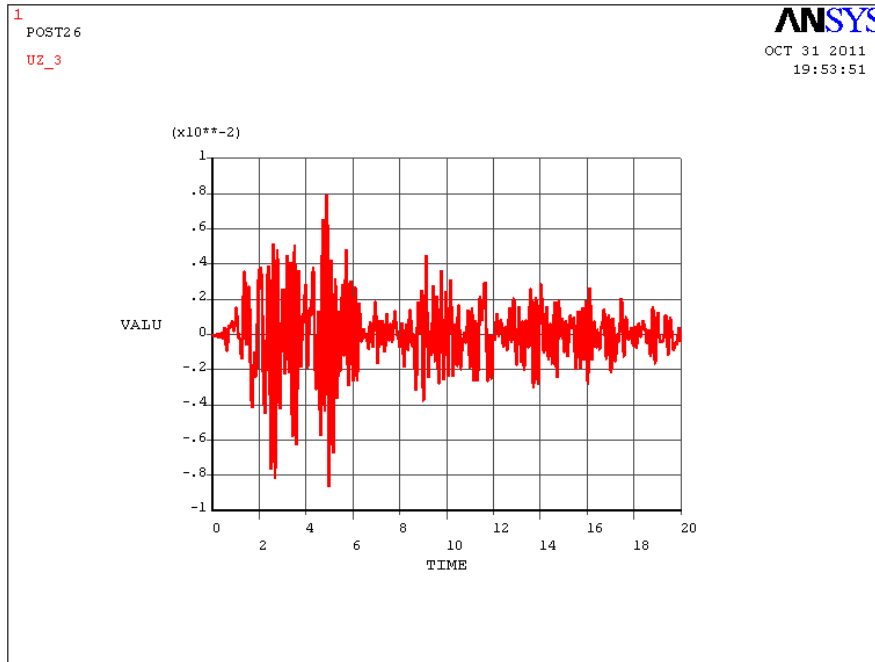
Fig. 5.30 Time-history response of deflection u_z (m) of the node at the center of top edge of long wall in structure Type A
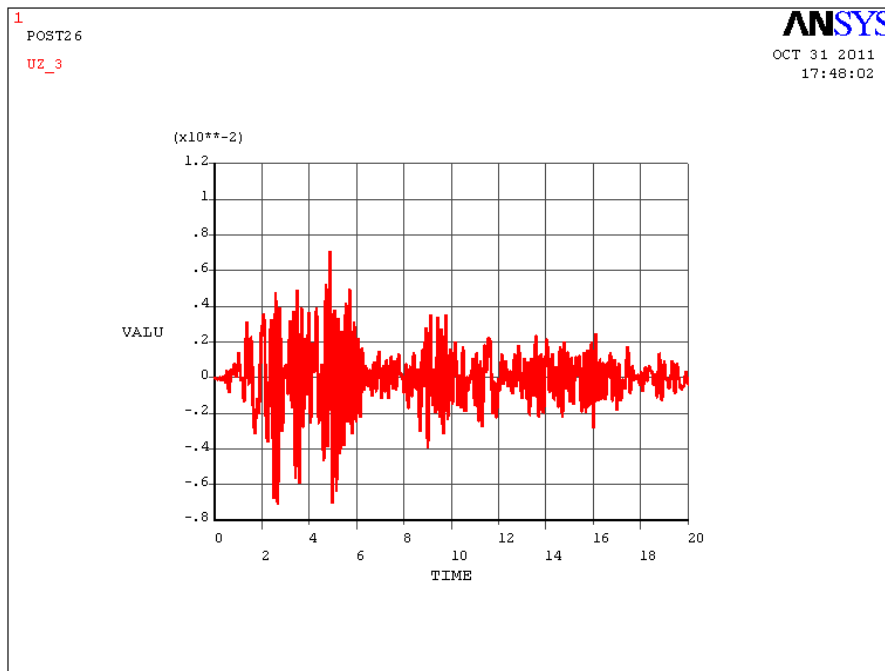
Fig. 5.31 Time history response of deflection u_z (m) of the node at the center of top edge of long wall in structure Type AV
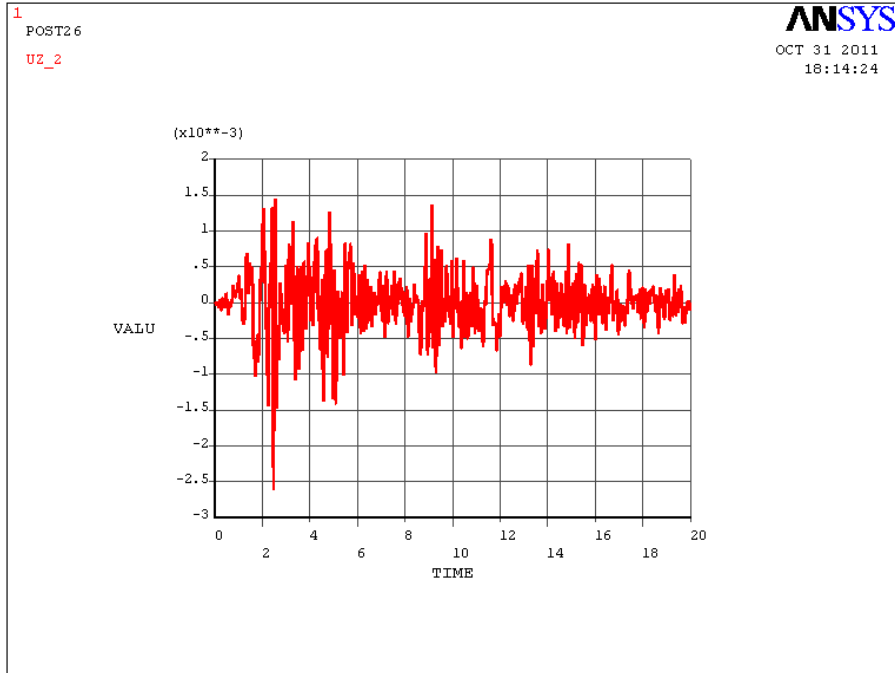
Fig. 5.32 Time history response of deflection u_z (m) of the node at the center of top edge of long wall in structure Type ALR
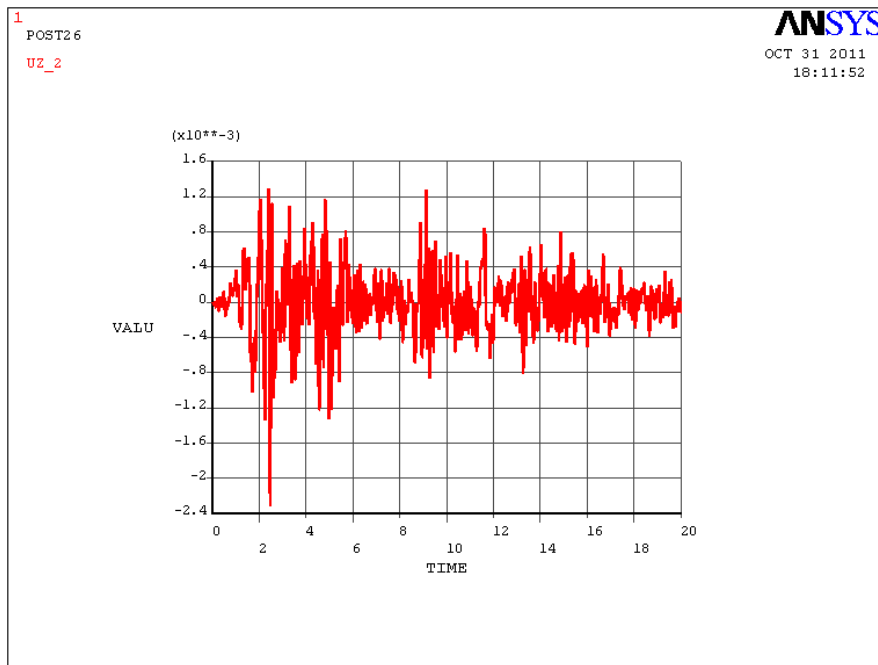
Fig. 5.33 Time history response of deflection u_z (m) of the node at the center of top edge of long wall in structure Type ALRV

The peak deflection in structure Type A was noted as 8.64 mm. This was observed to have reduced to 7.12 mm in structure AV, which is 18% less than that of structure Type A. The peak deflections in structure Type ALR and ALRV were similarly noted as 2.62 mm and 2.31 mm respectively, which are 70% and 73% less than that of structure Type A. The results show that in box type laterite masonry structures without roof, RC bands help to reduce the out of plane deflections significantly. Fig. 5.34 shows a comparison of the time history response u_z of the most vulnerable node observed from equivalent static analysis for structures without roof.
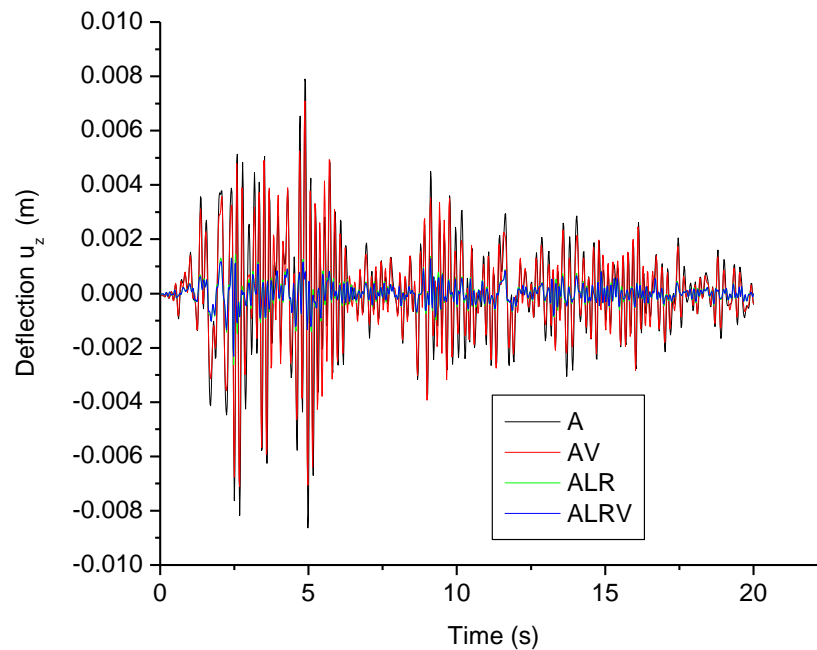
Fig. 5.34 Comparison of time history response of deflection u_z (m) of the node at the center of top edge of long wall in structures without roof

The ground accelerations are generally indicated as numerical values at discrete time instants. These time instants should be closely spaced to describe accurately the highly irregular variation of acceleration with time. Typically, in any direct time integration scheme, the time step is chosen as $1/10^{th}$ to $1/15^{th}$ of the fundamental period of the structure.

In the El-Centro acceleration record, the data points are at equal time steps of 0.02 s and the same had been used as time step in all the analyses of box-type laterite masonry structures under El-Centro earthquake reported so far. In order to verify the accuracy of such responses obtained, an analysis was repeated with time step of 0.01s for ground acceleration for the building Type ALRV.

Deflection u_z for building Type ALRV with time step of ground acceleration selected as 0.01 s is shown in Fig. 5.35. The responses obtained for the said problem with 0.01 s as time step is quite similar to the one obtained with 0.02 s as time step. Hence, the time interval for ground acceleration was kept at 0.02 s for all the other analyses with El Centro acceleration records.
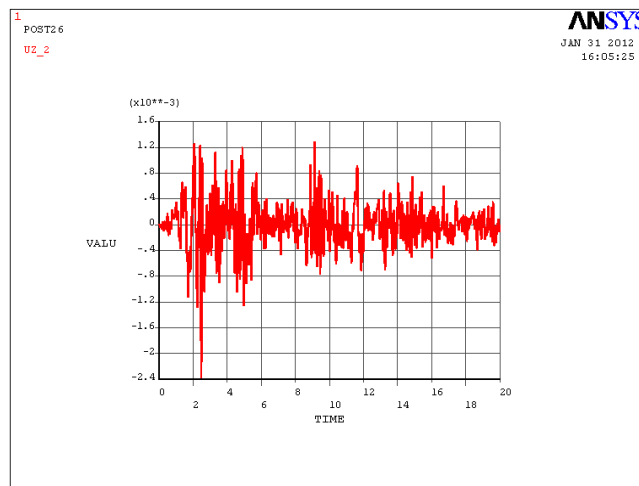
Fig. 5.35 Time history response of deflection u_z (m) of the node at the center of top edge of long wall in structure Type ALRV for δt=0.01s

Results of equivalent static analysis on box type laterite masonry structures with roof (B, BV, BL and BLV), indicates that the out-of-plane deflection of these structures were quite small as compared to those without roof. Nodes with peak deflections were identified from equivalent static analysis and the time history responses of those nodes under El-Centro earthquake were taken. Fig. 5.36 to Fig. 5.39 shows the time history responses of deflection u_z of the nodes at 2.25 m height, along the center of the wall in all the four cases (B, BV, BL and BLV).
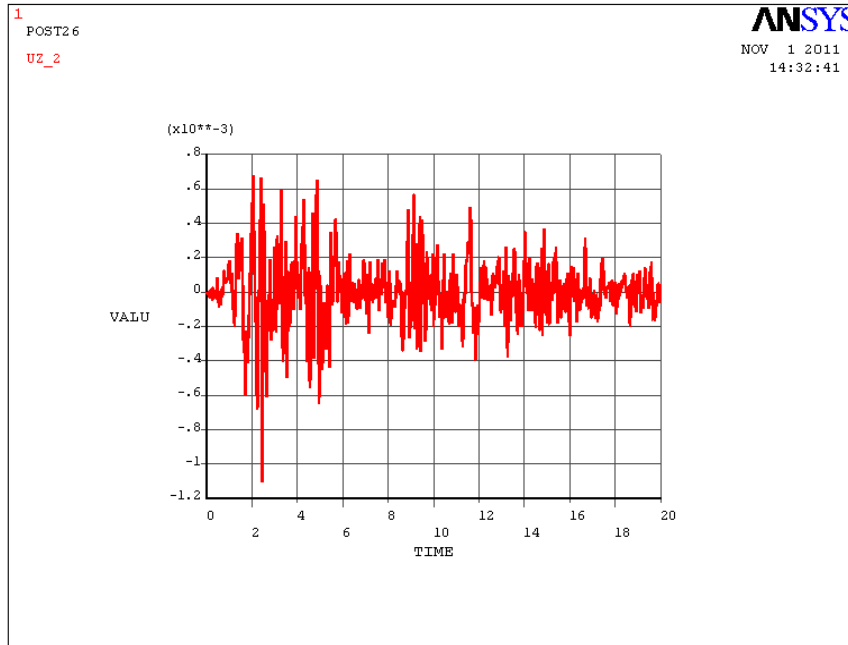
Fig. 5.36 Time history response of deflection u$_z$ (m) of the node at center of long wall at ¾th height of structure Type B
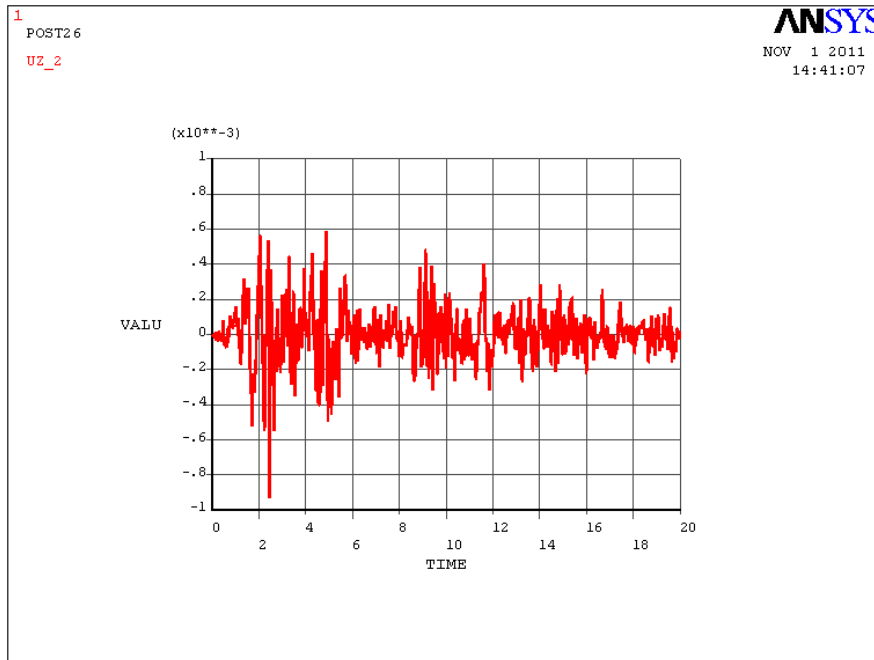
Fig. 5.37 Time history response of deflection u$_z$ (m) of the node at center of long wall at ¾th height of structure Type BV
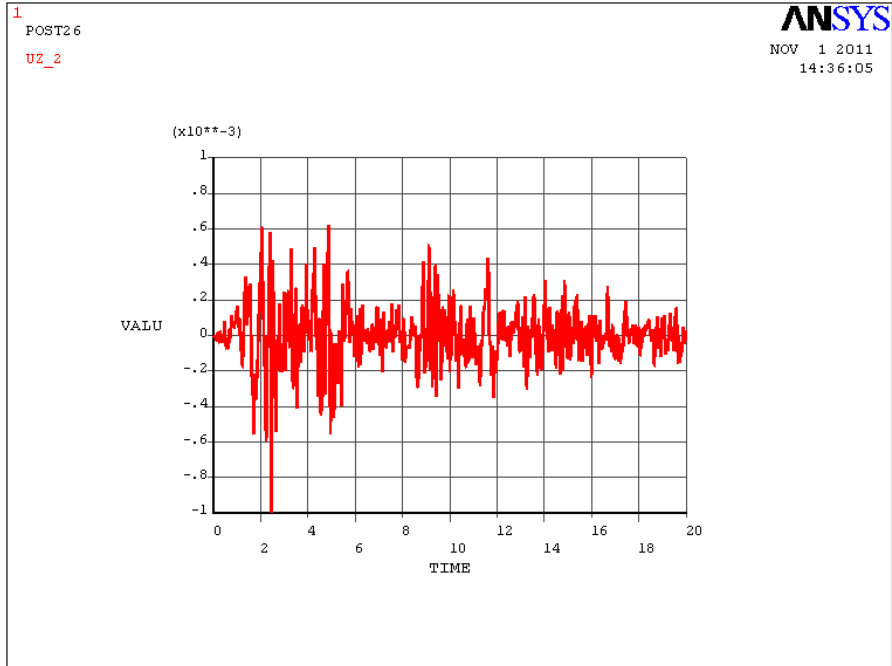
Fig. 5.38 Time history response of deflection u_z (m) of the node at center of long wall at ¾ [th] height of structure Type BL
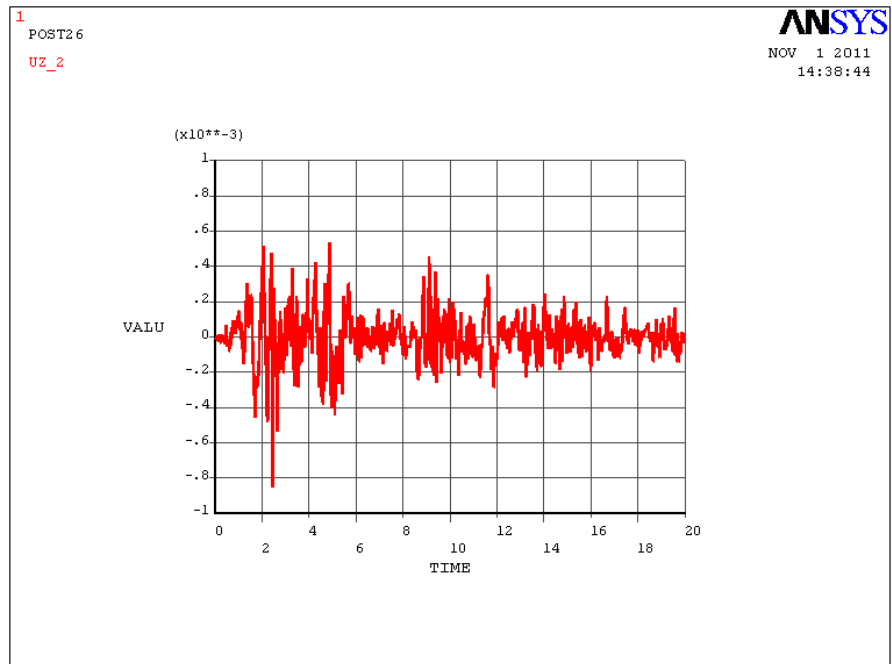
Fig. 5.39 Time history response of deflection u_z (m) of the node at center of long wall at ¾ [th] height of structure Type BLV

The peak deflection in structure Type B was noted as 1.1 mm. This was observed to have reduced to 0.93 mm in structure BV, which is 16% less than that of structure Type B. The corresponding peak deflections were noted as 0.995 mm and 0.85 mm respectively, in structure Type BL and BLV, which are 10% and 23% less than that of structure Type B. Fig. 5.40 shows a comparison of the time history response u_z of the most vulnerable node observed from equivalent static analysis for structures with roof.
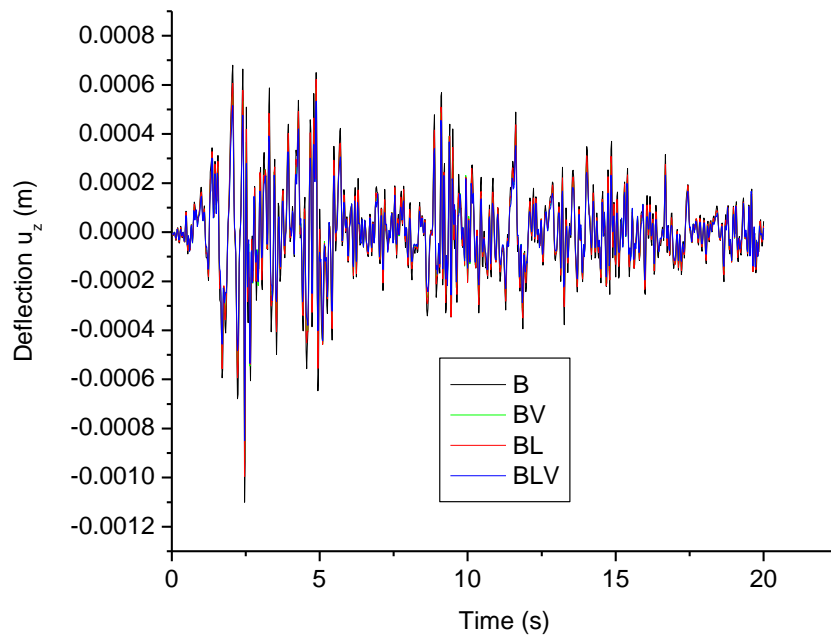
Fig. 5.40 Comparison of time history response of deflection u_z (m) of the node at center of long wall at ¾ th height of structures with roof

The results show that the rigid roof itself has helped to reduce the out-of-plane deflections significantly. Containment reinforcement has helped to reduce the deflection further while the lintel band alone has not helped to reduce the out-of-plane deflection significantly, but provision of lintel band employed along with containment reinforcement has helped to reduce the out-of-plane deflection by 23%. Fig. 5.41 shows a comparison of the time history response u_z for structure without roof Type A and structure with roof Type B.
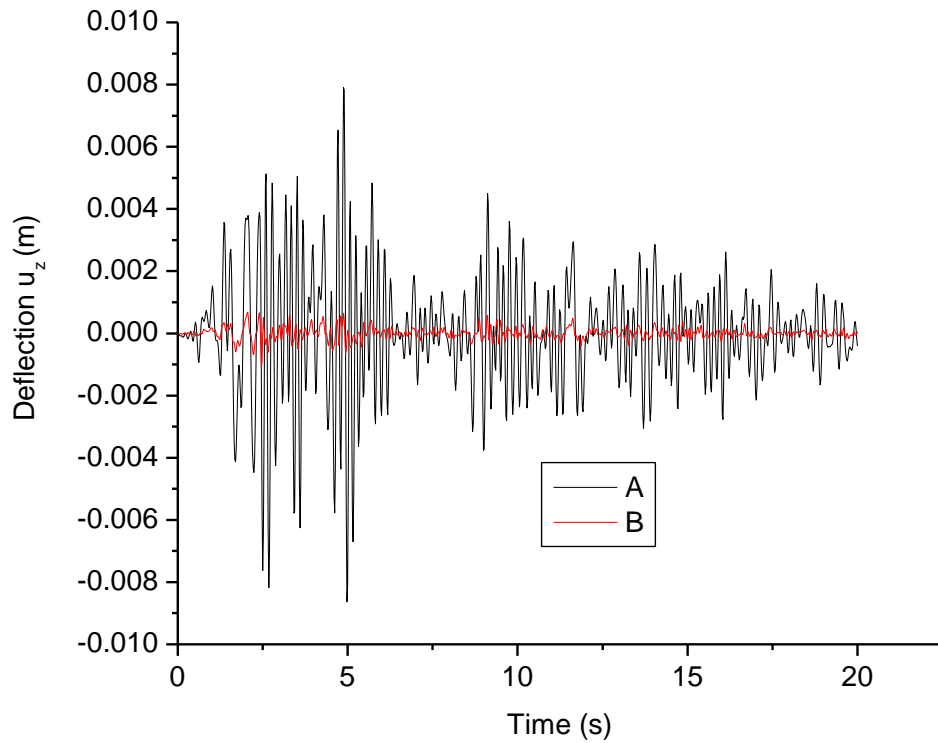
**Fig. 5.41 Comparison of time history response of deflection u_z (m)
of the most vulnerable node of structure Type A and Type B**

5.3.2 Time-History Response of Stress σ_y in Long Walls

Nodes with maximum stress σ_y had been identified from equivalent static analysis and time history responses of stress σ_y at those nodes were plotted. Fig. 5.42 to Fig. 5.45 show the time history responses of vertical stress σ_y for building Types A, AV, ALR and ALRV.
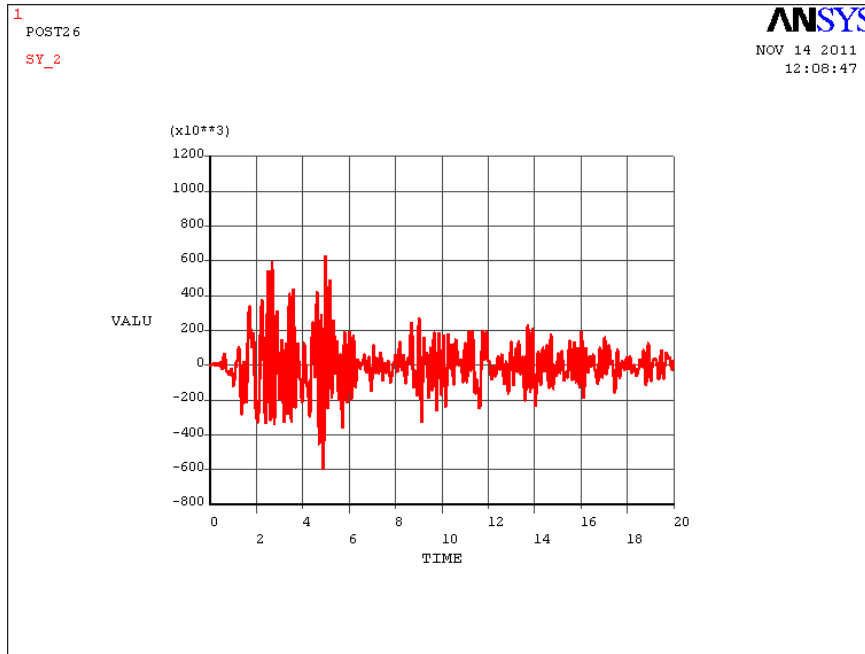
Fig. 5.42 Time history response of stress σ_y (N/m^2) of the node near the center of bottom edge of long wall in structure Type A
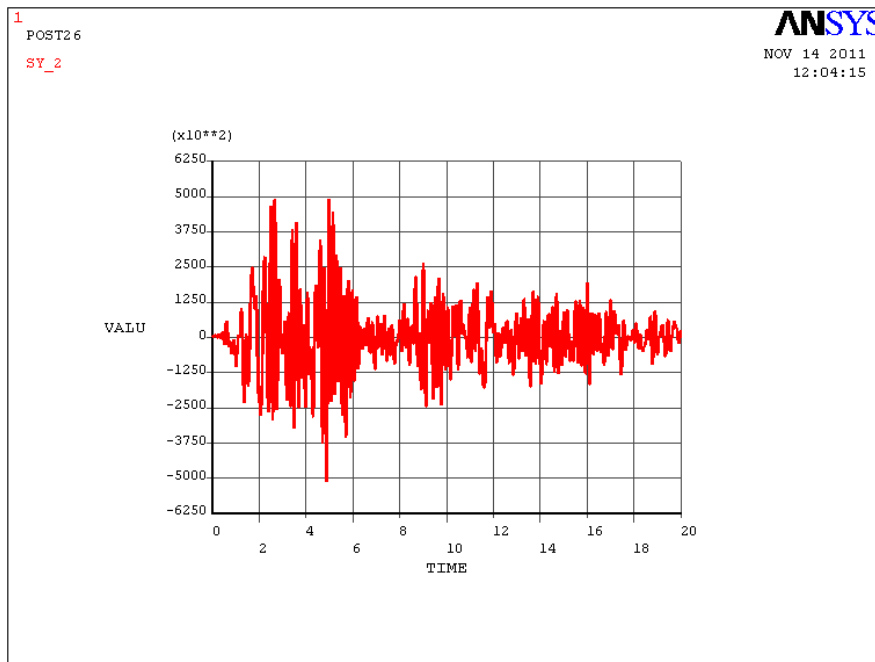
Fig. 5.43 Time history response of stress σ_y (N/m^2) of the node near the center of bottom edge of long wall in structure Type AV
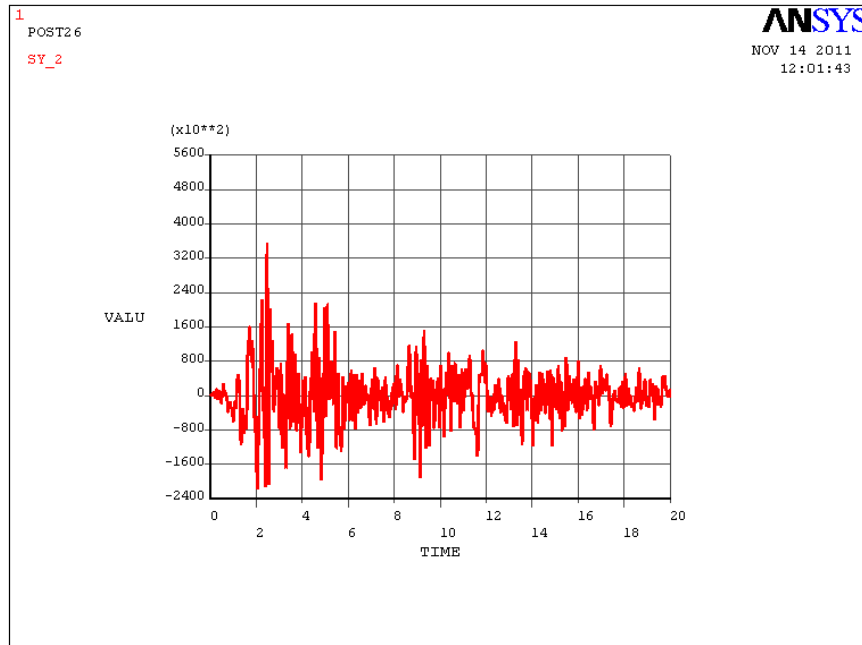
Fig. 5.44 Time history response of stress σ_y (N/m^2) of the node near the center of bottom edge of long wall in structure Type ALR
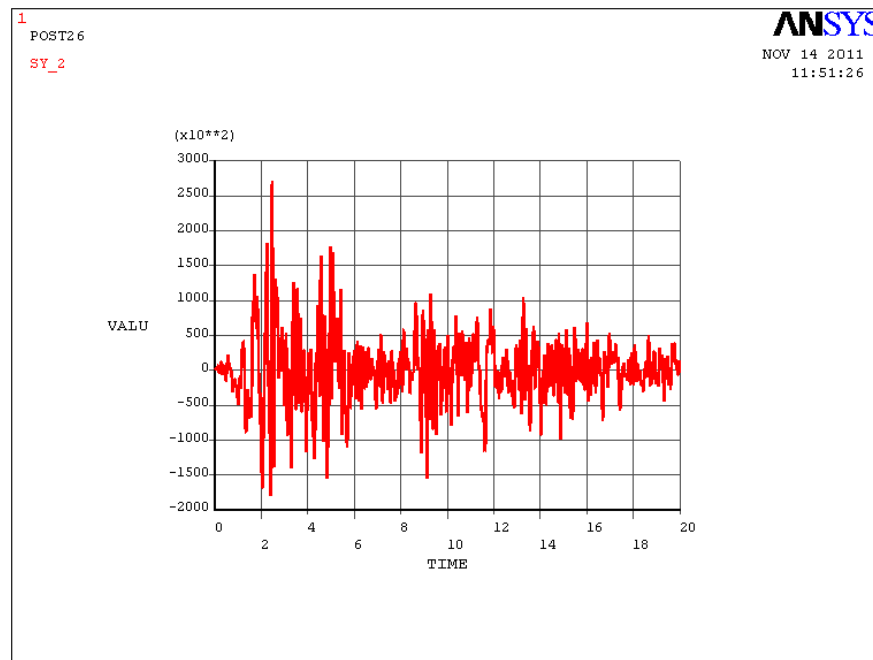
Fig. 5.45 Time history response of stress σ_y (N/m^2) of the node near the center of bottom edge in structure Type ALRV

108

The maximum value of σ_y was observed as 0.63 MPa in building Type A. This has reduced to 0.49 MPa in building Type AV, a reduction of 22%. The maximum values of σ_y in building Type ALR and ALRV were noted as 0.35 MPa and 0.27 MPa respectively, reductions of 44% and 57% respectively, from that of building Type A. Fig. 5.46 shows a comparison of the time history response σ_y of the most vulnerable node observed from equivalent static analysis for structures without roof.
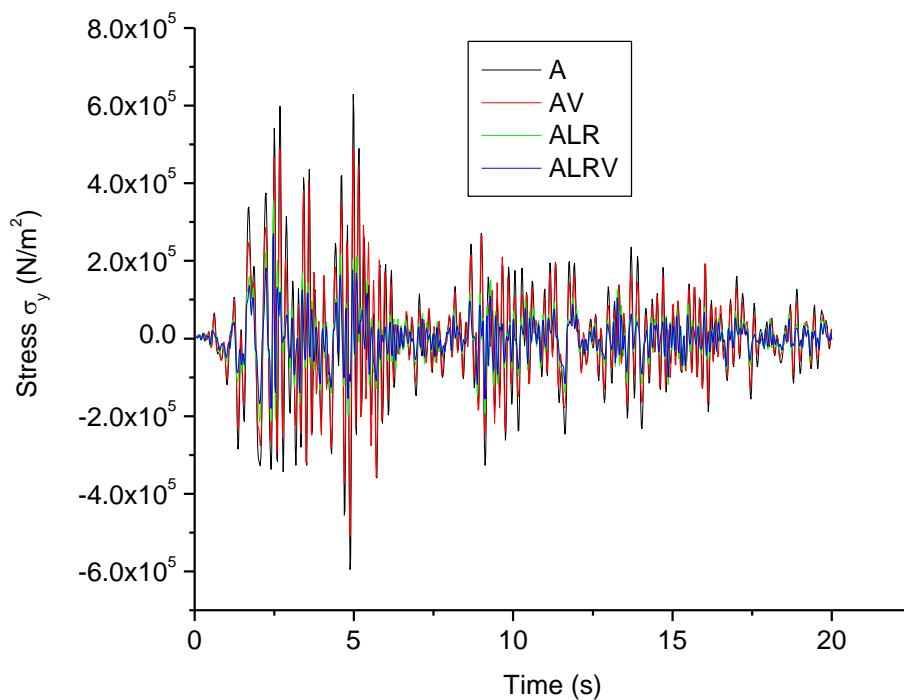
Fig. 5.46 Comparison of time history response of stress σ_y (N/m^2) of the node near the center of bottom edge in structures without roof

In box-type laterite masonry structures without roof, RC bands have helped to reduce the stresses σ_y considerably. Still vertical containment reinforcement has helped to reduce the stresses σ_y further. Thus in box-type laterite masonry structures without roof, provision of RC bands along with containment reinforcement helps to reduce the stresses σ_y and thus reduce the chances of horizontal cracks in the masonry.

In box-type laterite masonry structures with roof, maximum stress σ_y was observed at the corner of base of long wall. Fig. 5.47 to Fig. 5.50 show the time history responses of the node near the corner of base edge, for stresses σ_y for building types B, BV, BL and BLV.
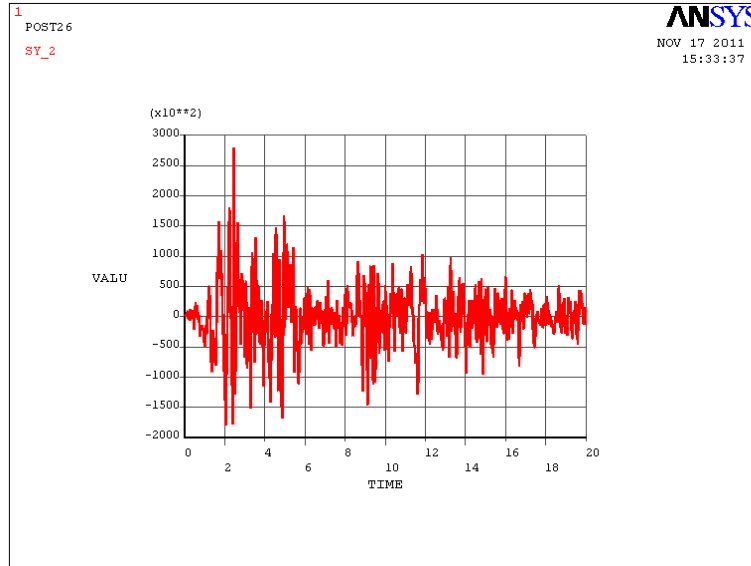
Fig. 5.47 Time history response of stress σ_y (N/m^2) of the node near the corner of bottom edge of long wall in structure Type B
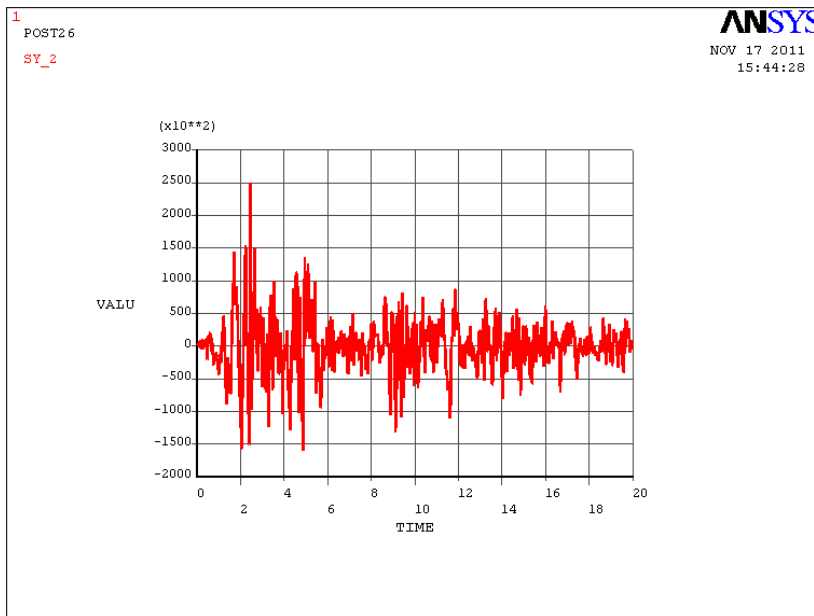
Fig. 5.48 Time history response of stress σ_y (N/m^2) of the node near the corner of bottom edge of long wall in structure Type BV
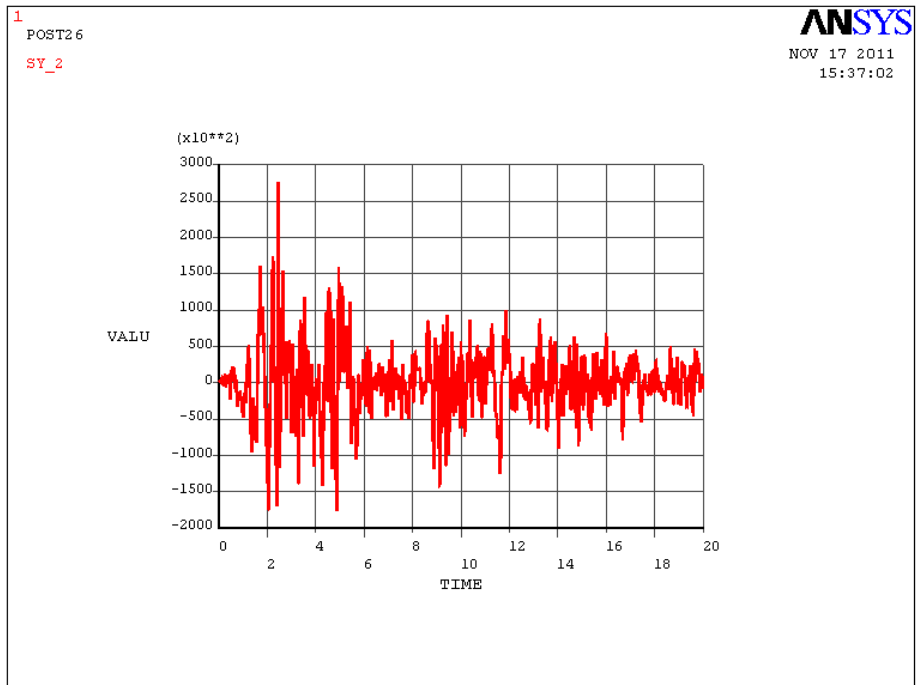
Fig. 5.49 Time history response of stress σ_y (N/m²) of the node near the corner of bottom edge of long wall in structure Type BL
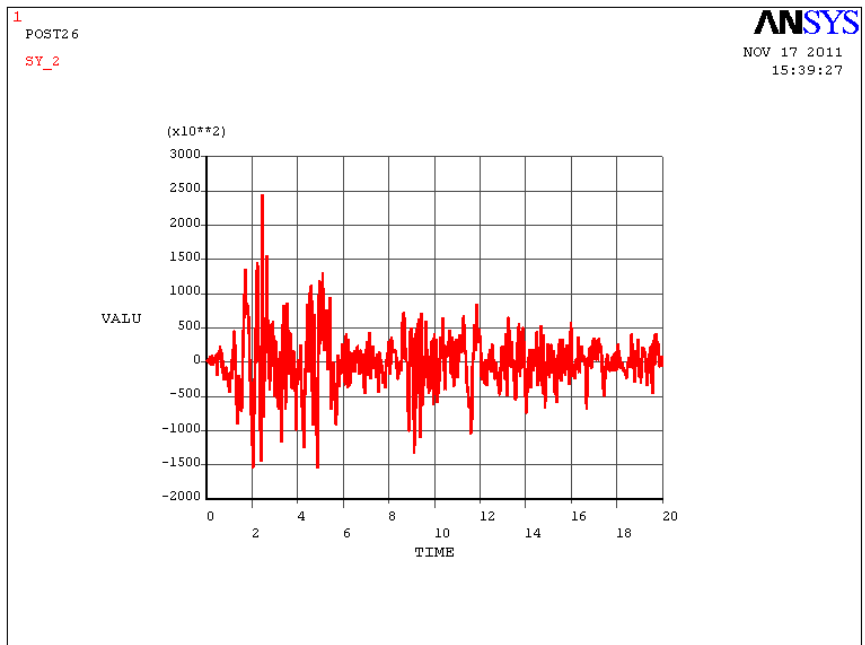
Fig. 5.50 Time history response of stress σ_y (N/m²) of the node near the corner of bottom edge of long wall in structure Type BLV

Fig. 5.51 shows a comparison of time history response of stress σ_y for structures with roof.
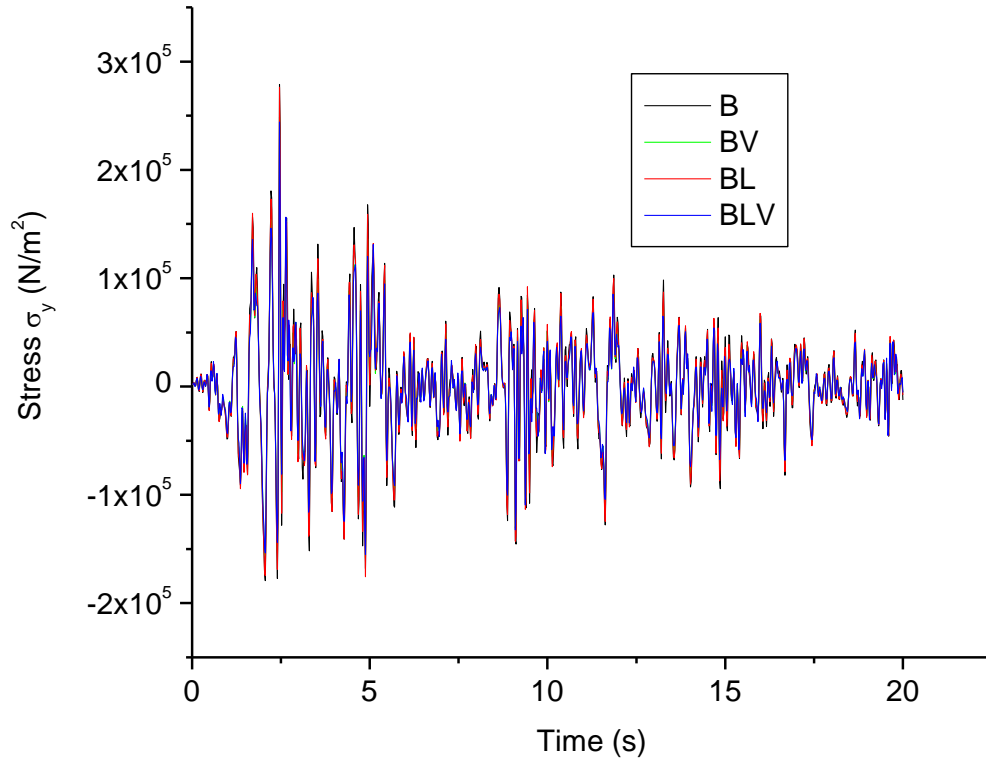
Fig. 5.51 Comparison of time history response of stress σ_y (N/m^2) of the node near the corner of bottom edge of long wall in structures with roof

The maximum value of σ_y was observed to be, 0.28 MPa in building Type B. This just reduced to 0.25 MPa in building Type BV, a reduction of 11%. The maximum value of σ_y in building Type BL was noted as 0.28 MPa which was the same as the maximum value in building Type B. In case of BLV, the maximum value was 0.24 MPa a reduction of 14% from that of building Type B. Thus in box-type laterite masonry structures with roof, provision of the containment reinforcement may prove structurally more efficient than a lintel band in reducing the stress σ_y.

Fig. 5.52 shows a comparison of time history response of stress σ_y in structure Type A and Type B. In box-type laterite masonry structure with roof (B), the maximum value of stress σ_y was observed to be almost 55% less than that of structure without roof (A).
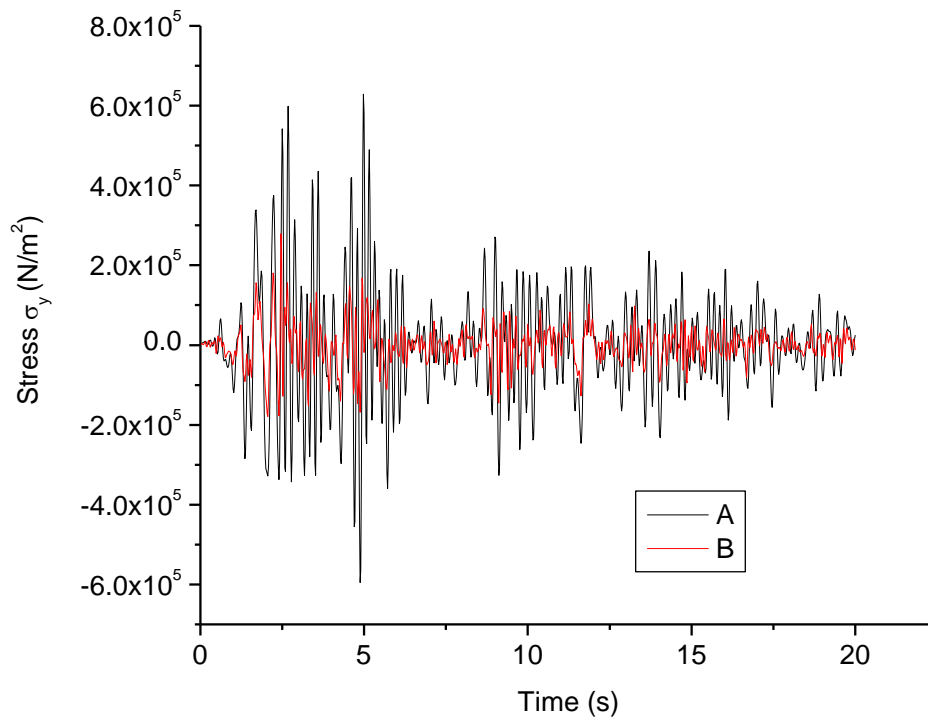
**Fig. 5.52 Comparison of time history response of stress σ_y (N/m^2)
of the most vulnerable node of structure Type A and Type B**

5.3.3 Time-History Response of Stress σ_x in Long Walls

For box-type laterite masonry structures without roof, the maximum value of σ_x was observed around the center near the top edge of the long wall. Fig. 5.53 to Fig. 5.56 shows the time history response σ_x of the nodes where maximum value of σ_x was observed in building Types A, AV, ALR and ALRV respectively.
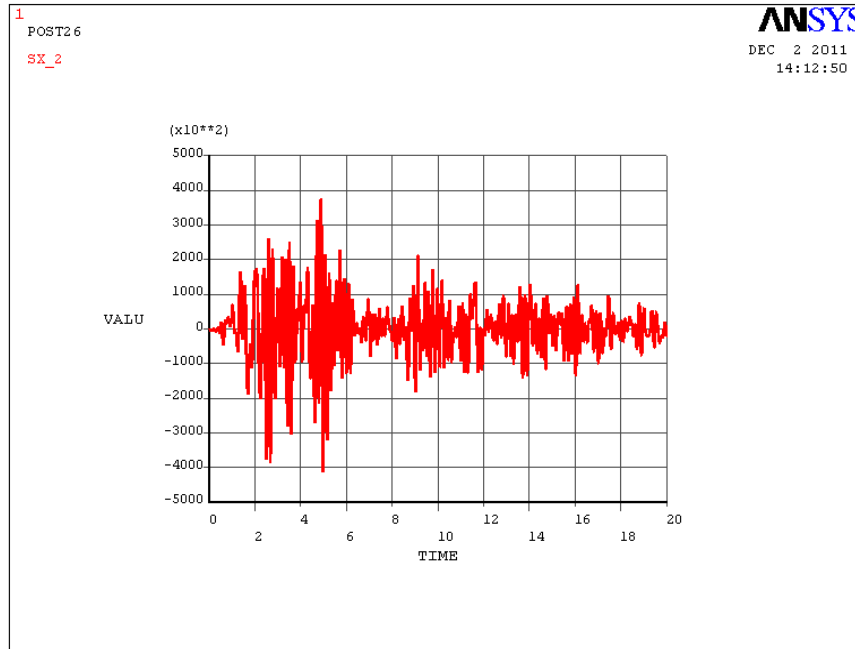
Fig. 5.53 Time history response of stress σ_x (N/m^2) of the node around the center near the top edge of long wall in structure Type A
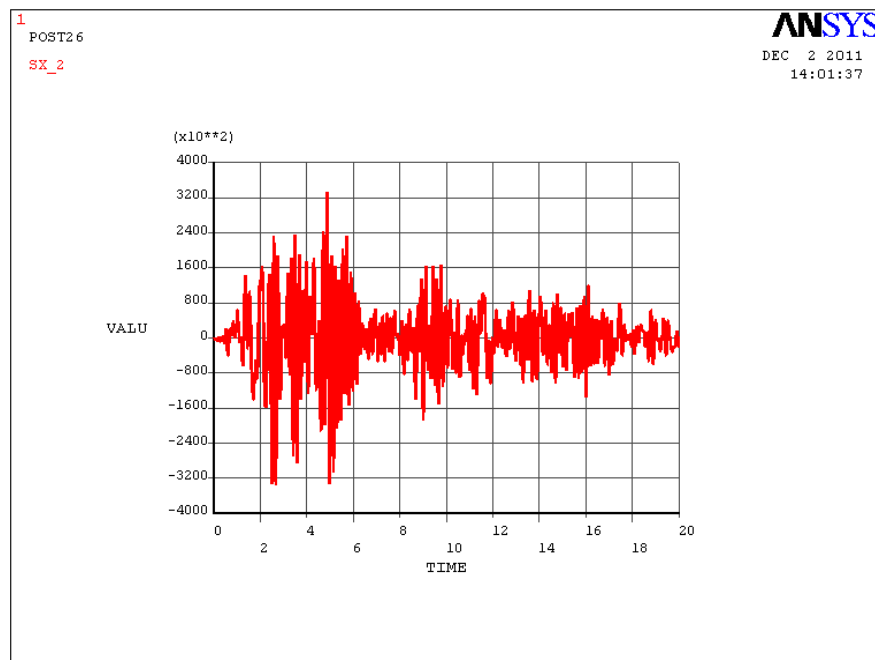
Fig. 5.54 Time history response of stress σ_x (N/m^2) of the node around the center near the top edge of long wall in structure Type AV
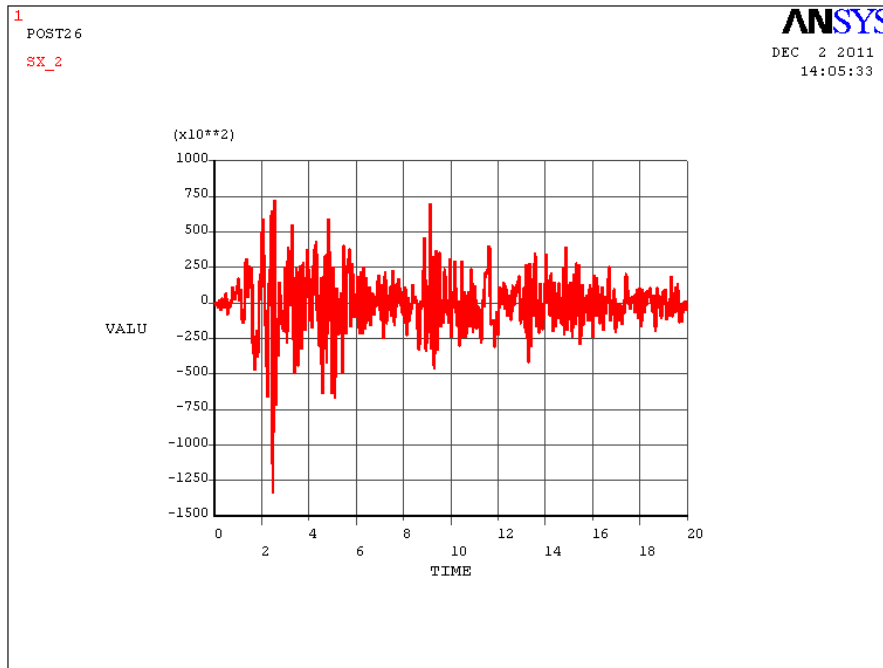
Fig. 5.55 Time history response of stress σ$_x$ (N/m^2) of the node around the center near the top edge of long wall in structure Type ALR
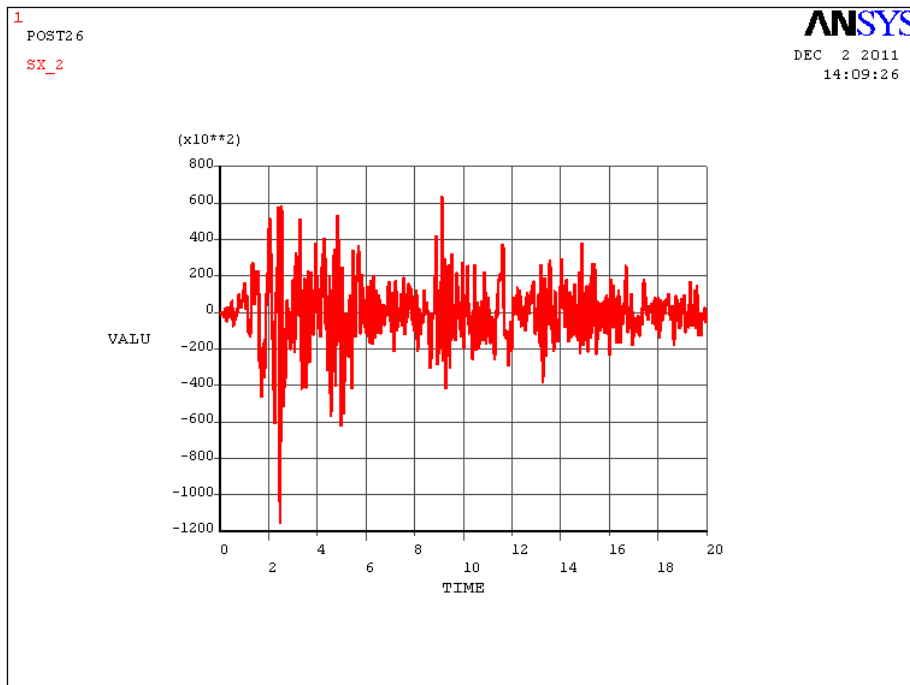
Fig. 5.56 Time history response of stress σ$_x$ (N/m^2) of the node around the center near the top edge of long wall in structure Type ALRV

The maximum value of σ_x was observed as 0.42 MPa in building Type A. This has reduced to 0.34 MPa in building Type AV, a reduction of 19%. Correspondingly the maximum values of σ_x in building Type ALR and ALRV were noted as 0.13 MPa and 0.12 MPa respectively, which are 69% and 71% less than the maximum σ_x in building Type A. Thus in box type laterite masonry structures without roof, RC bands have helped to reduce the stresses σ_x considerably and the effect of vertical containment reinforcement is not appreciable. Fig. 5.57 show a comparison of time history response σ_x in structures without roof, for the most vulnerable node obtained from equivalent static analysis.
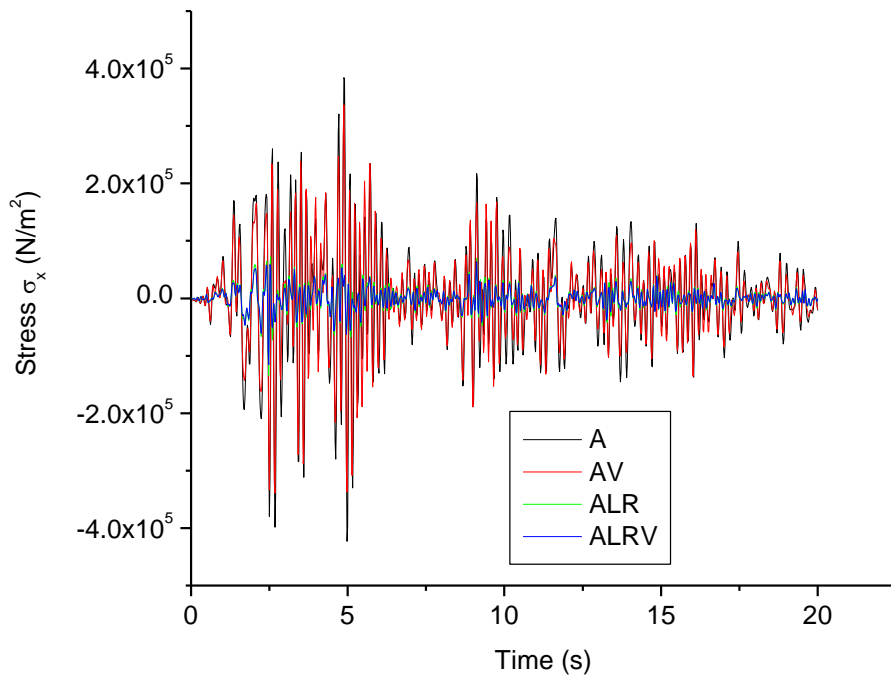
**Fig. 5.57 Comparison of time history response of stress σ_x (N/m^2)
of the most vulnerable node in structures without roof**

Fig. 5.58 to Fig. 5.61 show the time history responses for σ_x of the nodes at the sill level, where maximum value of σ_x was observed in building types B, BV, BL and BLV respectively.

116
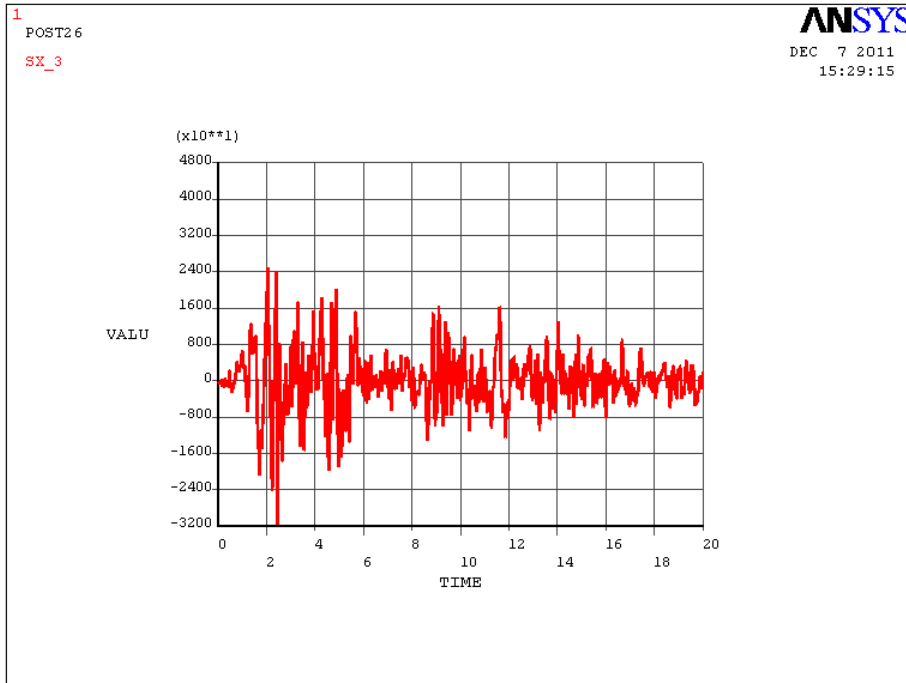
Fig. 5.58 Time history response of stress σ_x (N/m^2) of a node at sill level of long wall in structure Type B
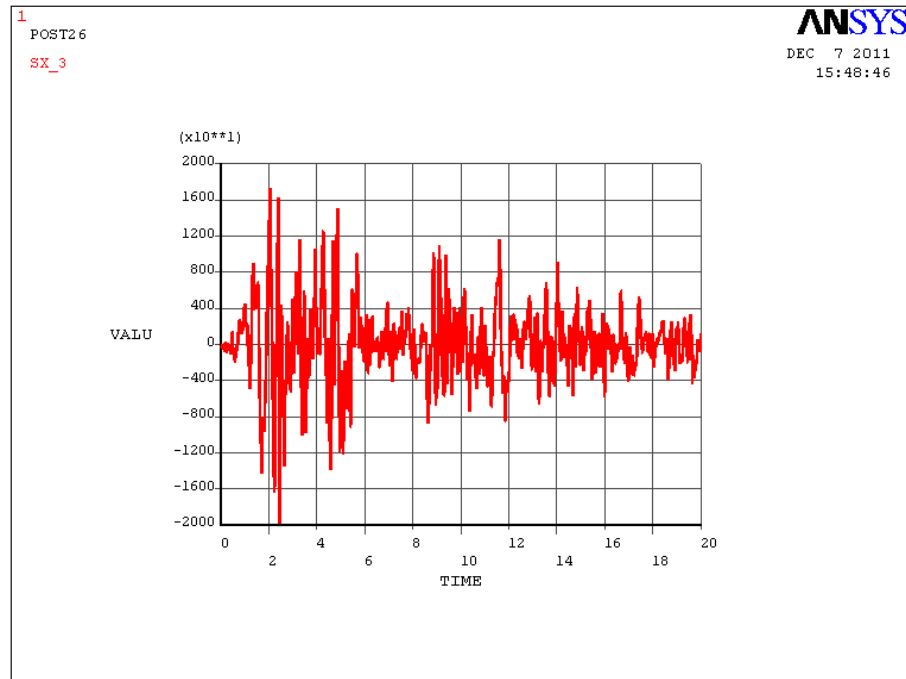
Fig. 5.59 Time history response of stress σ_x (N/m^2) of a node at sill level of long wall in structure Type BV
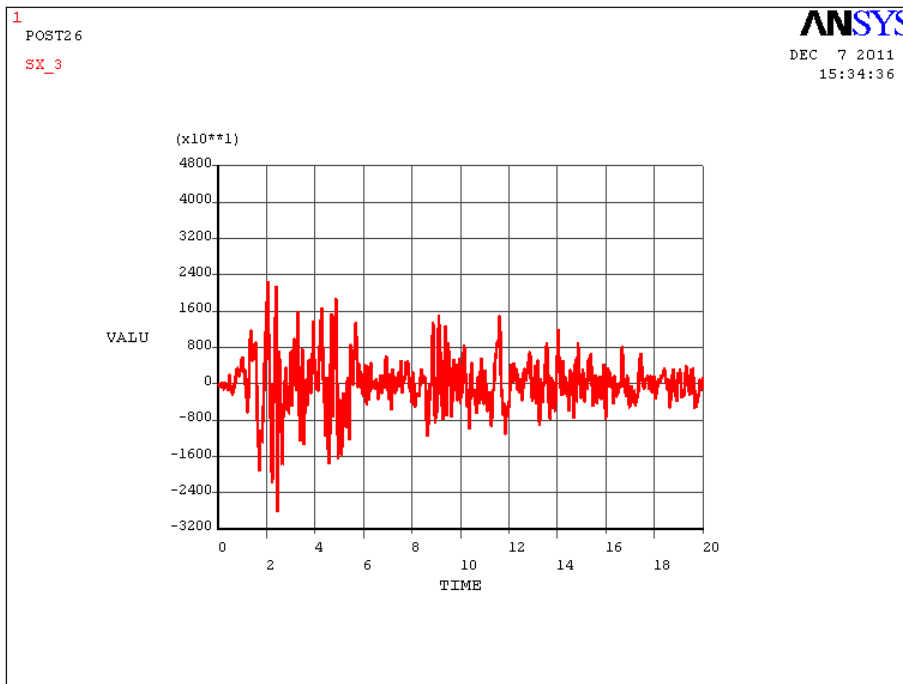
Fig. 5.60 Time history response of stress σ_x (N/m^2) of a node at sill level of long wall in structure Type BL
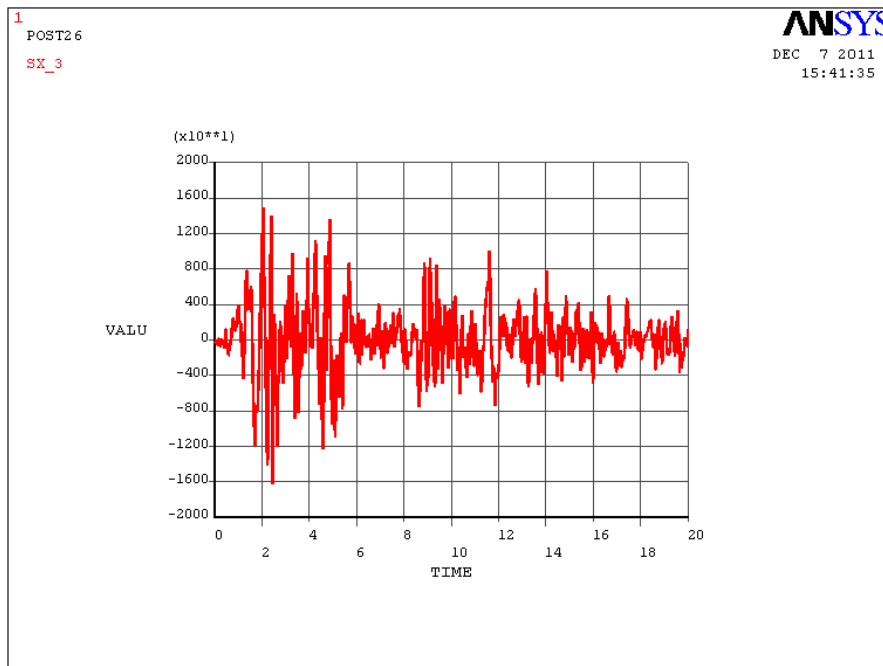
Fig. 5.61 Time history response of stress σ_x (N/m^2) of a node at sill level of long wall in structure Type BLV

The maximum value for stress σ_x in laterite masonry structure B was noted as 0.032 MPa. This got reduced to 0.028 MPa, 0.02 MPa and 0.016 MPa in structure Types BL, BV and BLV respectively, which are 13%, 38% and 50% lesser than that of structure Type B. Fig. 5.62 show a comparison of time history response σ_x in structures with roof, for the most vulnerable node obtained from equivalent static analysis.
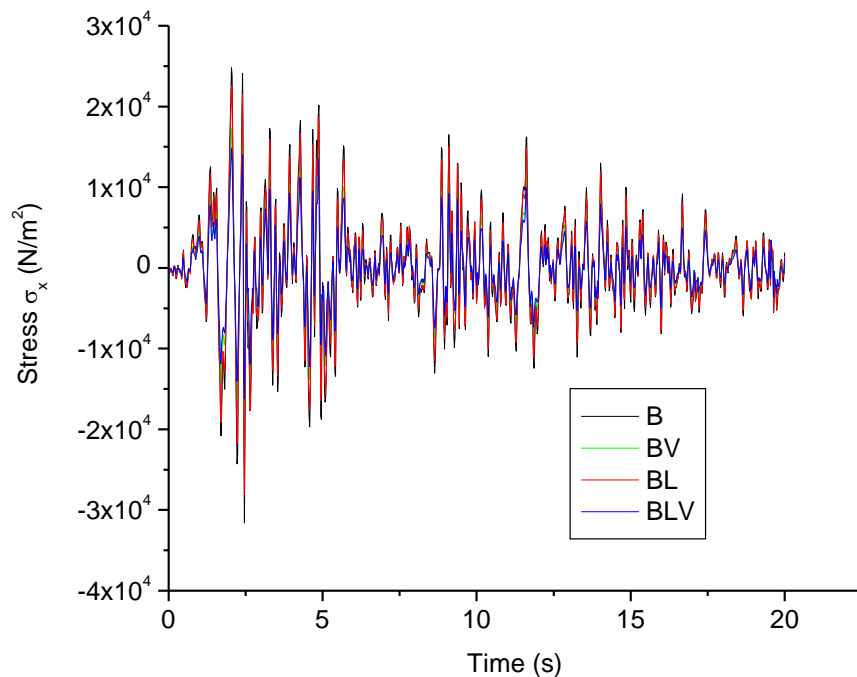
Fig. 5.62 Comparison of time history response of stress
σ_x (N/m^2) of the most vulnerable node in structures with roof

The maximum value of stress σ_x in box type laterite masonry structure with roof (B) is almost 92% less than that in structure without roof (A). Fig. 5.63 shows a comparison of time history response of stress σ_x in structure Type A and Type B. In structures with roof, however, containment reinforcement has proved to be more effective than providing a lintel band in reducing the stress σ_x. Containment reinforcement together with lintel band has helped to further reduce the maximum stress σ_x by more than 50%.
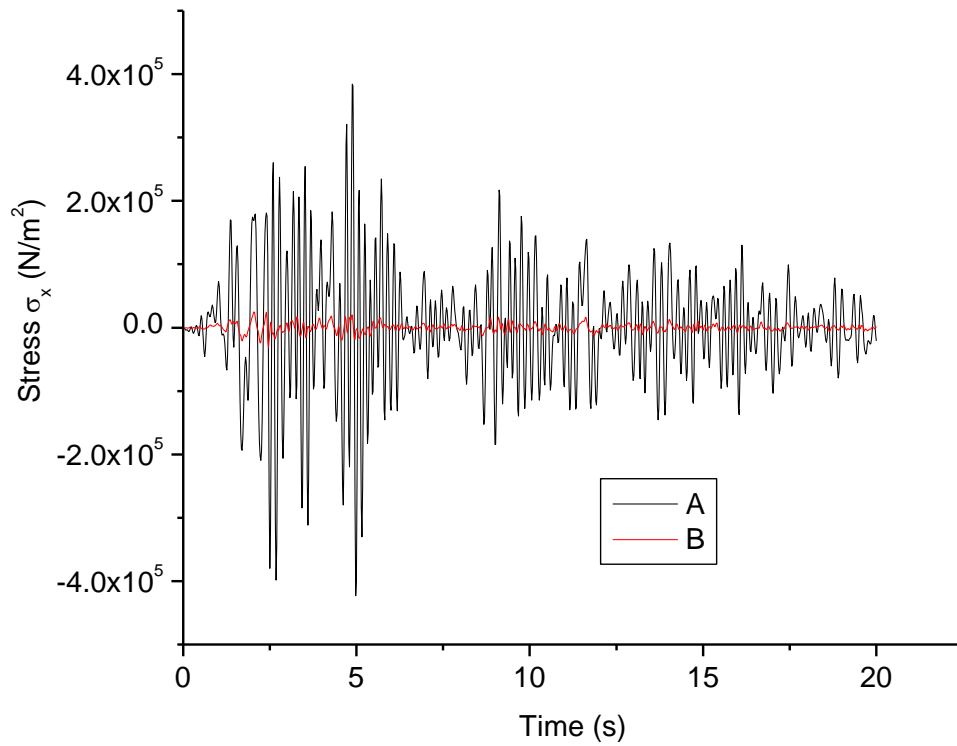
**Fig. 5.63 Comparison of time history response of stress σ_x (N/m^2)
of the most vulnerable node of structure Type A and Type B**

5.3.4 Time-History Response of Shear Stress σ_{yz} in Short Walls

For box-type laterite masonry structures without roof, the maximum value of σ_{yz} in short wall, was observed at the corner of opening at lintel level. Fig. 5.64 to Fig. 5.67 shows the time history response σ_{yz} of the nodes where maximum value of σ_{yz} was observed in building Types A, AV, ALR and ALRV respectively.
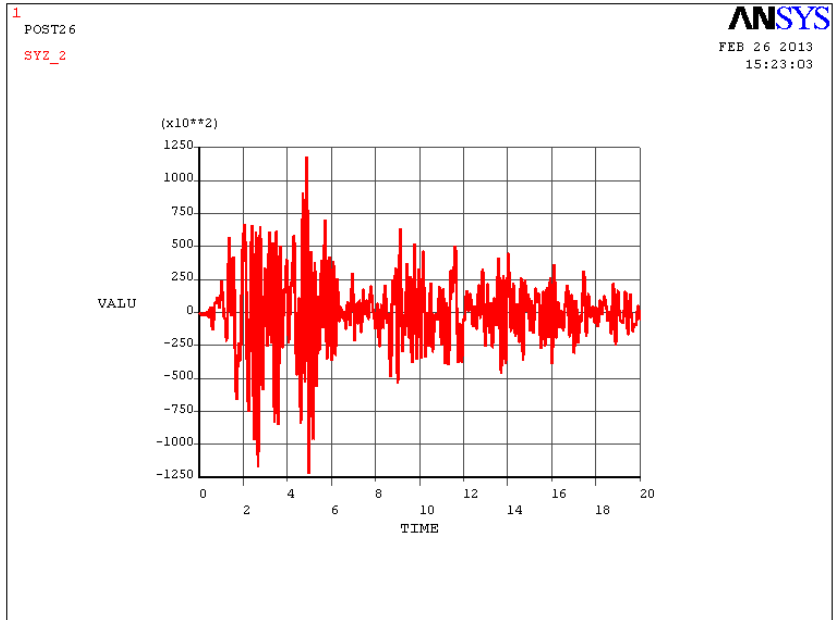
Fig. 5.64 Time history response of shear stress σ$_{yz}$ (N/m^2) of the node at corner of opening at lintel level in structure Type A
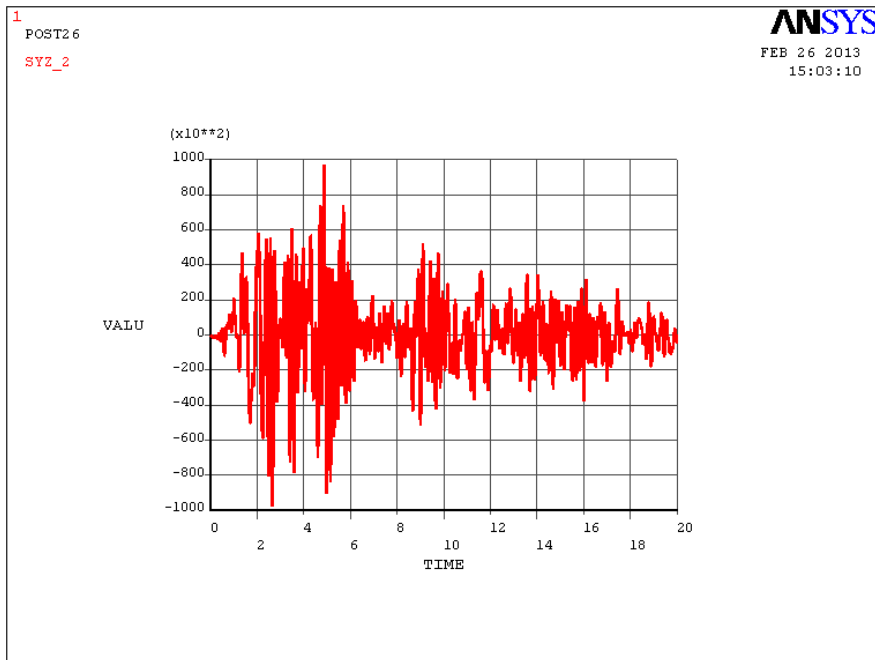
Fig. 5.65 Time history response of shear stress σ$_{yz}$ (N/m^2) of the node at corner of opening at lintel level in structure Type AV
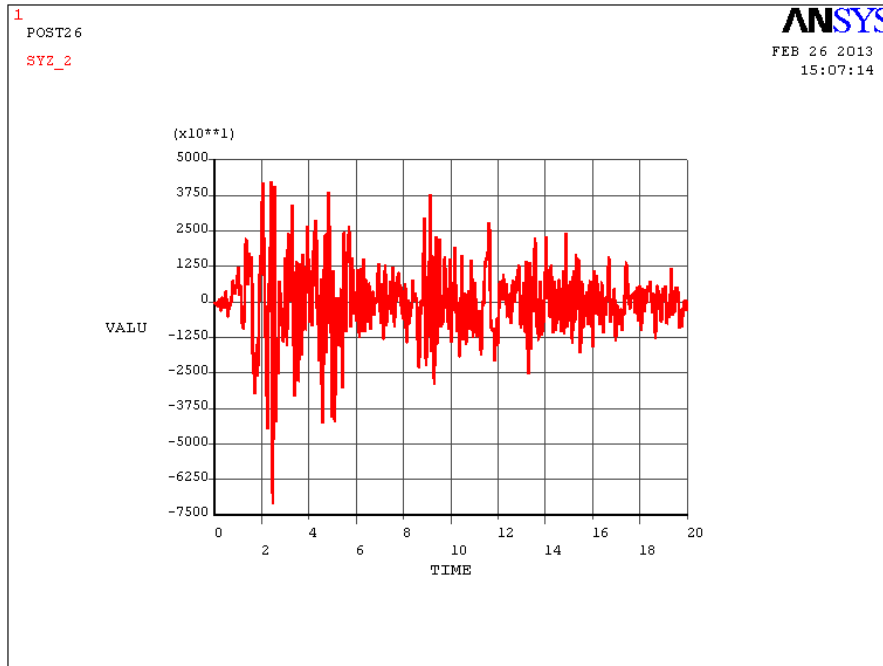
**Fig. 5.66 Time history response of shear stress σ$_{yz}$ (N/m^2) of
the node at corner of opening at lintel level in structure Type ALR**
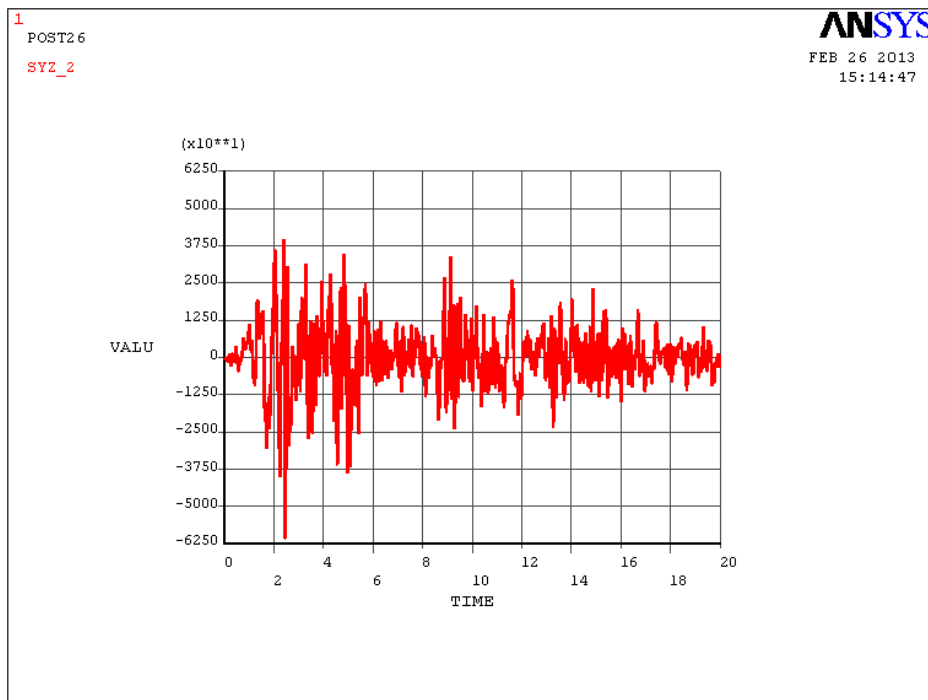
**Fig. 5.67 Time history response of shear stress σ$_{yz}$ (N/m^2) of
the node at corner of opening at lintel level in structure Type ALRV**

The maximum value for stress σ_{yz} in laterite masonry structure A was noted as 0.122MPa. This got reduced to 0.097 MPa, 0.071 MPa and 0.061 MPa in structure Types AV, ALR and ALRV respectively, which are 20%, 42% and 50% lesser than that of structure Type A. In structures without roof, RC bands seems to be effective in reducing the shear stress, but RC bands with vertical reinforcement seems to be better.

Fig. 5.68 shows a comparison of time history response σ_{yz} in structures without roof, for the most vulnerable node obtained from equivalent static analysis.
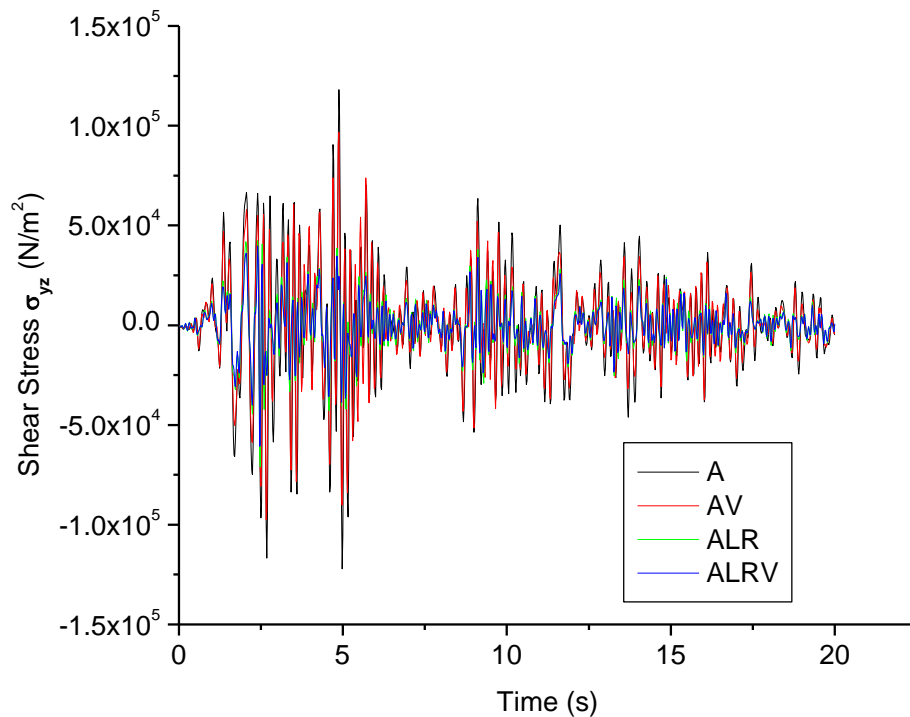
Fig. 5.68 Comparison of time history response of shear stress σ_{yz} (N/m^2) of the most vulnerable node in structures without roof

Fig. 5.69 to Fig. 5.72 show the time history responses for σ_{yz} of the nodes below sill level, where maximum value of σ_{yz} was observed in building types B, BV, BL and BLV respectively.
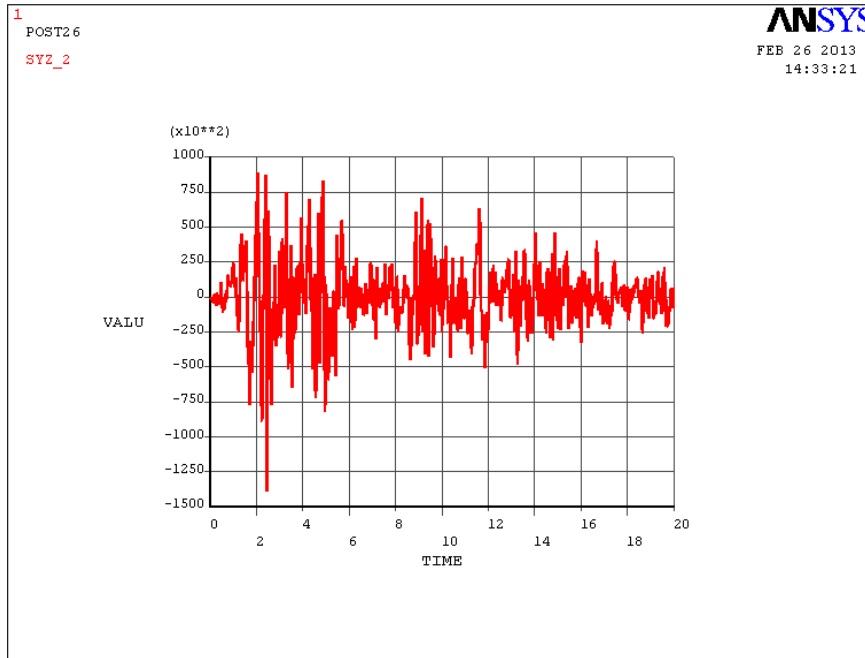
Fig. 5.69 Time history response of shear stress σ_{yz} (N/m^2) of a node below sill level of short wall in structure Type B
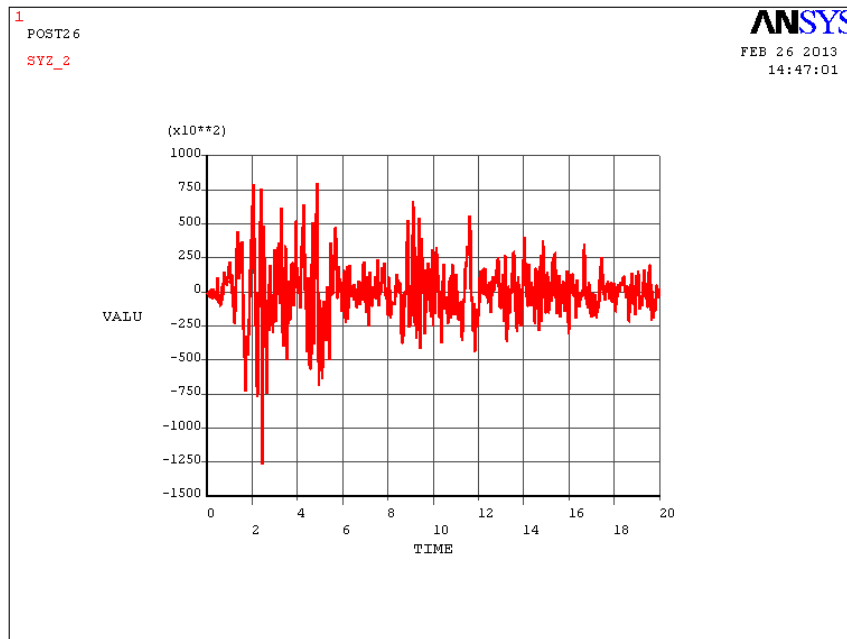
Fig. 5.70 Time history response of shear stress σ_{yz} (N/m^2) of a node below sill level of short wall in structure Type BV
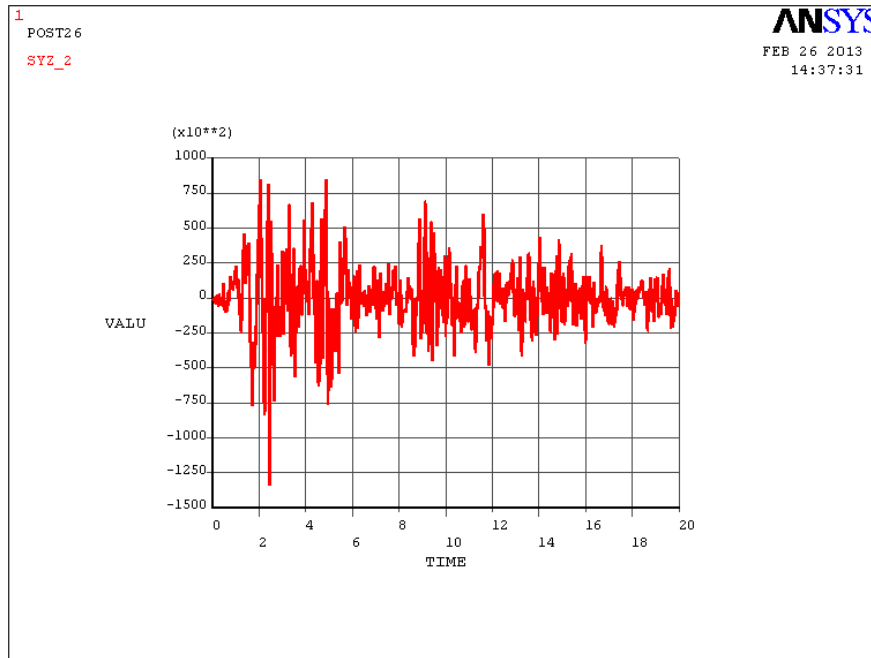
Fig. 5.71 Time history response of shear stress σ_{yz} (N/m^2) of a node below sill level of short wall in structure Type BL
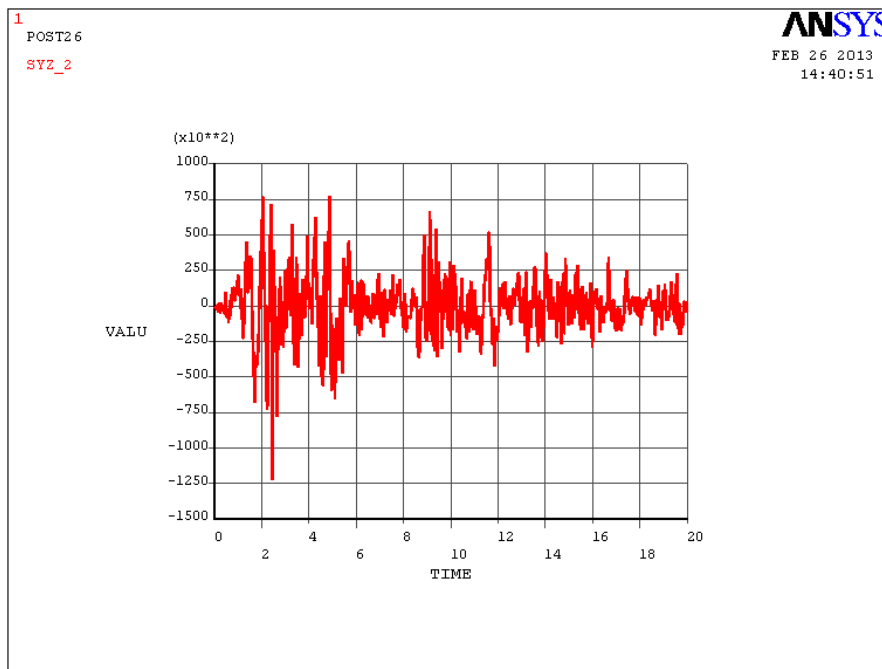
Fig. 5.72 Time history response of shear stress σ_{yz} (N/m^2) of a node below sill level of short wall in structure Type BLV

The maximum value for stress σ_{yz} in laterite masonry structure B was noted as 0.138 MPa. This got reduced to 0.134 MPa, 0.126 MPa, and 0.122 MPa in structure Types BL, BV, and BLV respectively, which are 3%, 9%, and 12% less than that of structure Type B. In structures with roof, vertical reinforcement seems to be more effective than lintel band in reducing the stresses, but lintel band with vertical reinforcement has proved to be better.

Fig. 5.73 show a comparison of time history response σ_{yz} in structures with roof, for the most vulnerable node obtained from equivalent static analysis.
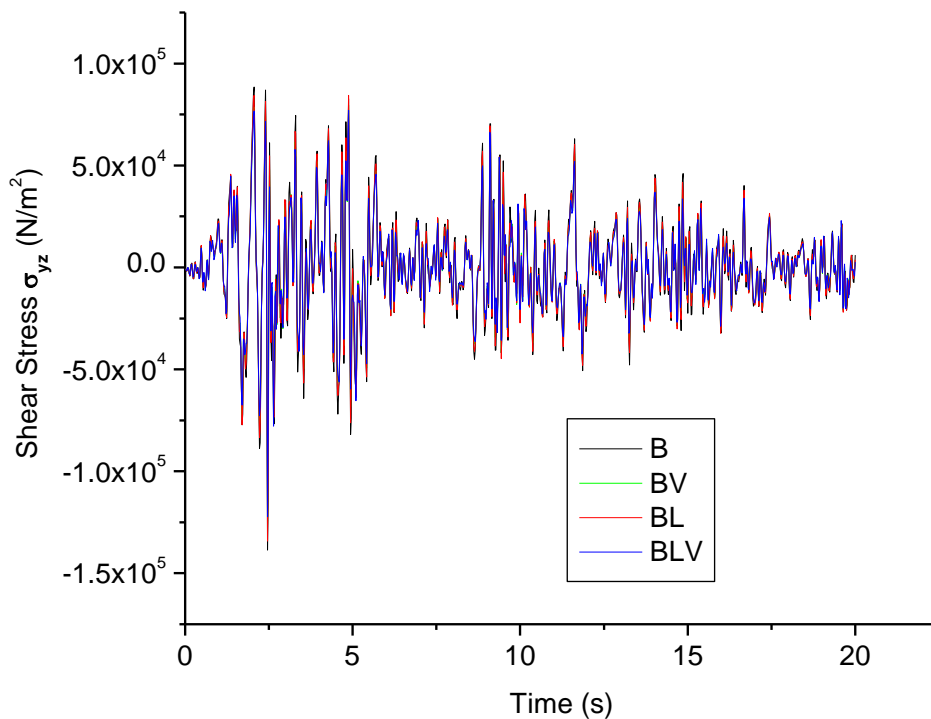
Fig. 5.73 Comparison of time history response of shear stress
σ_{yz} (N/m^2) of the most vulnerable node in structures with roof

Fig. 5.74 shows a comparison of time history response of shear stress σ_{yz} in structure Type A and Type B. Shear stress σ_{yz} was observed to be higher in structures with roof

126

compared to structures without roof. The maximum value of shear stress σ_{yz} in structure Type B was noted as 0.138 MPa which is 13% more than the maximum shear stress in Type A.
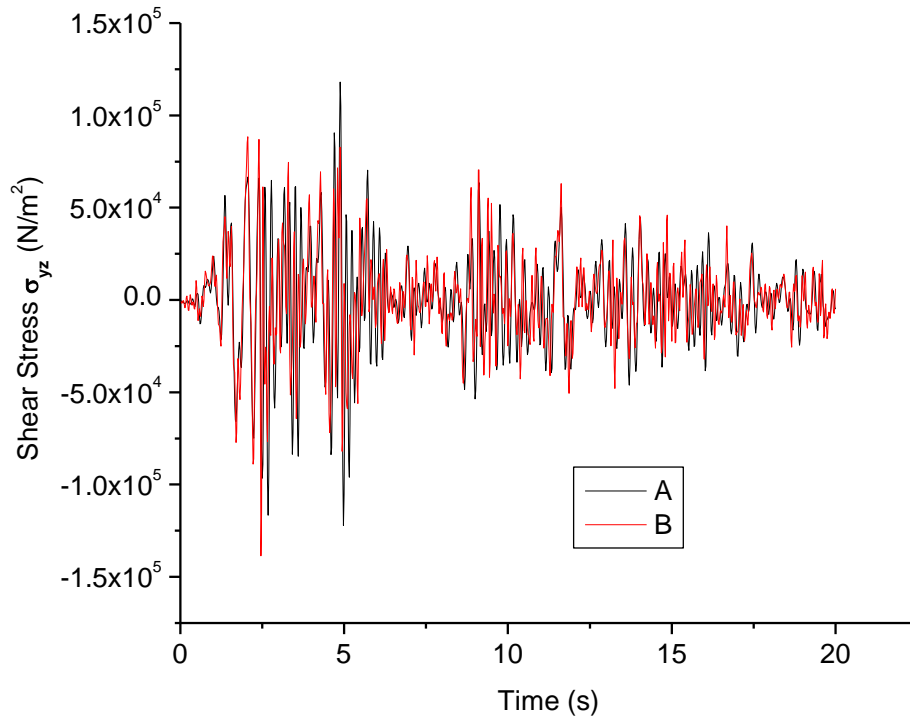
Fig. 5.74 Comparison of time history response of shear stress σ_{yz} (N/m^2) of the most vulnerable node of structure Type A and Type B

5.4 RESPONSE OF BOX TYPE LATERITE MASONRY STRUCTURES TO KOBE AND KOYNA ACCELERATIONS

As the effect of vertical reinforcements seem to be more effective in box type laterite masonry structures with roof, analyses were conducted to study the response of such structures due to Kobe and Koyna earthquake accelerations. Acceleration records of Kobe earthquake and Koyna earthquake used in the analyses are shown in Fig. 5.75 and Fig. 5.76.

127
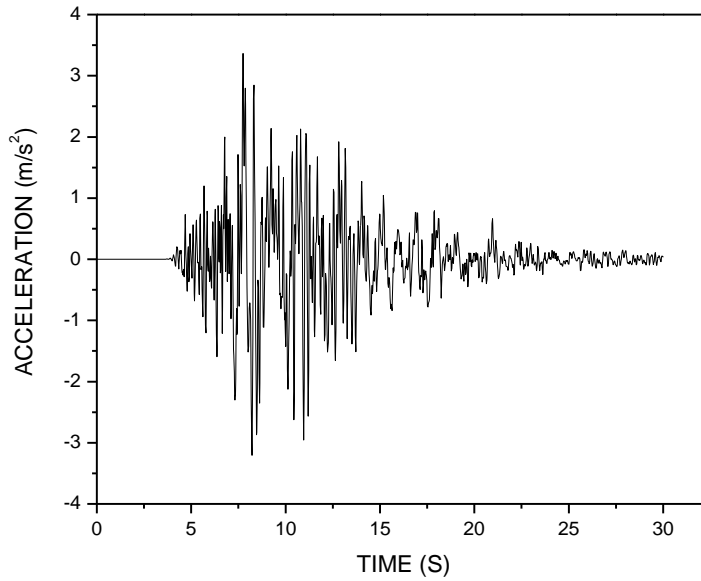
Fig. 5.75 Acceleration time history of Kobe earthquake
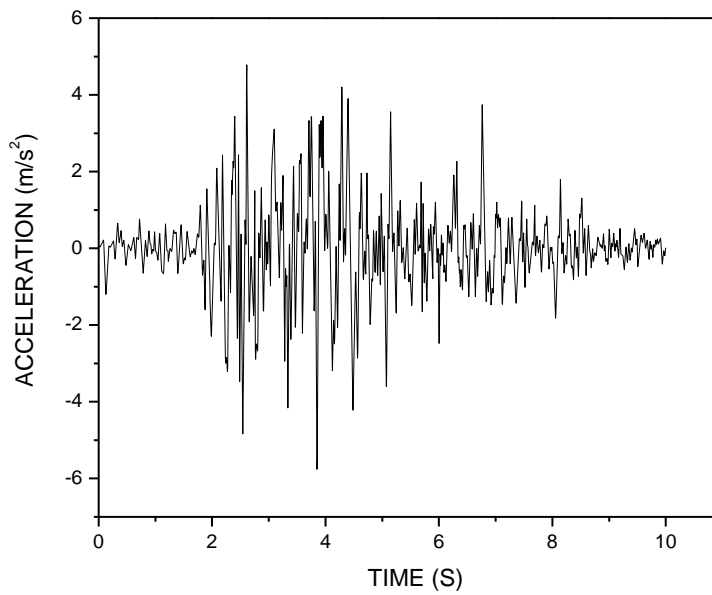
Fig. 5.76 Acceleration time history of Koyna earthquake

Fig. 5.77 and Fig. 5.78 show the Fourier amplitude spectrum of Kobe and Koyna earthquake. The predominant frequency content of Kobe acceleration record is around 0.98 Hz and that of Koyna acceleration record is around 4.49 Hz, which are significantly lower than the fundamental frequency of the buildings analyzed. Only B, BV & BLV were analyzed with Kobe and Koyna inputs. The fundamental frequency of B, BV and BLV are 11.953, 12.88 and 13.508 Hz.
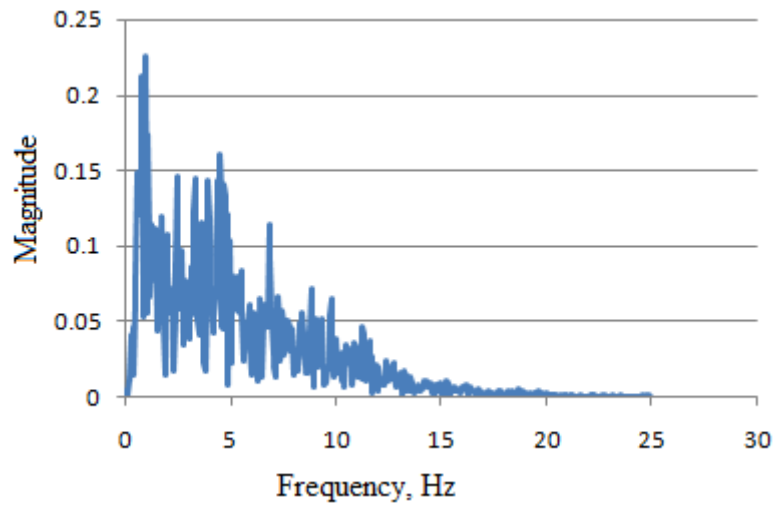
Fig.5.77 Fourier amplitude spectrum of Kobe
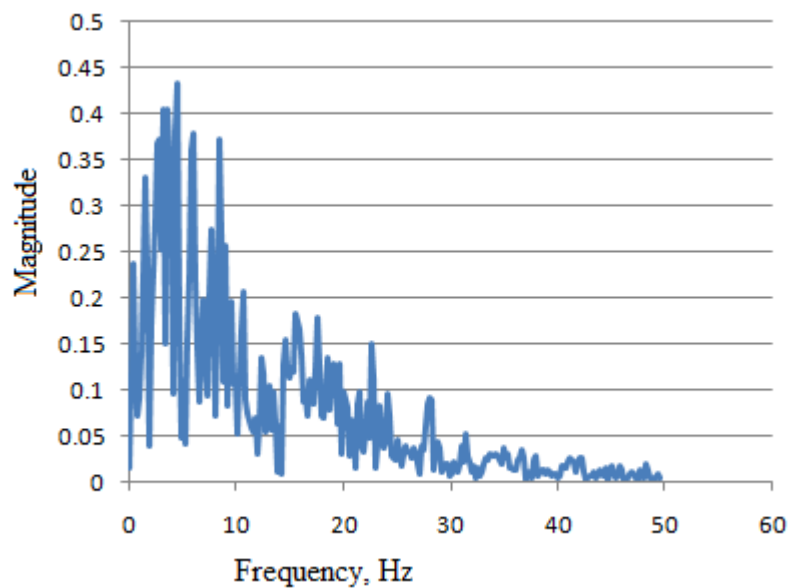
Fig.5.78 Fourier amplitude spectrum of Koyna

Linear transient analyses were conducted on single storeyed box type laterite masonry structures with roof, B, BV and BLV. Again the ground accelerations were applied perpendicular to the long wall. Time history responses of displacement (u_z) of critical nodes identified from equivalent static analyses are shown in Fig. 5.79 and Fig. 5.80.
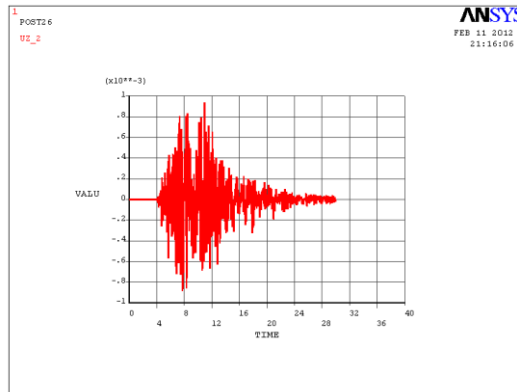
(a) Type B
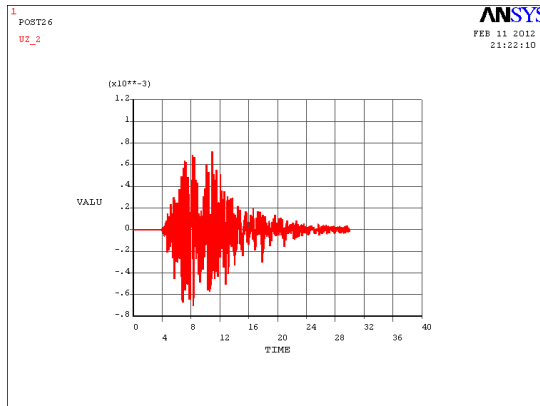
(b) Type BV
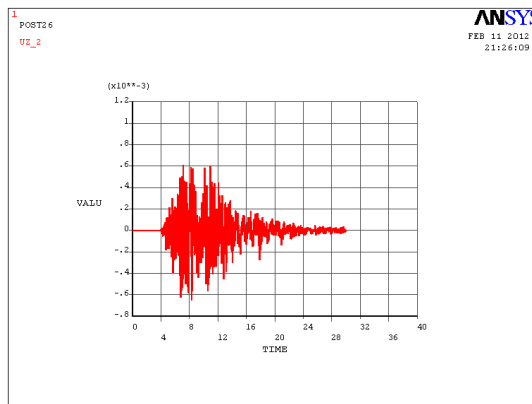
(c) Type BLV

Fig. 5.79 Time history response of deflection u_z (m) for structures subjected to Kobe earthquake
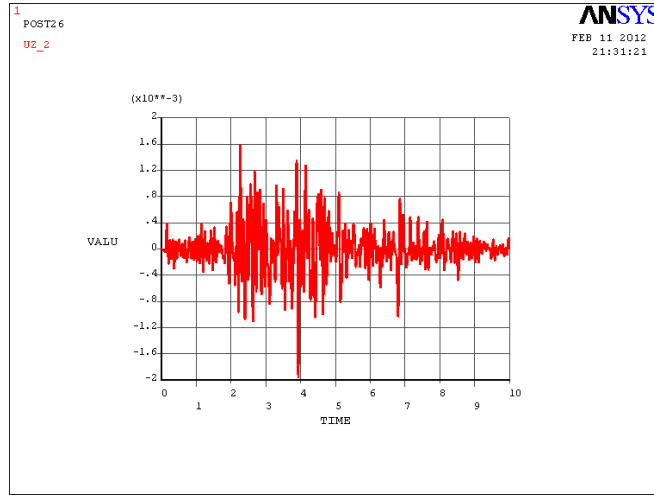
(a) Type B
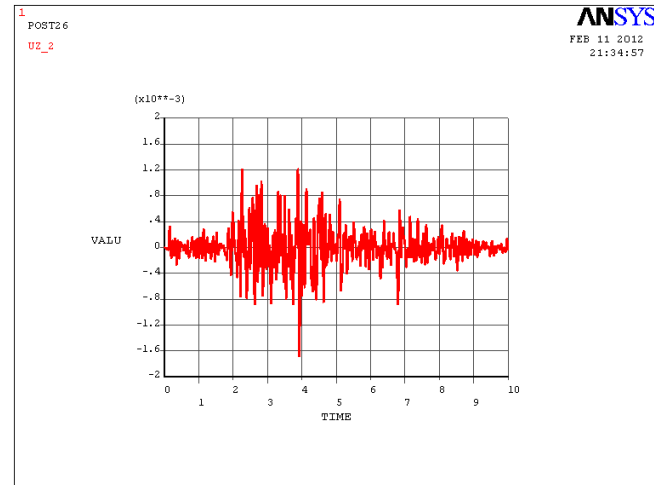
(b) Type BV
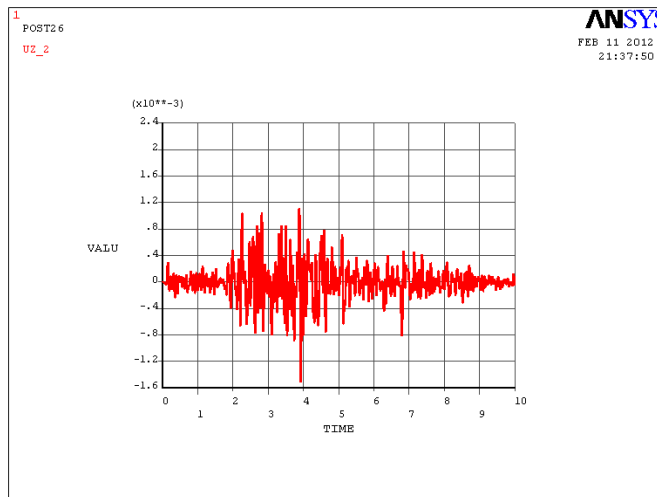
(c) Type BLV

Fig. 5.80 Time history response of deflection u$_z$ (m) for structures subjected to Koyna earthquake

131

The maximum deflection u_z for structure type B, when it is subjected to Kobe acceleration was noted as 0.93 mm, which got reduced to 0.72 mm in case of structure type BV, which is a reduction of 23% from that of structure type B. In case of structure type BLV the maximum deflection was noted as 0.65 mm which is a reduction of 30% from that of structure type B.

For structure type B subjected to Koyna acceleration, the maximum deflection u_z was noted as 1.9 mm whereas for structure type BV it was noted as 1.7 mm, which is 11% less than that of structure type B. This was noted to have reduced to 1.5 mm in case of structure type BLV which is 21% less than that of structure type B.

Again the studies on structures under Kobe and Koyna accelerations also reveal the effectiveness of containment reinforcement.

5.5 CONCLUSIONS

1. Equivalent-static analyses conducted by applying a horizontal acceleration of 0.5g, perpendicular to the long wall, revealed that the long walls of box-type laterite masonry structures without roof undergo a cantilever mode of deflection, with maximum deflection (u_z) at the center of top edge. The reduction in maximum out of plane deflection (u_z) in structures AV, ALR and ALRV were observed as 11%, 70% and 72% respectively from that of structure A. Again in box-type laterite masonry structures without roof, provision of a lintel band and a roof band seems to be more effective in reducing the lateral displacement (u_z), than the containment reinforcement.

   In a similar study on box-type laterite masonry structures with roof, the maximum deflection was observed at about ¾[th] height, along the center of the long wall in all the four cases (B, BV, BL and BLV). The deflections seem to increase up to 2.25m height and then gradually decrease up to the top edge. The reduction in maximum out of plane deflection (u_z) in structures BV, BL and BLV were observed as 16%, 10% and 24% respectively from that of structure B. Lintel band

along with containment reinforcement reduced the out-of-plane deflection by 24%. The effect of containment reinforcement in reducing the out of plane deflection (u_z) is also observed to be more in structures with roof, compared to structures without roof.

2. From equivalent static analyses, the maximum stress normal to bed joint σ_y was observed to occur near the center of the base of the long wall for building Types A, AV, ALR and ALRV. Although providing containment reinforcement alone helps to reduce the bending stress σ_y in box-type laterite masonry structures without roof, provision of RC bands instead appears to be more effective in reducing the stresses. In box-type laterite masonry structures without roof, RC bands along with containment reinforcement leads to a reduction of the stresses σ_y by almost 53%. Maximum stress σ_y was observed at the corners of base of the long wall for building Types B, BV, BL and BLV. However, provision of containment reinforcement appears to be more effective in reducing the stress σ_y than provision of a lintel band, in these structures. The results indicate that, during an earthquake, horizontal flexure cracks could develop at the base of the long walls in box type laterite masonry structures, both with and without rigid roof.

3. Equivalent static analyses reveal the maximum values of stress σ_x, parallel to bed joints, at the center of long walls near the top edge for box type laterite masonry structures without roof (A, AV, ALR and ALRV) thus, indicating a tendency of vertical crack formation in the center of long walls. In box type laterite masonry structures without roof, just the provision of RC bands can lead to an appreciable reduction in the stress σ_x (71% reduction in maximum stress σ_x from A to ALR). In box type laterite masonry structures with roof, B, BV, BL and BLV, maximum stress σ_x was observed at sill level of window opening in the long walls. In these structures, providing containment reinforcement proves to be more effective than lintel bands in reducing the stresses σ_x. Containment reinforcement along with RC

bands can lead to substantial reduction in the stresses σ_x (41% reduction in maximum stress from B to BLV), in these structures.

4. Equivalent static analyses reveal the maximum values of shear stress σ_{yz}, at the corners of opening at lintel level of short walls for box type laterite masonry structures without roof (A, AV, ALR and ALRV). In box type laterite masonry structures with roof, B, BV, BL and BLV, maximum shear stress σ_{yz} was observed at mid length of short wall below sill level. Compared to structures without roof, shear stress is more in structures with roof. Maximum shear stress in structure Type B is 41% more than that in Type A.

5. Time history analyses of box-type laterite masonry structures subjected to El-Centro (NS component) acceleration reveal that in structures without roof (Types A, AV, ALR and ALRV), the maximum deformations occur at the top free edge. In box type laterite masonry structures without roof, the reinforced concrete bands, when provided, were able to control the total deformation significantly. In structures with roof (B, BV, BL and BLV) the maximum deformations occur near the openings and at the corners of the rigid roof. In these structures, the rigid roof itself was able to reduce the total displacement significantly. Containment reinforcement seems to have further reduced the total deformation in single storeyed box-type laterite masonry structures with roof compared to those of structures without roof.

6. Trends in reduction of out-of-plane deflection and bending stresses in transient analysis with earthquake accelerations match with those obtained from equivalent static analyses.

CHAPTER 6

CONCLUSIONS AND SCOPE FOR FUTURE WORK

6.1 INTRODUCTION

Experimental investigations were carried out on the strength characteristics of laterite blocks, cement mortar specimens and stack-bonded laterite masonry prisms under uniaxial vertical pressure. Parametric studies were also conducted by finite element analyses on laterite masonry prisms. Free vibration studies were conducted to find the natural frequencies and mode shapes of box-type laterite masonry structures without and with roof. The effect of strengthening factors like lintel band, roof band and 'containment reinforcement on the natural frequencies and mode shapes were analyzed. Response of single storeyed box-type laterite masonry structures, to El-Centro acceleration was obtained using time-history analysis. Responses of some of these structures to Kobe and Koyna accelerations were also studied. Based on the results of all these studies, the following conclusions are made:

1. Based on experimental investigations:

- When laterite blocks of sizes used in practice were tested, the compressive strengths obtained were much lower than the strengths of the standard-sized mortar cubes tested.
- Average modulus of elasticity of laterite blocks tested was found to be less than that of mortar used in making the laterite masonry; hence, laterite masonry can be classified as soft unit-stiff mortar masonry.
- Laterite masonry prisms were observed to have failed by bond failure and subsequent splitting of laterite blocks.

2. Based on analytical studies on laterite masonry prisms:

- When laterite masonry prisms are subjected to uniaxial vertical pressure, the laterite blocks (weak and soft) were observed to be in triaxial compression and the mortar joints (strong and stiff) in uniaxial compression and bilateral tension.

- Increase in Poisson's ratio of laterite or decrease in Poisson's ratio of mortar resulted in an increase in lateral tensile stresses in mortar, which in turn would result in reduction of prism compressive strength. The larger the difference between the Poisson's ratios of the block and the mortar, lower the compressive strength of the prism.

- Reduction in modulus of elasticity of laterite blocks or increase in modulus of elasticity of mortar, results in increase in the lateral tensile stresses in mortar joints of the laterite masonry prism, at a given vertical pressure. As the ratio of modulus of elasticity of laterite block to modulus of elasticity of mortar is reduced (only $E_{lt}/E_m<1$ considered), there is an increase in the lateral tensile stresses in the mortar.

- Increase in thickness of mortar joint, results in a decrease in lateral tensile stresses in mortar joint, indicating higher prism strength, if bond remains intact.

- Prism strength will improve with better bond strength, higher ratio of elastic modulus of laterite and mortar (only $E_{lt}/E_m<1$ considered) and lower Poisson's ratio of laterite blocks.

3. Based on free vibration studies on box type laterite masonry structures:

- Introduction of RC bands or containment reinforcement tends to increase the natural frequencies of box-type laterite masonry structures, both with and without roof. But it does not seem to affect the fundamental mode shapes of these structures. While the fundamental mode shape of box-type laterite masonry structures without roof is the 'breathing mode', it gets

shifted to a 'sway mode' for box-type laterite masonry structures with roof. This change in the fundamental mode shape then brings greater differences in the dynamic response of the structures with provision of a rigid RC roof.

- Provision of roof also substantially changes the magnitude of the first few natural frequencies of single storeyed box type laterite masonry structures. The fundamental frequency of unreinforced laterite masonry structures with roof (B) is more than double that of a structure without roof (A). These changes in the magnitude of the frequencies and the change in the fundamental mode shape can lead to large differences in the seismic response of the structures with and without roof.

4. Based on equivalent static analysis and time history analysis:

- Equivalent-static analyses conducted by applying a horizontal acceleration of 0.5g, perpendicular to the long wall, reveal that the long walls of box-type laterite masonry structures without roof underwent a cantilever mode of deflection, with maximum deflection (u_z) at the center of top edge. In these structures, lintel band and roof band has proved to be more effective in reducing the lateral displacement (u_z), than the vertical containment reinforcement. In case of box-type laterite masonry structures with roof the maximum deflection is observed at around $3/4^{th}$ height, along the center of the long wall. The effect of vertical containment reinforcement in reducing the out of plane deflection (u_z) is slightly more in structures with roof, compared to structures without roof.

- Maximum stress σ_y was observed at the base edge of the long wall near the center for single storeyed box-type laterite masonry structures without roof. Although vertical containment reinforcement has helped to reduce the out of plane stresses (σ_y) in box-type laterite masonry structures without roof, RC bands have played a better role in the stress reduction.

137

Maximum stress σ_y was observed at the base edge of the corners of long wall for structures with roof. Vertical containment reinforcement along with RC bands will help to reduce the stresses σ_y and hence the horizontal cracks in single storeyed box type laterite masonry structures.

- Maximum stress σ_x was observed at the center of long walls near the top edge for single storeyed box type laterite masonry structures without roof. In these structures, RC bands have enabled to reduce the stress σ_x also considerably. Maximum stress σ_x was observed at sill level in long walls of single storeyed box type laterite masonry structures with roof. In these structures, however, vertical containment reinforcement has proved to be more effective than lintel band in reducing the stresses σ_x. Vertical containment reinforcement along with RC bands will help to reduce the stresses σ_x and hence the vertical cracks, in box-type laterite masonry structures.

- Maximum values of shear stress σ_{yz}, was observed at the corners of opening at lintel level of short walls for box type laterite masonry structures without roof. In box type laterite masonry structures with roof, maximum shear stress σ_{yz} was observed at mid length of short wall below sill level. Compared to structures without roof, shear stress is more in structures with roof. Maximum shear stress in structure Type B is 41% more than that in Type A.

5. Time history analyses of box type laterite masonry structures subjected to El-Centro (NS component) acceleration reveals that:

- In structures without roof (Types A, AV, ALR and ALRV) the maximum deformations occur at the top free edge. In box type laterite masonry structures without roof, the reinforced concrete bands themselves were able to control the total deformation significantly. In structures with roof (B, BV, BL and BLV), however, the maximum deformation occurs near

138

the openings and at the corners of the rigid roof. In these structures, the rigid roof was able to reduce the total displacement significantly. Containment reinforcement seems to have further reduced the total deformation in single storeyed box-type laterite masonry structures with roof compared to that of structures without roof.

6. Trends in reduction of out-of-plane deflection and bending stresses in analyses with earthquake accelerations match with those obtained from equivalent static analyses.

7. Time history analyses with Kobe and Koyna earthquake acceleration inputs also reveal the relative effectiveness of vertical containment reinforcement in reducing the displacements and stresses in box-type laterite masonry structures under earthquakes.

6.2 SCOPE FOR FURTHER STUDIES

In continuation of this research, the following studies may be carried out:

- Only a limited number of samples were tested in the experimental study. However, considering the scarce data available on laterite masonry, the results of the present study may prove to be valuable. Studies may be taken up with large sample size, possibly with laterites from different quarries from different parts of India.

- Laterite monumental structures were constructed with lime mortar. It is seen that such structures have performed well. Hence extensive experiments on bond strength of laterite with lime mortar and also cement-lime mortar may be conducted.

- Isotropic material properties were assumed for laterite masonry. Detailed experimental work for obtaining orthotropic material properties may be conducted.

- A detailed experimental work for the characterization of laterite masonry can be attempted.

- Linear elastic material assumption is a first step to understand the seismic response of box-type laterite masonry structures. Nonlinear dynamic analysis is necessary in further understanding the crack-behaviour in box-type laterite masonry structures.

- Shake table studies on scaled models of laterite masonry structures may be attempted.

- Seismic response of laterite masonry structures with asymmetry in plan, multi-storey buildings and buildings with vertical irregularities may be attempted.

REFERENCES

Agarwal P. and Shrikhande M. (2007), "Earthquake resistant design of structures", *Prentice Hall of India Private Limited*, New Delhi, India.

Anderson D and Brzev S (2009), "Seismic design guide for masonry buildings", *Canadian Concrete Masonry Producers Association* (CCMPA), Toronto, April.

Andreaus U. (1996), "Failure criteria for masonry panels under in-plane loading", *Journal of Structural Engineering*, Vol.122, No.1, January, pp.37-46.

ANSYS (2005), "ANSYS User's Manual Revision 10" ANSYS Inc.

Bakhteri J., Makhtar A.M. & Sambasivam S. (2004), "Finite element modelling of structural clay brick masonry subjected to axial compression", *Jurnal Teknologi*, 41(B) February, pp.57-68.

Berto L., Saetta A., Scotta R. and Vitaliani R. (2005), "Failure mechanism of masonry prism loaded in axial compression: computational aspects", *Materials and Structures*, 38, pp.249-256.

BMTPC Guidelines (2000), Improving earthquake resistance of housing, *Building Materials and Technology Promotion Council,* New Delhi, India.

Bruneau M. (1994), "State-of-the-art report on seismic performance of unreinforced masonry buildings", *Journal of Structural Engineering*, ASCE, Vol.120, No.1, January, pp.231-251.

Buchanan F. (1807), "A journey from Madras through countries of Mysore, Canara and Malabar", *East India Company*, London, pp.436-461.

Das S. (2008), "Decay diagnosis of Goan laterite stone monuments", 11DBMC *International Conference on Durability of Building Materials and Components*, ISTANBUL, Turkey, 11-14 May.

Felix Ip. (1999), "Compressive strength and modulus of elasticity of masonry prisms", *Master of Engineering thesis*, Dept. of Civil and Environmental Engineering, Carleton University, Ottawa, Ontario.

Gidigasu M.D. (1974), "Degree of weathering in the identification of laterite materials for engineering purposes-A review", *Engineering Geology*, 8, pp.213-266.

Gumaste K.S., Rao N.K.S., Reddy V.B.V. and Jagadish K.S. (2007), "Strength and elasticity of brick masonry prisms and wallettes under compression", *Materials and Structures*, 40, pp.241-253.

Hamid A.A. and Chukwunenye A.O. (1986), "Compression behavior of concrete masonry prisms", *Journal of Structural Engineering*, ASCE, Vol.112, No.3, pp.605-613.

IS 1121(Part 1)-1974 (Reaffirmed 2003), "Methods of test for determination of strength properties of natural building stones – compressive strength", *Bureau of Indian Standards*, New Delhi, India.

IS 1124-1974 (Reaffirmed 1998), "Method of test for determination of water absorption, apparent specific gravity and porosity of natural building stones", *Bureau of Indian Standards*, New Delhi, India.

IS 1893(Part 1)-2002, "Indian standard criteria for earthquake resistant design of structures", *Bureau of Indian Standards*, New Delhi, India.

IS 1905-1987, "Indian standard code of practice for structural use of unreinforced masonry", *Bureau of Indian Standards*, New Delhi, India.

IS 2250-1981 (Reaffirmed 2000), "Indian standard code of practice for preparation and use of masonry mortars", *Bureau of Indian Standards*, New Delhi, India.

IS 3620-1979 (Reaffirmed 1998), "Indian standard specification for laterite stone block for masonry", *Bureau   of Indian Standards*, New Delhi, India.

IS 4326-1993, "Earthquake resistant design and construction of buildings – Code of practice", 2nd revision, *Bureau of Indian Standards*, New Delhi, India.

Jagadish K.S., Raghunath S. and Rao N.K.S. (2002), "Shock table studies on masonry building model with containment reinforcement", *Journal of Structural Engineering*, Vol.29, No.1, April-June, pp.9-17.

Jagadish K.S., Raghunath S. and Rao N.K.S. (2003), "Behaviour of masonry structures during the Bhuj earthquake of January 2001", *Proc. Indian Acad. Sci. (Earth Planet. Sci.)*, 112, No.3, September, pp.431-440.

Jain S.K., Murty C.V.R, Chandak N., Seeber L., and Jain N.K. (1994), "The September 29, 1993, M6.4 Killari, Maharashtra Earthquake in Central India", EERI Special Earthquake Report, *EERI Newsletter*, Vol.28, No.1, January.

Jain S.K., Murty C.V.R, Arlekar J.N., Sinha R., Goyal A. and Jain C.K. (1997), "Some Observations on Engineering Aspects of the Jabalpur Earthquake of 22 May 1997", EERI Special Earthquake Report, *EERI Newsletter*, Vol.32, No.2, August.

Jhung M.J, (2009), "Seismic analysis of mechanical components by ANSYS", *Korea Institute of Nuclear Safety*, KINS/RR-685.

Karantoni F.V. and Fardis M.N. (1992), "Computed versus observed seismic response and damage of masonry buildings", *Journal of Structural Engineering*, Vol.118, No.7, July, pp.1804-1821.

Kasthurba A.K (2005a), Characterisation and study of weathering mechanisms of Malabar laterite for building purposes, *Unpublished PhD thesis*, Department of Civil Engineering, Indian Institute of Technology, Madras, India.

Kasthurba A.K. and Santhanam M. (2005b), "A re-look into the code specifications for the strength evaluation of laterite stone blocks for masonry purposes", *Journal of Institution of Engineers (India)*, Architecture Division, Vol.86, April, pp.1-6.

Kasthurba A.K., Santhanam M. and Mathews M.S. (2006), "Weathering forms and properties of laterite building stones used in historic monuments of western India", *Structural Analysis of Historical Constructions*, New Delhi, pp.1323-1328.

Kasthurba A.K., Santhanam M. and Mathews M.S. (2007), Investigation of laterite stones for building purpose from Malabar region, Kerala state, SW India –Part 1: field studies and profile characterization", *Construction and Building Materials*, 21, pp.73-82.

Kaushik H.B., Rai D.C. and Jain S.K. (2007a), "Uniaxial compressive stress-strain model for clay brick masonry", *Current Science*, Vol.92, No.4, February, pp.497-501.

Kaushik H.B., Rai D.C. and Jain, S.K. (2007b), "Stress-strain characteristics of clay brick masonry under uniaxial compression", *Journal of Materials in Civil Engineering*, Vol.19, No.9, September, pp.728-739.

Krishna J. and Chandra B. (1965), "Strengthening of brick buildings against earthquake forces", *Proc. 3rd World Conference on Earthquake Engineering*, New Zealand, Vol.3, pp.IV 324-IV341.

Manu F. W., Baiden-Amissah P. D., Boadi J. K., Amoa-Mensah K. (2009), "Some material improvement options for earth construction in Northern Ghana: a key factor in reducing the impact of recent floods on housing", *Proceedings of the 11th international conference on non-conventional materials and technologies* (NOCMAT 2009), Bath, UK.

McNary S.W. and Abrams D.P. (1985), "Mechanics of masonry in compression", *Journal of Structural Engineering*, Vol. 111, No. 4, April, pp. 857-870.

Murty C.V.R. (2005), "Earthquake tips", IITK - BMTPC, *Building Materials and Technology Promotion Council,* New Delhi, India.

Murty C.V.R., Rai D.C., Jain S.K., Kaushik H.B., Mondal G., and Dash S.R. (2006), "Performance of Structures in the Andaman and Nicobar Islands (India) during the December 2004 Great Sumatra Earthquake and Indian Ocean Tsunami", *Earthquake Spectra*, Vol.22, No.S3, June, pp.S321-S354, Earthquake Engineering Research Institute.

Pradhan P.L., Murty C.V.R., Hoiseth K.V. and Aryal M.P. (2009), "Nonlinear simulation of stress-strain curve of infill materials using PLP fit model", *Journal of the Institute of Engineering*, Vol. 7, No.1, pp 1-12.

Raghunath S., Rao K.S.N., and Jagadish K.S. (2000), "Studies on the Ductility of Brick Masonry Walls with Containment Reinforcement", *Proc. 6th International Seminar on Structural Masonry for Developing Countries*, 11-13 October, IISc, Bangalore, India.

Raghunath S. (2003), "Static and dynamic behaviour of brick masonry with containment reinforcement", *Unpublished PhD thesis*, Department of Civil Engineering, Indian Institute of Science, Bangalore, India.

Rai D.C. and Goel S.C. (1996), "Seismic strengthening of unreinforced masonry piers with steel elements", *Earthquake Spectra*, Vol.12, No.4, November, pp.845-862.

Rao S.S., Reddy V.B.V. and Jagadish K.S. (1995), "Strength characteristics of soil-cement block masonry", *The Indian Concrete Journal*, 69(2), February, pp.127-131.

Rao N.K.S., Raghunath, S. and Jagadish, K.S. (2004), "Containment reinforcement for earthquake resistant masonry buildings", *13th World Conference on Earthquake Engineering*, Vancouver, B.C., Canada, August 1-6, Paper No. 1968.

Reddy V.B.V., Lal R. and Rao N.K.S (2009), "Influence of joint thickness and mortar-block elastic properties on the strength and stresses developed in soil-cement block masonry", *Journal of Materials in Civil Engineering*, ASCE, Vol.21, No. 10, October, pp.535-542.

Şahin A. (2010), "ANSeismic – A Simple Assistant Computer Program for Implementing Earthquake Analysis of Structures with ANSYS and SAP2000", *The Ninth International Congress on Advances in Civil Engineering (ACE 2010)*, September 27-30, Trabzon, Turkey.

Saikia B., Vinod K.S., Raghunath S. and Jagadish K.S. (2006), "Effect of reinforced concrete bands on dynamic behaviour of masonry buildings", *The Indian Concrete Journal*, October, pp.9-16.

Sarangapani G., Reddy V.B.V. and Jagadish K.S. (2005), "Brick-mortar bond and masonry compressive strength", *Journal of Materials in Civil Engineering*, Vol. 17, No.2, April, pp.229-237.

SP 20 (S&T):1991, "Handbook on masonry design and construction", *Bureau of Indian Standards*, New Delhi, India.

SP 22-1982, "Explanatory handbook on codes for earthquake engineering", *Bureau of Indian Standards,* New Delhi, India.

Tavarez F.A. (2001), "Simulation of behavior of composite grid reinforced concrete beams using explicit finite element methods," *Master's Thesis*, University of Wisconsin, Madison, Wisconsin.

Thakkar K.S. and Agarwal P. (2000), "Seismic evaluation of earthquake resistant and retrofitting measures of stone masonry houses", 12WCEE *12th World Conference on Earthquake Engineering*, Jan 30-Feb 4, Auckland, New Zealand, Paper No. 0110.

Tomazevic M. (1999), "Earthquake resistant design of masonry buildings", *Imperial College Press*, London, UK.

Vyas Ch.U.V. and Reddy V.B.V. (2010), "Prediction of solid block masonry prism compressive strength using FE model", *Materials and Structures*, Vol. 43, No. 5, July, pp.719-735.

West W.D. (1936), "Preliminary geological report on the Baluchistan (Quetta) earthquake of 31st May 1935", *Records of the Geological Survey of India*, Vol. LXIX, Part 2, pp.203-240.

Wikipedia, "Angadipuram laterite", Retrieved on 7/2/2010.

Wolanski A.J. (2004), "Flexural behavior of reinforced and prestressed concrete beams using finite element analysis," *Master's Thesis*, Marquette University, Milwaukee, Wisconsin.

Zharikov V.A., Pertsev N.N., Rusinov V.L., Callegari E. and Fettes D.J. (2007), "Metasomatism and metasomatic rocks", *Recommendations by the IUGS Subcommission on the Systematics of Metamorphic Rocks: Web Version*,
01.02.07, www.bgs.ac.uk/scmr/home.html.

http://www.vibrationdata.com/elcentro.htm

http://www.eerc.berkeley.edu/, National Information Service for Earthquake Engineering (NISEE), University of California at Berkeley.

Appendix 1: APDL Seismic analysis code [Sahin 2010]

```
FINISH
/CONFIG,NRES,20000
/PREP7
DAMPRATIO = 0.05
*SET,NT,1000
*SET,DT,0.02
*DIM,AC,,NT
*VREAD,AC(1),a-g1-20,TXT
(F10.5)
/SOLU
ANTYPE,2
MODOPT,LANB,6
MXPAND,6,,,1
SOLVE
FINISH
*GET,FREQ1,MODE,1,FREQ
/SOLU
ANTYPE,TRANS
TRNOPT,FULL
ALPHAD,2*DAMPRATIO*FREQ1*2*3.1415926
BETAD,2*DAMPRATIO/(FREQ1*2*3.1415926)
*DO,I,1,1000
ACEL,0,0,AC(I)
TIME,(I)*0.02
OUTRES,ALL,ALL
SOLVE
*ENDDO
FINISH
```

PUBLICATIONS FROM PRESENT RESEARCH WORK

1. Sujatha Unnikrishnan, Mattur C. Narasimhan and Katta Venkataramana (2011), "Studies on uniaxial compressive strength of laterite masonry prisms", International Journal of Earth Sciences and Engineering, April, Volume 4, No.2, pp.336-350.

2. Sujatha Unnikrishnan, Mattur C. Narasimhan and Katta Venkataramana (2012), "Free vibration studies of box type laterite masonry structures", Journal of Structural Engineering, SERC, Chennai, India, August-September, Volume 39, No. 3, pp.332-346.

3. Sujatha Unnikrishnan, Mattur C. Narasimhan and Katta Venkataramana (2010), "Uniaxial compressive strength of laterite masonry prisms- an evaluation", International Conference (ICEE-2010), Hyderabad, India, 21-22 August.

4. Sujatha Unnikrishnan, Mattur C. Narasimhan and Katta Venkataramana, "Effect of containment reinforcement on the seismic response of box type laterite masonry structures – An analytical evaluation", accepted for publication in Earthquake and Structures, An International Journal.

PERSONAL PROFILE

Name : Sujatha Unnikrishnan

Date of Birth : 02-11-1971

Permanent Address : "UJJAINI", TC 36/1433, J.P.Nagar,

Thiruvananthapuram-695008

Sl No.	Certificate/Degree	University/Board
1	SSC	Kerala Board of Secondary Education
2	PUC	Kerala University
3	B.Tech (Civil)	Kerala University
4	M.Tech (Structures)	Visvesvaraiah Technological University

Teaching Experience: 8 Years
Publications :

1. Sujatha Unnikrishnan, Mattur C. Narasimhan and Katta Venkataramana (2009), "Stress strain characteristics of laterite masonry", NITK Research Bulletin, Vol. 18, No. 1, June, pp. 27-31.

2. Sujatha Unnikrishnan, Mattur C. Narasimhan and Katta Venkataramana (2010), "Uniaxial compressive strength of laterite masonry prisms- an evaluation", International conference (ICEE-2010), 21-22 August.

3. Sujatha Unnikrishnan, Mattur C. Narasimhan and Katta Venkataramana (2011), "Studies on uniaxial compressive strength of laterite masonry prisms", International Journal of Earth Sciences and Engineering, April, Volume 4, No. 2, pp.336-350.

4. Sujatha Unnikrishnan, Mattur C. Narasimhan and Katta Venkataramana (2012), "Free vibration studies of box type laterite masonry structures", Journal of Structural Engineering, SERC, Chennai, India, August-September, Volume 39, No. 3, pp.332- 346.

5. Sujatha Unnikrishnan, Mattur C. Narasimhan and Katta Venkataramana, "effect of containment reinforcement on the seismic response of box type laterite masonry structures – an analytical evaluation", accepted for publication in Earthquake and Structures, An International Journal.